Galaxy Clusters in Optic and X-Rays

Elena Panko

I.I. Mechnikov Odessa National University
Odessa, Ukraine

Some key ideas about galaxy clusters

1. Galaxies tend to gather into Groups and Clusters.
2. Galaxy clusters are rare extremes in the galaxy distribution, with local overdence $\Delta\rho/\langle\rho\rangle \sim 10^3$.
3. Galaxy groups and clusters are not the largest known gravitationally bound objects.
4. Superclusters are largest bound structures identified in the Universe.
5. Galaxy clusters are the element of large-scale structure of Universe.
6. Clusters are part of a continuous range of structures:

   Galaxies ⇨ Groups ⇨ Clusters ⇨ Superclusters ⇨ Large Scale Structure.

Note: clusters are not necessarily the largest bound structures in the universe ⇨ superclusters may be bound, but haven't yet turned around and virialized.
On these large scales, components have not had a chance to separate during collapse ⇨ a cluster is probably a representative sample of the Universe.

YES or NO?

If YES: we measure Dark Matter (DM) content in clusters and:

$$(M_{DM} / M_{baryons})_{cluster} = (M_{DM} / M_{baryons})_{Universe}$$

If NO: WHY?

Galaxy clusters are the element of large-scale structure of Universe.
Clusters are part of a continuous range of structures:

Galaxies ⇨ ("Local Groups") ⇨ Groups ⇨ Clusters ⇨
Superclusters ⇨ Large Scale Structure

Galaxies : $t_{virial} = 10^8$ yr <<< t_{Hubble}

Clusters : $t_{virial} = 10^9$ yr << t_{Hubble}

Galaxy clusters are the largest virialized structures in the Universe.

Groups:
3 to 30 bright galaxies

Clusters:
30 to 300+ bright galaxies

Superclusters : $t_{virial} = 10^{10.5}$ yr > t_{Hubble}

Structures larger than clusters have not had time to "turn around", collapse, and virialize.

Superclusters:
Clusters of Clusters? No!

LSC: Superclusters, Voids
Filaments, Walls

Very roughly (depending on definitions) the total galaxy content of the universe is divided: 1-2% in rich clusters, 5-10% in clusters and
50-100% in "Local Group"s and/or looser groupings.

Local Galaxy Grope:

Milky Way, Andromeda (M31, largest galaxy in the group) and Triangulum galaxies (M33) and more than 50 satellite small galaxies.

The radius of zero-acceleration surface around the LG ≃2 Mpc (V. Dolgachev, L. Domozhilova & A. Chernin. AZ, 2003, **80**, 792).

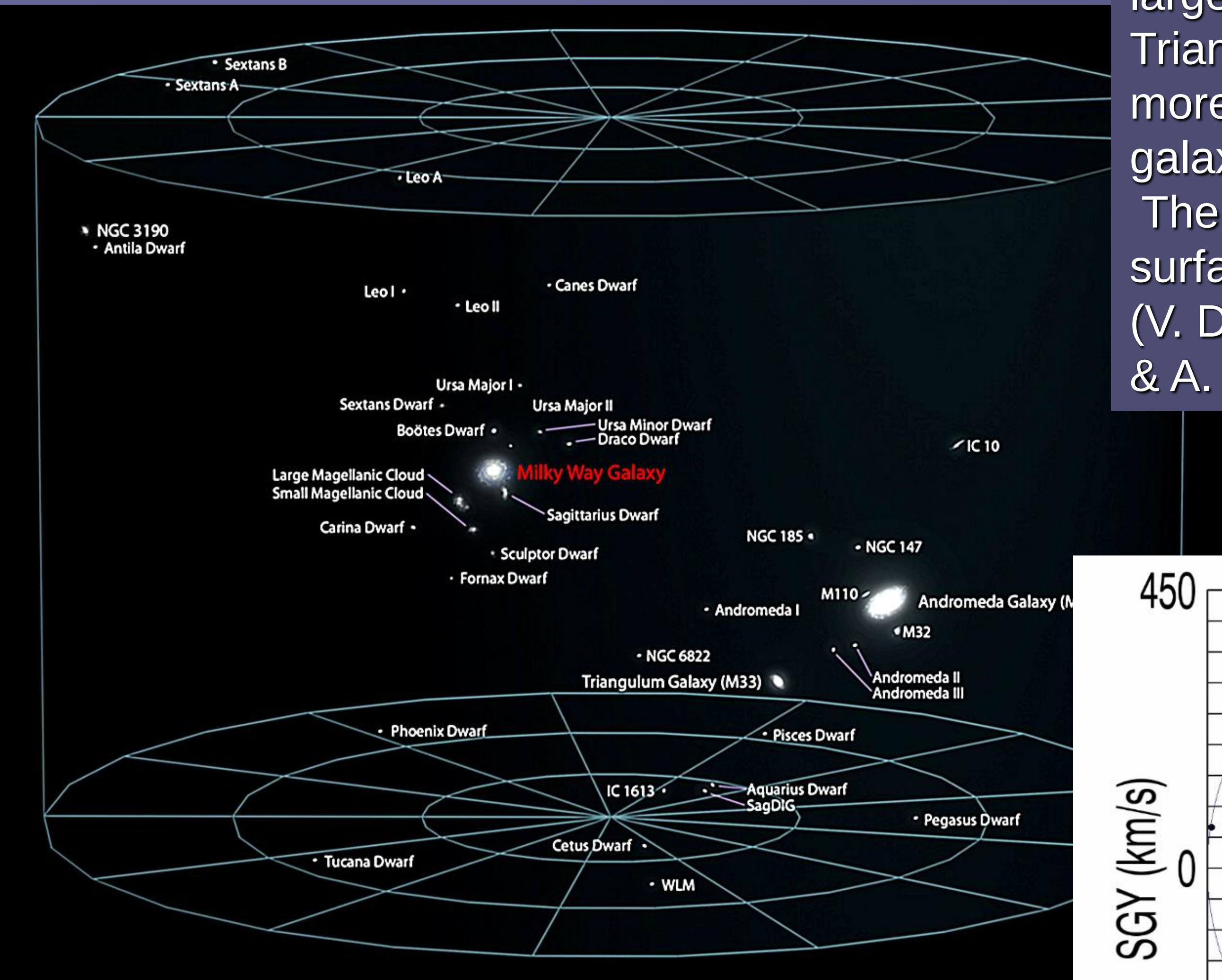

Credit: Jason Maron
http://www.jaymaron.com/astro/Earth's_Location_in_the_Universe_SMALLER_(JPEG).jpg

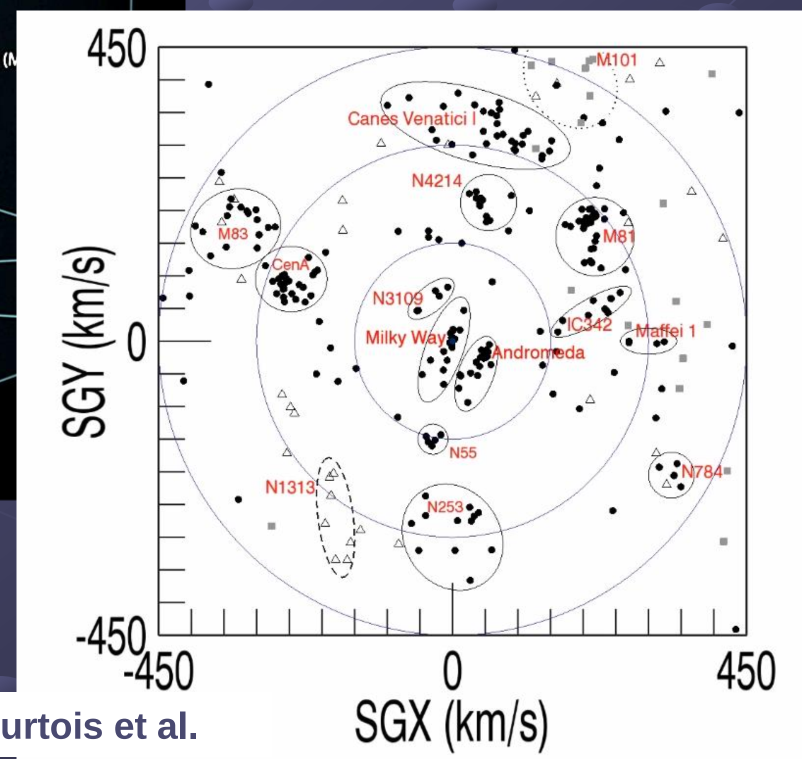

Courtesy H. Courtois et al.

Virgo Supercluster

Virgo, Fornax and Eridanus Clusters; Norma Cluster (located near the center of the Great Attractor, not shown), and a lot of galaxy groups, like to LGG, M81 group, Leo Group etc.

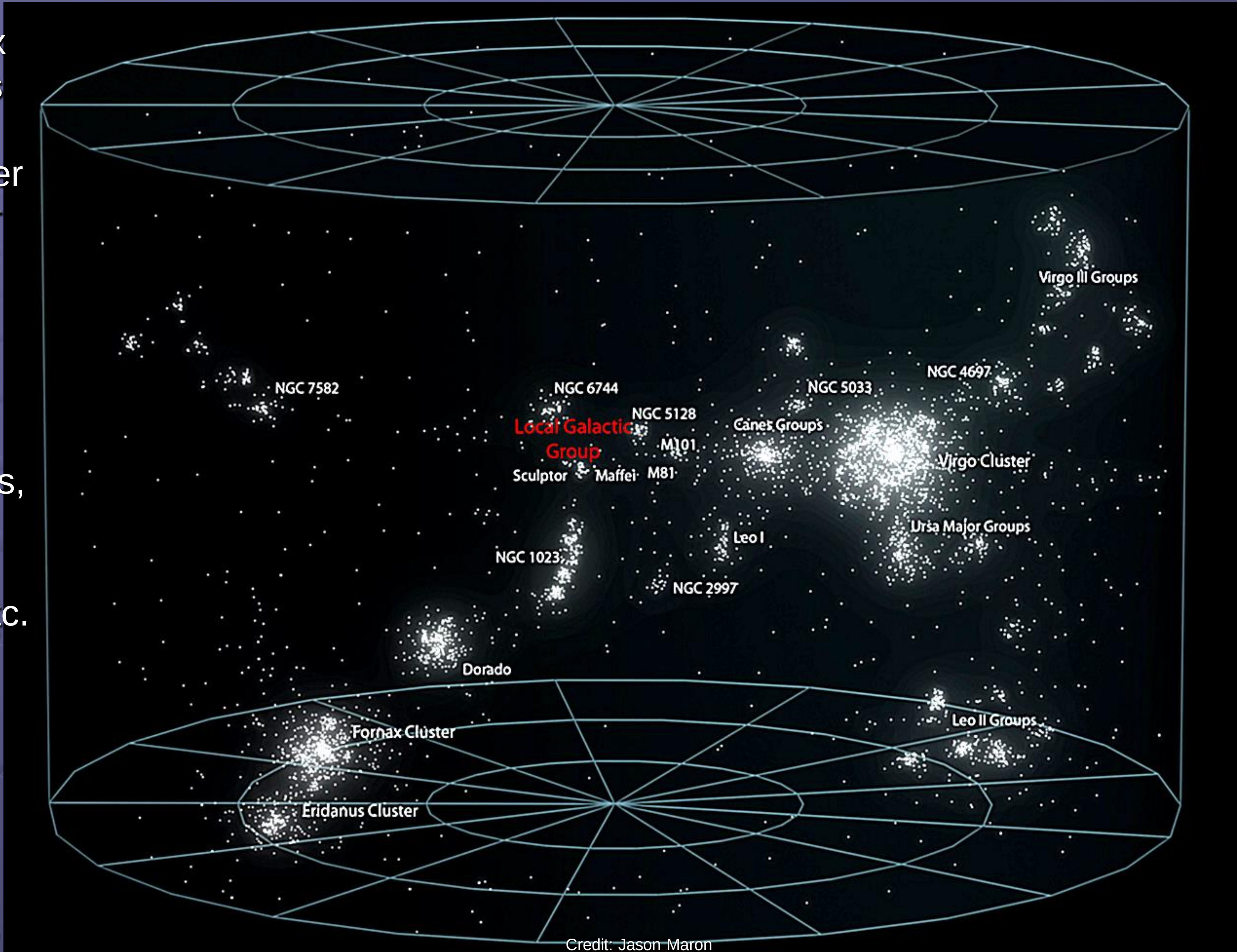

Credit: Jason Maron
http://www.jaymaron.com/astro/Earth's_Location_in_the_Universe_SMALLER_(JPEG).jpg

Local Supercluster: Laniakea

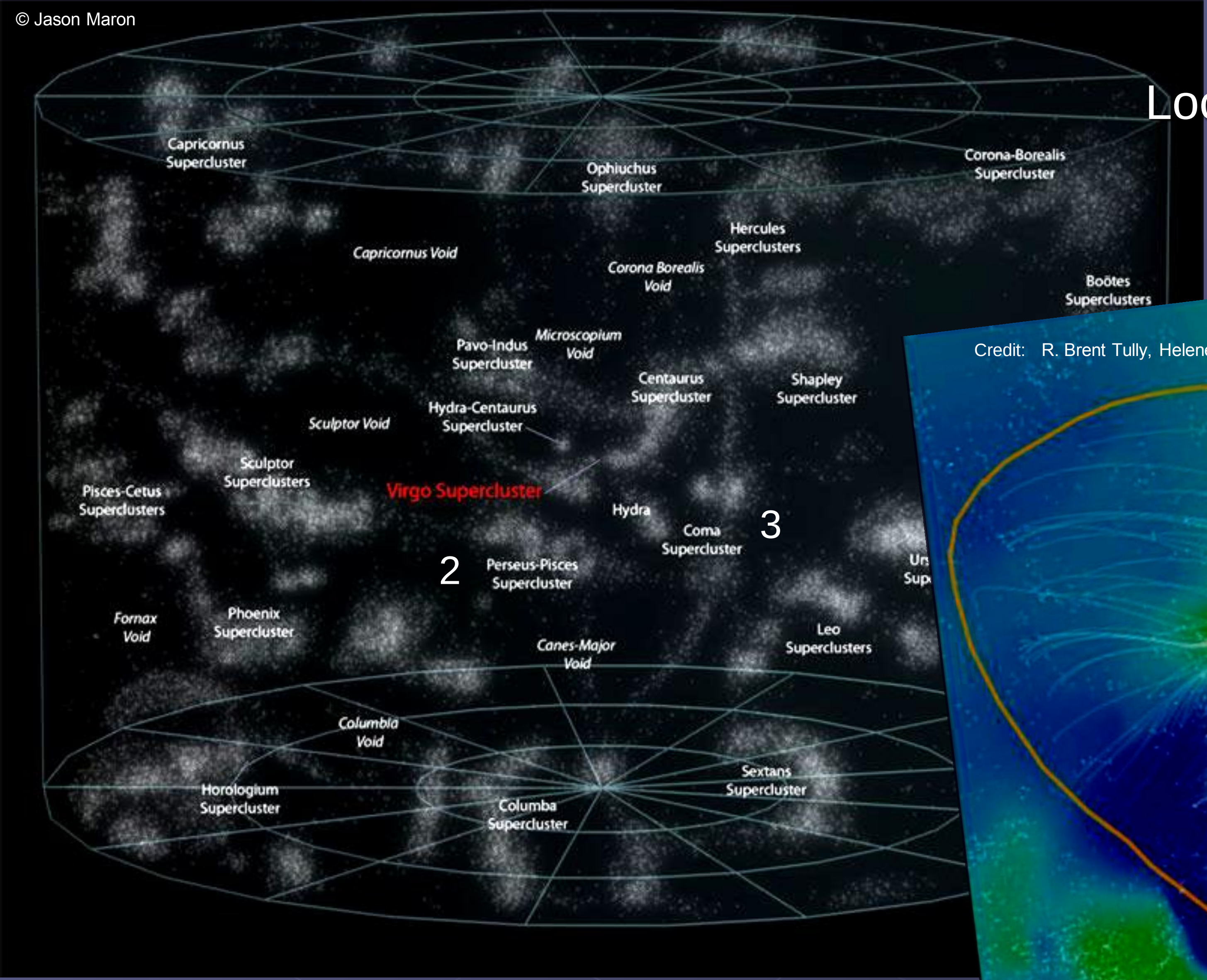

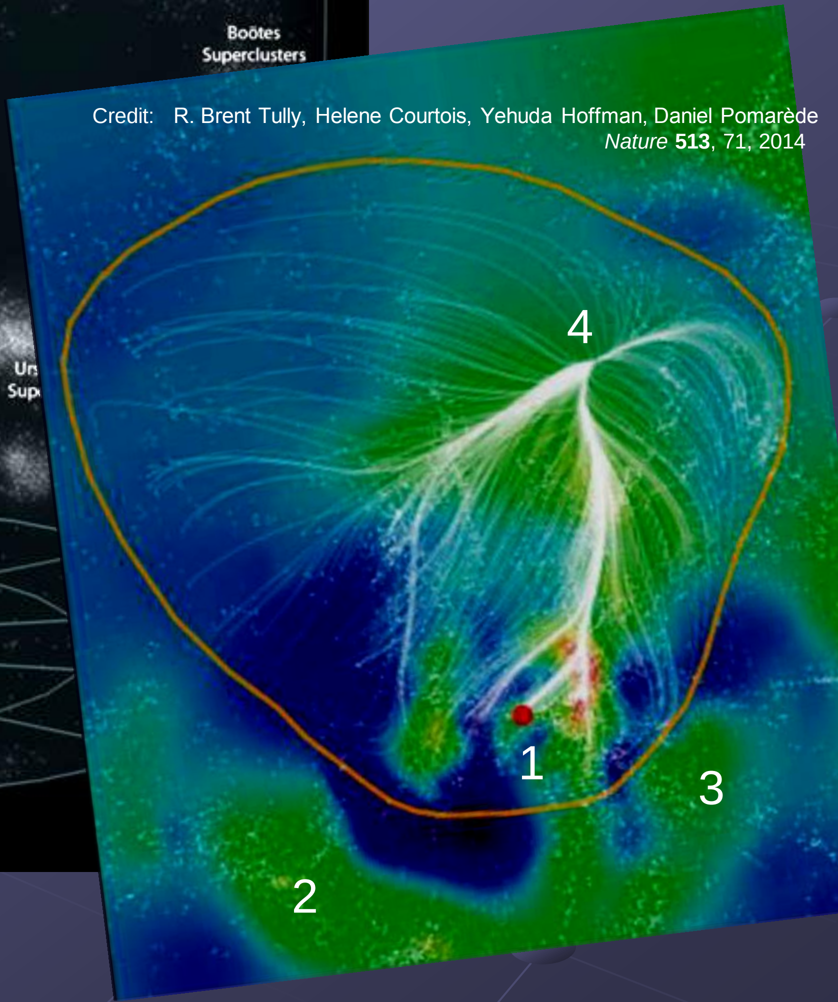

The radius of zero-acceleration surface around the Laniakea ≃80 Mpc.

1 – our position (Virgo); 2 – Perseus-Pisces; 3 – Coma, 4 – the Great Attractor

LCS subtypes

LCS -- larger than superclusters. The study began in the late 1980s.

1987 -- R. Brent Tully discover the Pisces–Cetus Supercluster Complex, type filament (*The ApJ,* **323**, 1–18. 1987).

1989 -- CfA2 Great Wall (*M. J. Geller & J. P. Huchra*, Science, **246**, 897)

- Filaments as supercluster complexes, 1*D* structures with a typical length 50 to 80 h^{-1} Mpc, having roughly similar values of major and minor axes in cross-section along the lengthwise axis

- Galaxy walls (sheets) 2*D* structures.

(CfA2 Great Wall, SDSS Great Wall, Sculptor Wall (Southern Great Wall), Hercules–Corona Borealis Great Wall, discovered in 2013, (Horvath et al., 2013 (arXiv1311.1104H)
3000 Mpc × 150 000 km/s (in z-space), the largest known structure in the universe?)

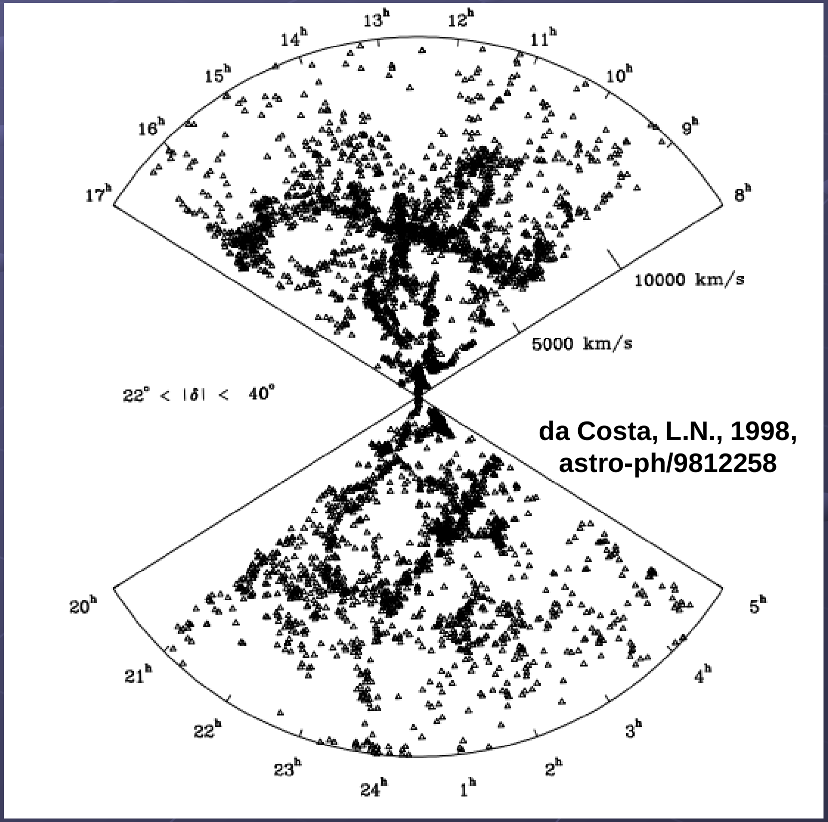

CfA2 Great Wall and Ursa Major Filament (left leg of Homunculus)

Galaxy clusters: some steps in optic

1. William, Caroline and John Herschel and their study of distribution and classifications of nebulae and description of "nebulous stratum of Coma Berenices", and several other nearby clusters and groups of galaxies, such as Leo, Ursa Major, Hydra, Pisces, Fornax etc.
2. John Herschel also hinted at the existence of the Local Supercluster, with the Virgo concentration "being regarded as the main body of this system", and our own Galaxy "placed somewhat beyond the borders of its densest portion, yet involved among its outlying members" (de Vaucouleurs' Supergalaxy).
3. Another star islands: BMC and SMC.
4. The Great Debate: the nature of M31.
5. Abell and Herzog, Wild & Zwicky and their "Catalogues Clusters of Galaxies“.
6. Modern 2D and 3D sky surveys and detail study of galaxy clusters.

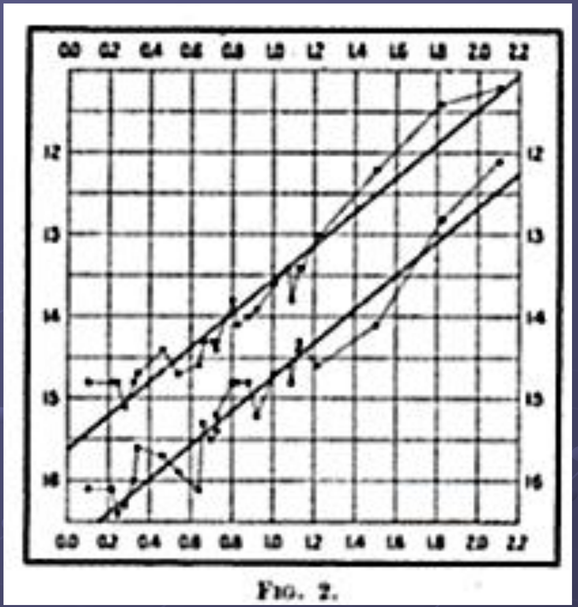

From: Harvard College Observatory, Circular 173

Magellanic clouds. In 1908 Henrietta Swan Leavitt based on dataset of 1777 variable, established "period–luminosity relationship" for cepheids. It allows to estimate the distance to nearest galaxies (GALAXIES ??)

Especial case was M31. It has regular spiral structure and spectrum different from a gaseous nebula. In 1864, William Huggins noted that the spectrum of Andromeda nebula has absorption lines.

Andromeda Galaxy

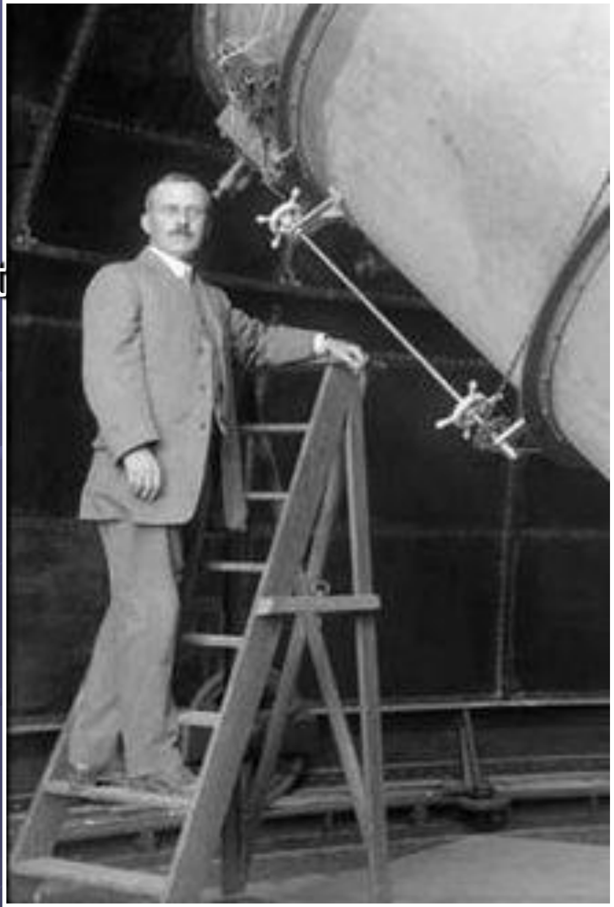

In 1917 Heber Curtis observed a nova within M31 (*Ibid.,* **29**, 206). Searching the photographic record, 11 more novae were discovered. Curtis noticed that these novae were, on average, 10^m fainter than those that occurred elsewhere in the sky.

As a result, he was able to come up with a distance estimate of 500'000 light-years The paper was published only in 1988 (*PASP,* **100**, 6), however the results noted to so-called "island universes" hypothesis, which held that spiral nebulae were actually independent galaxies.

More, the results were base for his position on "The Great Debate" about the nature of MW, spiral nebulae and the dimensions of the universe between Curtis and Shapley (1920). To support his claim of the Great Andromeda Nebula being, in fact, an external galaxy, Curtis also noted the appearance of dark lanes resembling the dust clouds in our own galaxy within Andromeda -- the MW -- as well as the significant Doppler shift that he had observed of Andromeda.

Andromeda Galaxy

Ernst Julius Öpik

In 1922 Ernst Öpik presented a method to estimate the distance of M31 using the measured velocities of its stars. His result placed the Andromeda Nebula far outside our galaxy at a distance of about 450 000 parsecs (1 500 000 LY). It was first published data. He also at first estimate the mass of Andromeda Nebula (4.5×10^9 solar masses, modern value $\sim 1.5 \times 10^{12}$ solar masses).

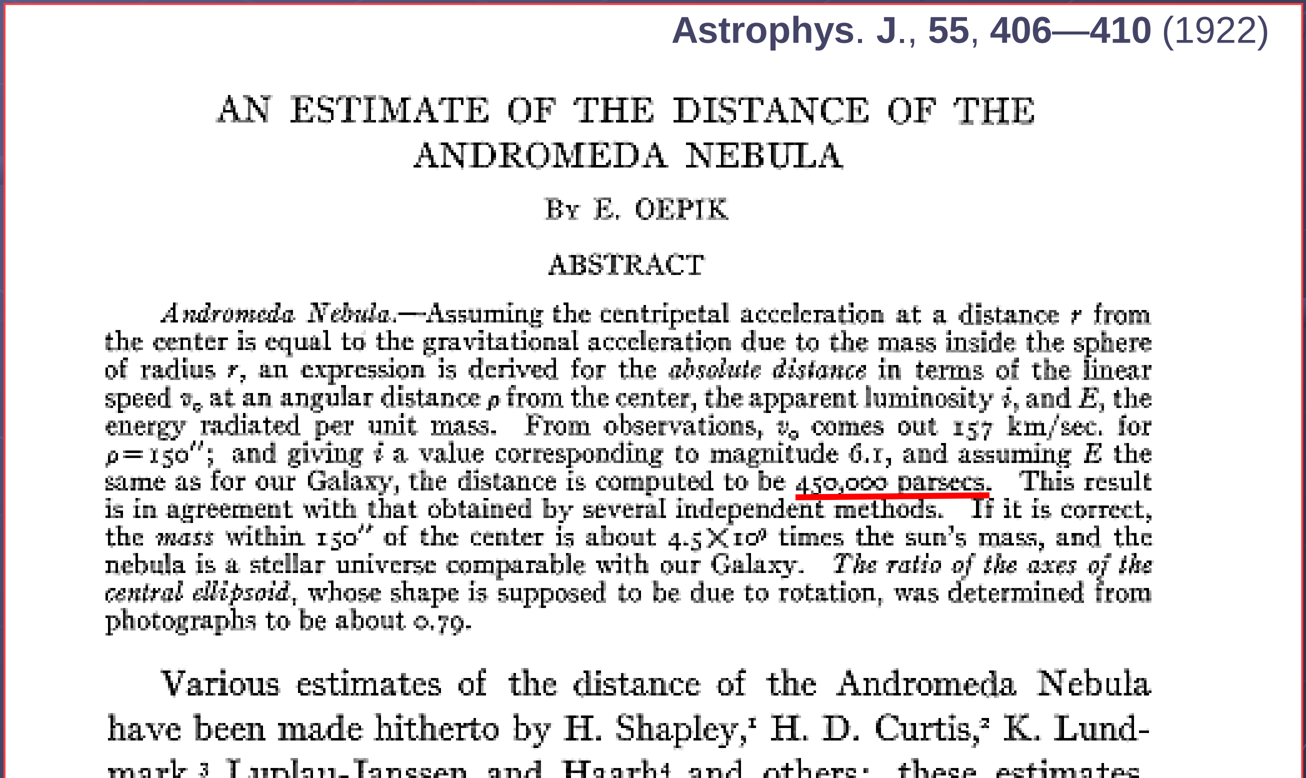

Astrophys. J., 55, 406—410 (1922)

AN ESTIMATE OF THE DISTANCE OF THE ANDROMEDA NEBULA

BY E. OEPIK

ABSTRACT

Andromeda Nebula.—Assuming the centripetal acceleration at a distance r from the center is equal to the gravitational acceleration due to the mass inside the sphere of radius r, an expression is derived for the *absolute distance* in terms of the linear speed v_0 at an angular distance ρ from the center, the apparent luminosity i, and E, the energy radiated per unit mass. From observations, v_0 comes out 157 km/sec. for $\rho = 150''$; and giving i a value corresponding to magnitude 6.1, and assuming E the same as for our Galaxy, the distance is computed to be 450,000 parsecs. This result is in agreement with that obtained by several independent methods. If it is correct, the *mass* within 150″ of the center is about 4.5×10^9 times the sun's mass, and the nebula is a stellar universe comparable with our Galaxy. *The ratio of the axes of the central ellipsoid*, whose shape is supposed to be due to rotation, was determined from photographs to be about 0.79.

Various estimates of the distance of the Andromeda Nebula have been made hitherto by H. Shapley,[1] H. D. Curtis,[2] K. Lundmark,[3] Luplau-Janssen and Haarh[4] and others; these estimates

On October 6, 1923 Hubble noted *N* for Nova and *Var* for variable star in M31.

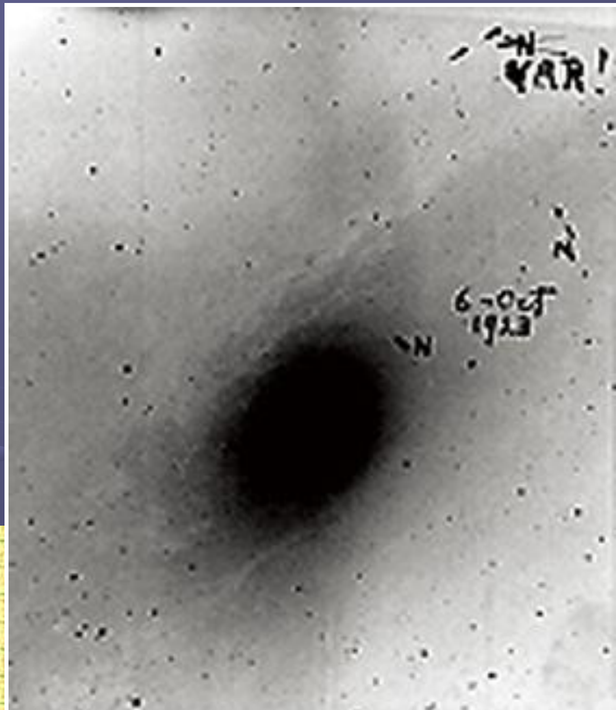

Credit: Mount Wilson Observatory Historical Archive

Hubble's observatory notebook observations fragment showing the changes in brightness of a star in M31.

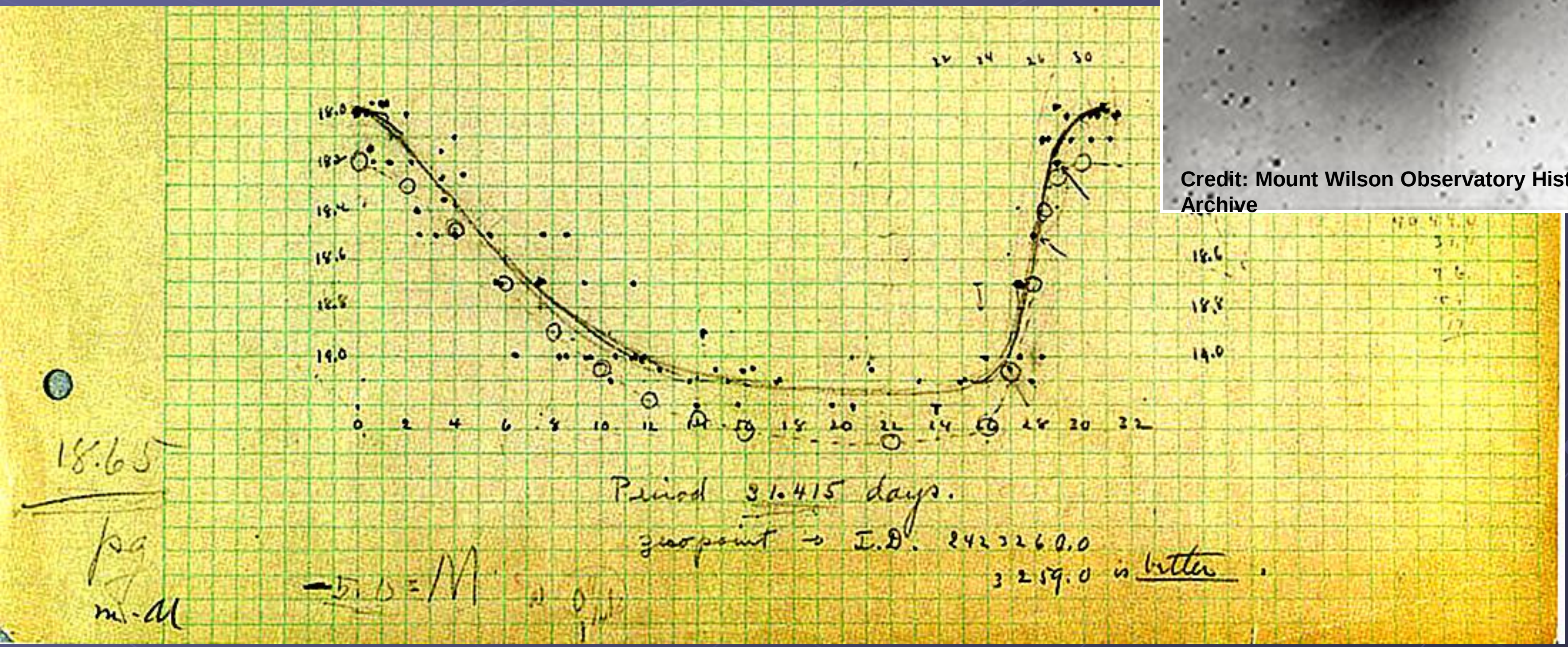

From:
http://faculty.humanities.uci.edu/bjbecker/ExploringtheCosmos/lecture17.html

E. Habble stargazes through the Hooker telescope at California’s Mount Wilson Observatory.

In the early twenties, Edwin Powell Hubble discovered cepheids in the Andromeda Nebula on 100-inch Hooker telescope at California’s Mount Wilson Observatory.
His measurement demonstrated conclusively that this feature was not a cluster of stars and gas within our own Galaxy, but an entirely separate galaxy located at significant distance from the Milky Way

He definitely established the extragalactic nature of M31
and finished "The Great Debate"
in 1925.

Great Galaxy Clouds on the sky

More galaxy systems were discovered in thirties of the XX century: Cancer, Hercules, Leo, and notably the "Centaurus cloud", today's Shapley concentration. Harlow Shapley correctly estimated it to be 14 times more distant than Virgo, and 10 times as rich in nebulae (1930).

3 years later Shapley published a list of 25 clusters and suggested the existence of "metagalactic clouds" in Coma Berenices, Centaurus and Hercules ("supercluster" term didn't exist), and Fritz Zwicky at first estimated the mass of a galaxy cluster, thus establishing the need for invisible matter – dark matter! He noted the observed dispersion in the radial velocity of the galaxies in the Coma cluster was very large and the gravity provided by the luminous matter in the cluster was not enough to hold the cluster together.

F. Zwicky
at the 18-inch Schmidt

Knut Lundmark (one of the first to suspect that the galaxies are remote stellar systems) plotted on the sky map the positions of "55 clusters of the anagalactic nebulae" in 1927. But he didn't divided galaxy group and clusters.

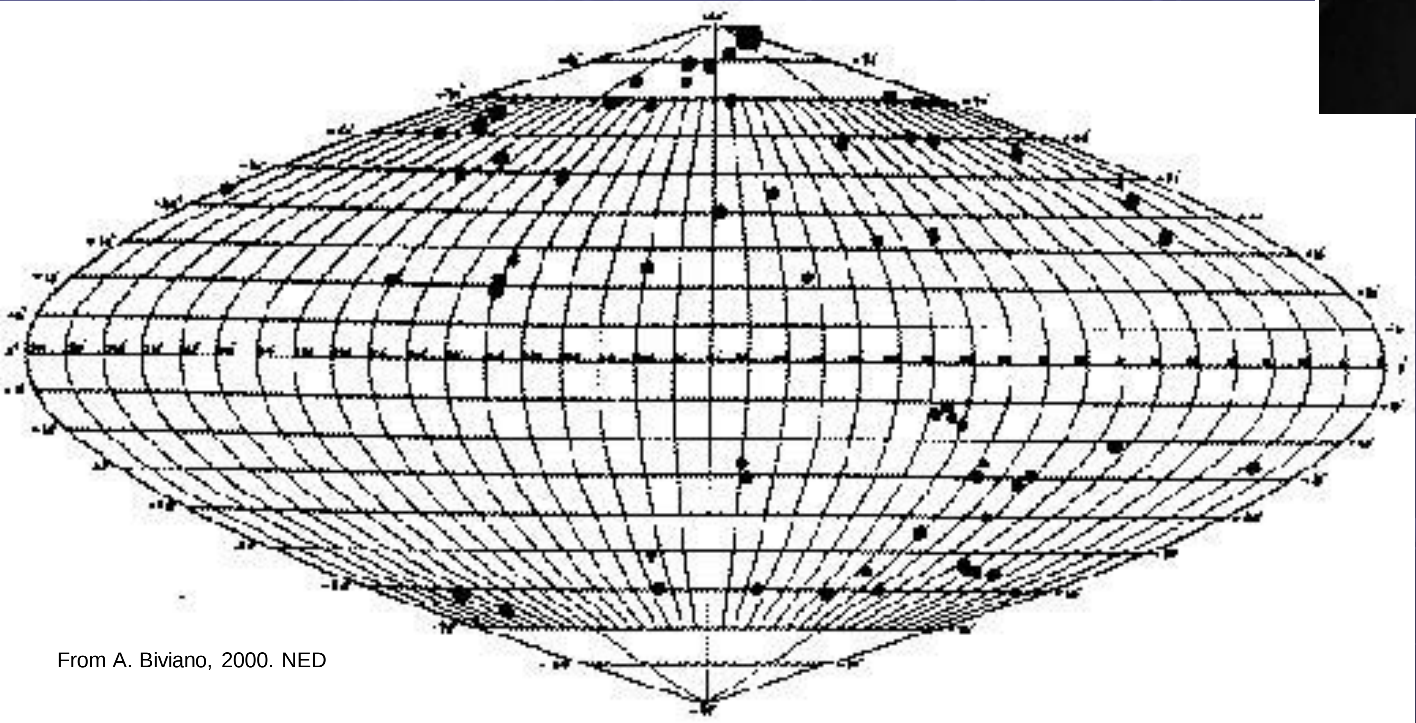

From A. Biviano, 2000. NED

In 1919 Lundmark estimate the distance (as photometrical parallax) to M31 using magnitudes of novae (*Astronomische Nachrichten*, **209**, 378).

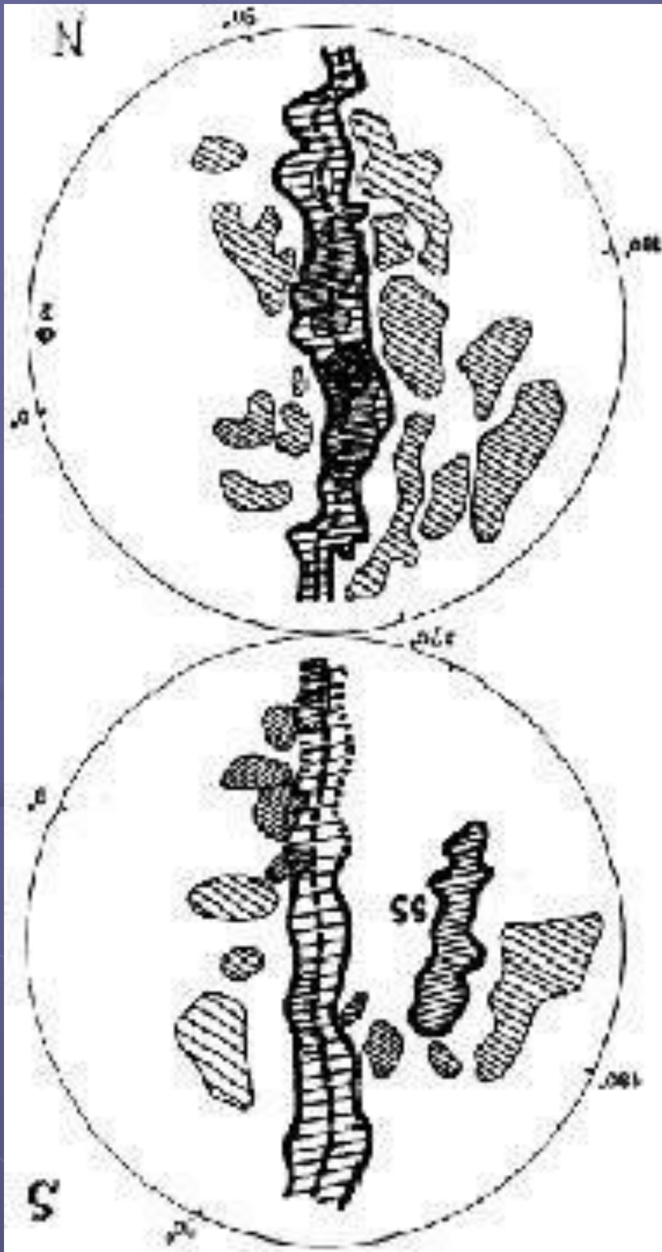

From de Vaucouleurs (1953), NED.

After the Second World War, the Lick and Palomar Observatory Sky Surveys (POSS) and the spectroscopic observations provided the essential data-base for the analysis of the distribution of galaxies and superclusters became one more element of Universe.

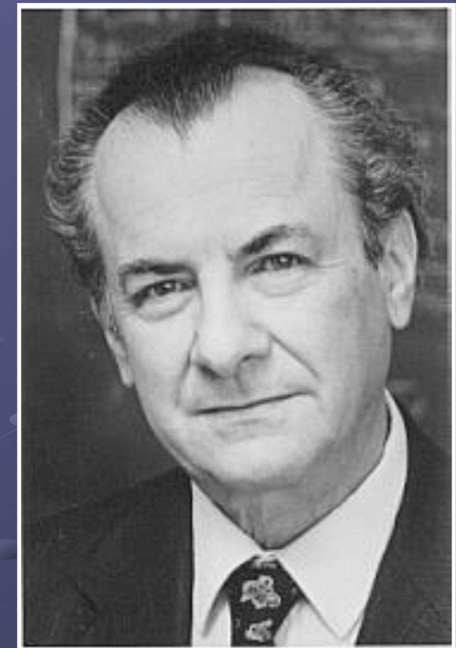

The evidence for the "Local Supergalaxy" and for many other superclusters grew stronger mainly through the works of Gérard Henri de Vaucouleurs, Shane & Wirtanen, van den Bergh, Abell.

New observational data gave the possibility for systematic search of nearby galaxy clusters.

In 1947 Herzog, Wild and Zwicky announced the construction of a "Catalogue of Galaxies and Clusters of Galaxies", however the final CGCG was published only in 1967.

Paper of George Ogden Abell
"The distribution of rich clusters of galaxies" was published in 1958 (ApJS, V.3, P.211).
The catalogue collected 2712 north sky galaxy clusters which were selected on red POSS plates.

Abell was the first to study of distribution of cluster richnesses.

Both Abell's catalogue and Abell, Corwin & Olowin paper (contained 1364 south clusters, ApJS, V.70, P. 1, 1989) were much more than a catalogues of clusters. From publication of Abell's catalogue a new era in the investigation of galaxy clusters began. Researchers obtained a catalogue of clusters, and they could start look at them as a population, rather than as individual objects.

The first volume of Zwicky et al. “Catalogue of Galaxies and Clusters of Galaxies” was published only a few years later Abell's paper, but it did not exert such a large influence on the study of clusters. Unfortunately the sizes of Zwicky's clusters were distance-dependent, since they were defined within the isopleth contour that represents twice the field density.

The common problem:
where is the edge?

M31 3.2×1.0°

Abell Clusters VS Zwicky et al. Clusters Based on Palomar Plates (POSS)

List of galaxy clusters

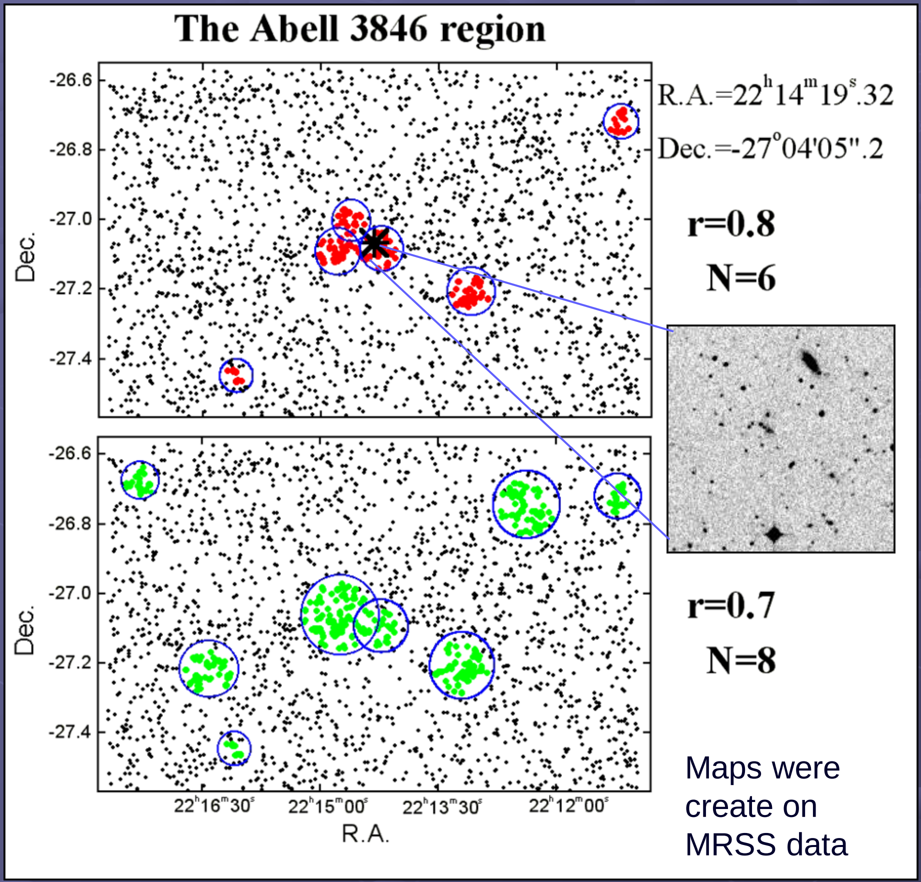

Zwicky et al.

Maps of galaxy clusters, different approach ⇨ different clusters

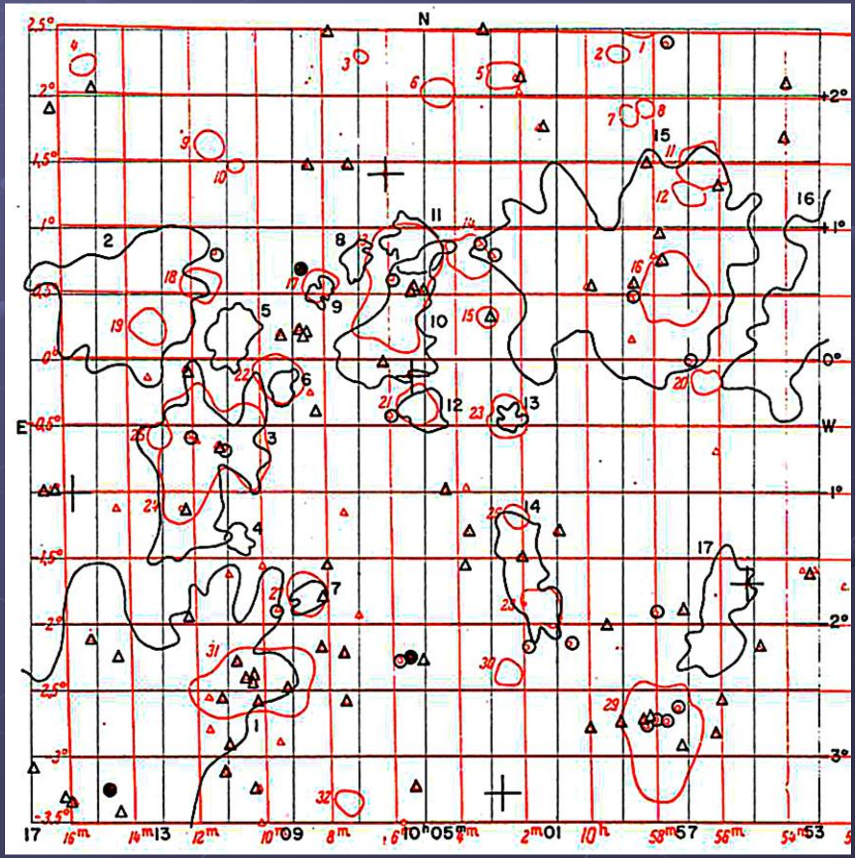

At present we have big set of galaxy clusters catalogues

The last *2D* surveys:

APM Galaxy survey

and

MRSS Galaxy

Catalogue

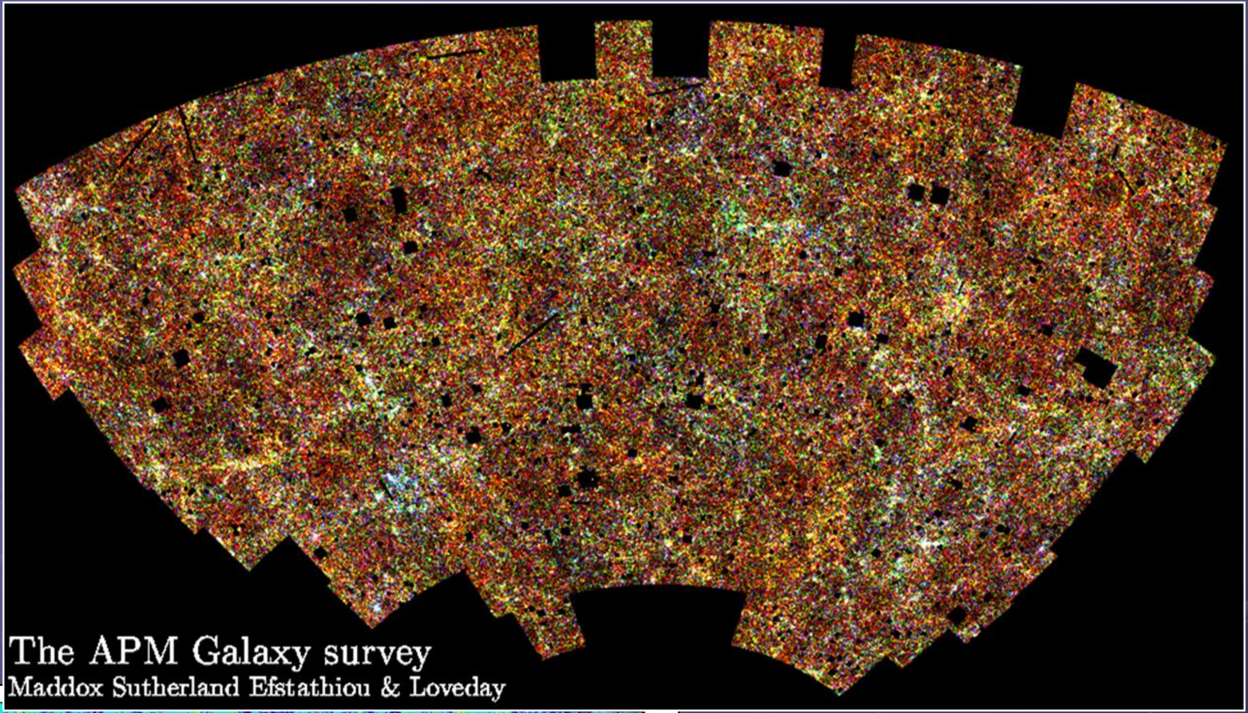

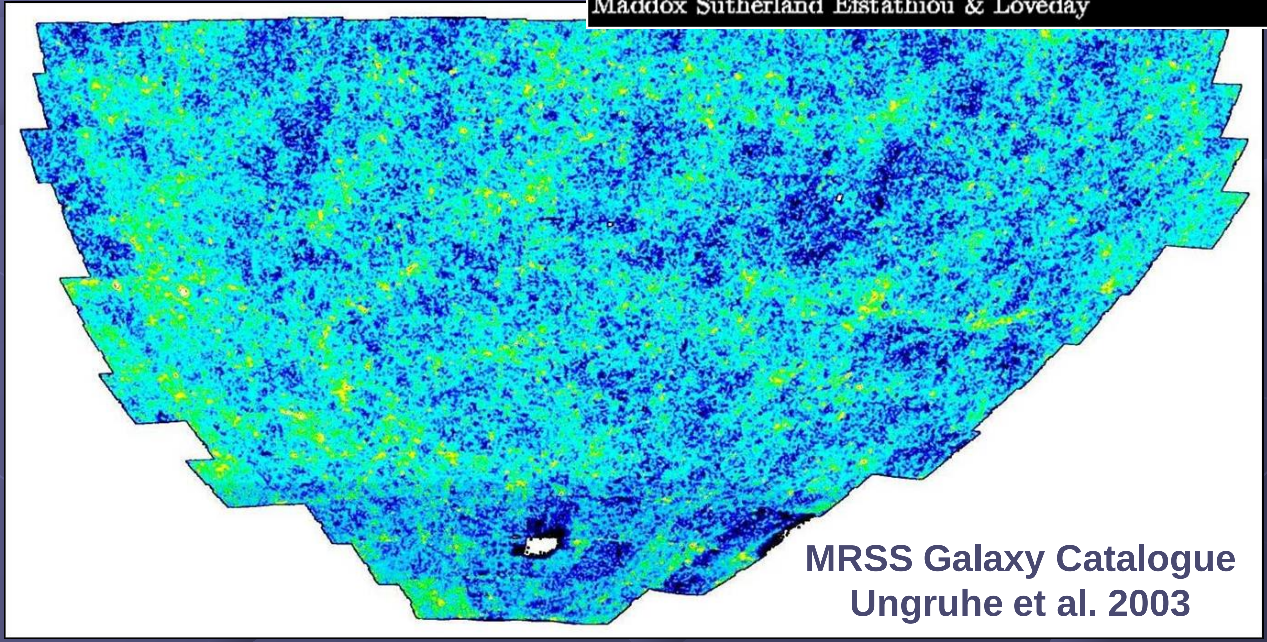

Do you see a problem?

We strongly need distances!

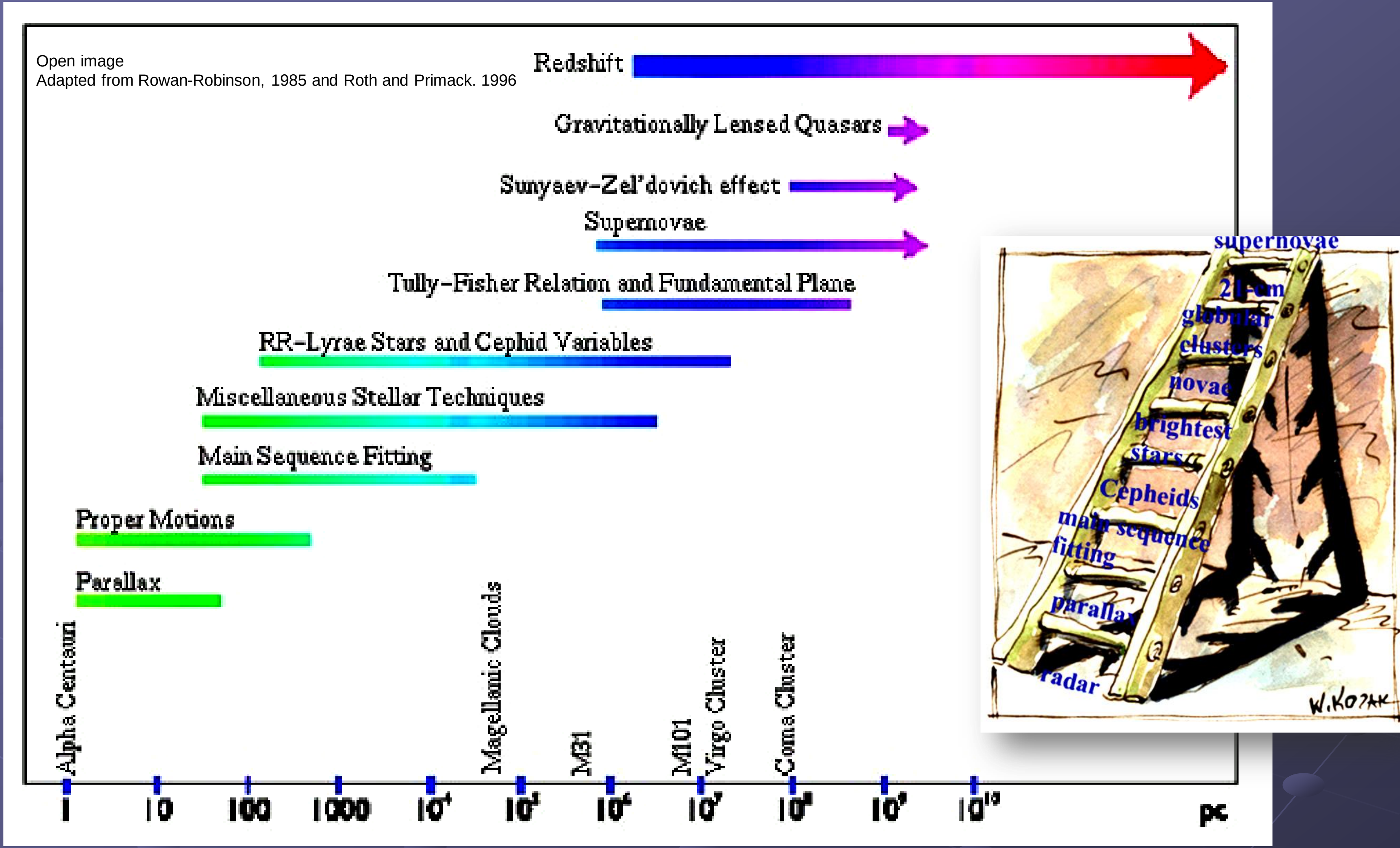

See more in:
DISTANCE MEASURES IN COSMOLOGY by David W. Hogg
https://ned.ipac.caltech.edu/level5/Hogg/Hogg_contents.html

The Distance Ladder

In 1929 Hubble published work "A Relation between Distance and Radial Velocity among Extra-Galactic Nebulae".

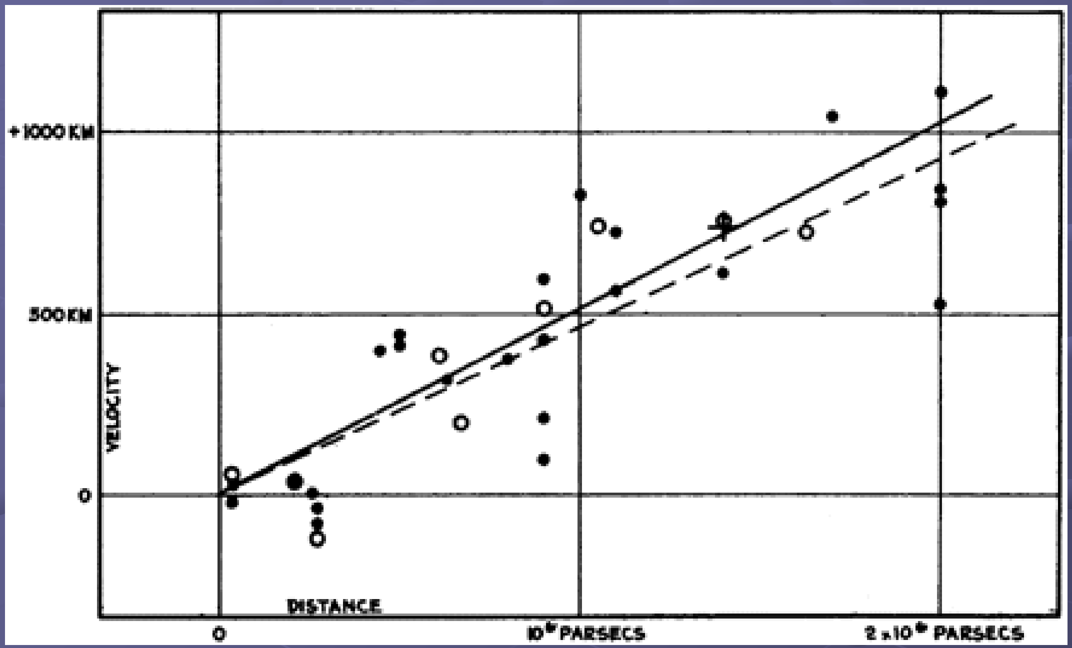

From:

Proceedings of the National Academy of Sciences of the United States of America, Volume 15, p. 168

Publication Date: 03/1929

$$\boxed{cz = Hr}$$

or

$$\boxed{\frac{\Delta\lambda}{\lambda} = \frac{H}{c}r}$$

It is a key to distance determination. But we need to establish distance markers for Hubble constant measurement.

See also Lundmark paper, line 20 in the Table I (MNRAS, **85**, 865,1925)

Communications from the Mount Wilson Observatory, to the
NATIONAL ACADEMY OF SCIENCES, No. 116.

Reprinted from the Proceedings of the NATIONAL ACADEMY OF SCIENCES,
Vol. 20, No. 5, pp. 264–268. May, 1934.

THE VELOCITY-DISTANCE RELATION FOR ISOLATED EXTRA-GALACTIC NEBULAE

BY EDWIN HUBBLE AND MILTON L. HUMASON

MOUNT WILSON OBSERVATORY, CARNEGIE INSTITUTION OF WASHINGTON

Read before the Academy, Monday, April 23, 1934

The velocity-distance relation was first established[1] for a few nebulae whose distances were derived from involved stars. With the aid of data from clusters whose relative distances were estimated from the mean apparent magnitudes of the many members of each cluster, the relation was confirmed in the form[2]

$$\log v = 0.2\,m + 0.51,$$

which, since

$$\log d = \frac{m - M + 5}{5},$$

In 1934 and 1936 Milton L. Humason confirmed the Hubble low for galaxies in far clusters. He measured velocities of 39 200 km/s and 42 000 km/s for galaxies in the Bootis and Ursa Major II clusters, making them the most distant clusters known at that time.

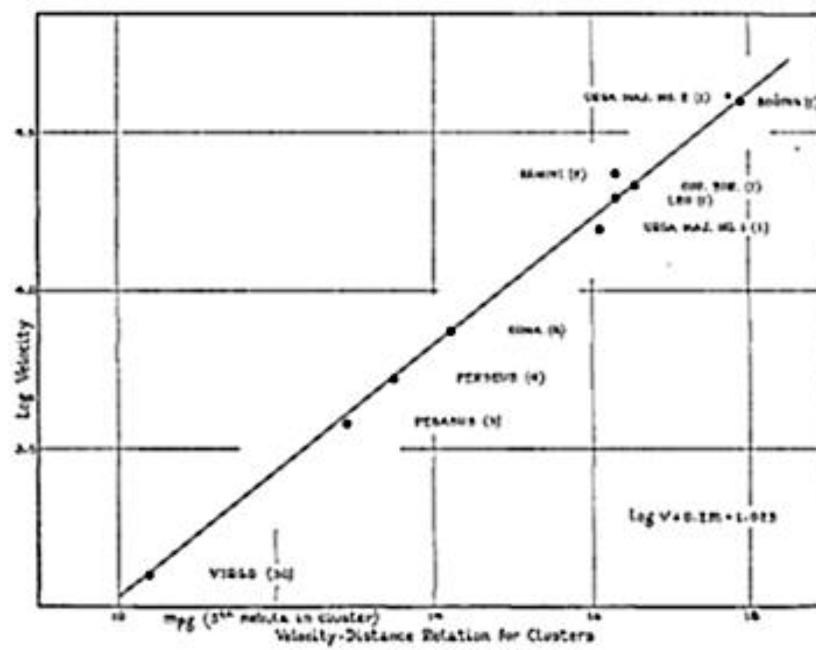

FIG. 2.—Figures in parentheses following the names of the clusters indicate the number of nebulae observed in each cluster.

Astronomical Society of the Pacific Leaflets, Vol. 2, No. 91, p.161,1936

LEAFLET 91—August, 1936

IS THE UNIVERSE EXPANDING?

By M. L. Humason
Of the Mount Wilson Observatory
Carnegie Institution of Washington

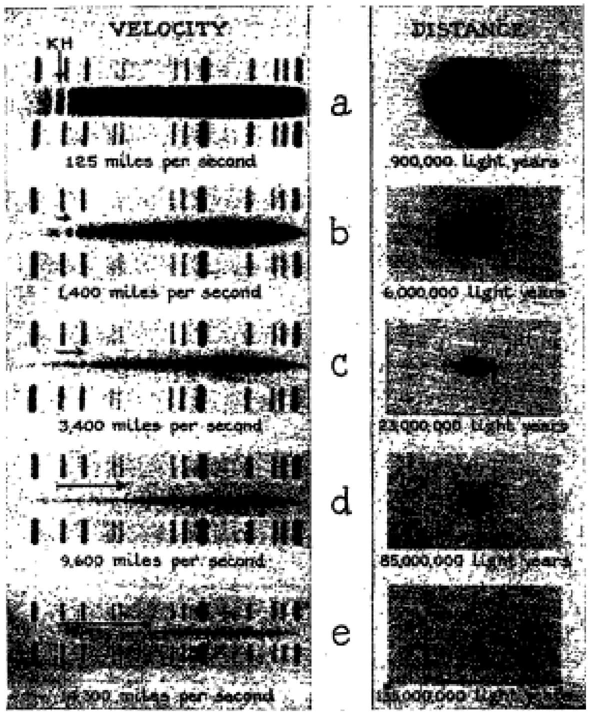

RED-SHIFTS IN SPECTRA OF EXTRA-GALACTIC NEBULAE
The arrows above the nebular spectra point to the H and K lines of calcium and show the amounts these lines are displaced toward the red end of the spectra. It is these red-shifts (interpreted as velocities of recession) which indicate the universe is expanding. The direct photographs (on the same scale and with approximately the same exposure times) illustrate the decrease in size and brightness with increasing velocity in passing to more and more distant objects. The nebulae illustrated are (a) NGC 221, (b) NGC 4473, (c) NGC 379, (d) nebula in Ursa Major I cluster, and (e) nebula in Gemini I cluster.

Humason, M. L. *ApJ*, **83,** 10, 1936

PLATE III

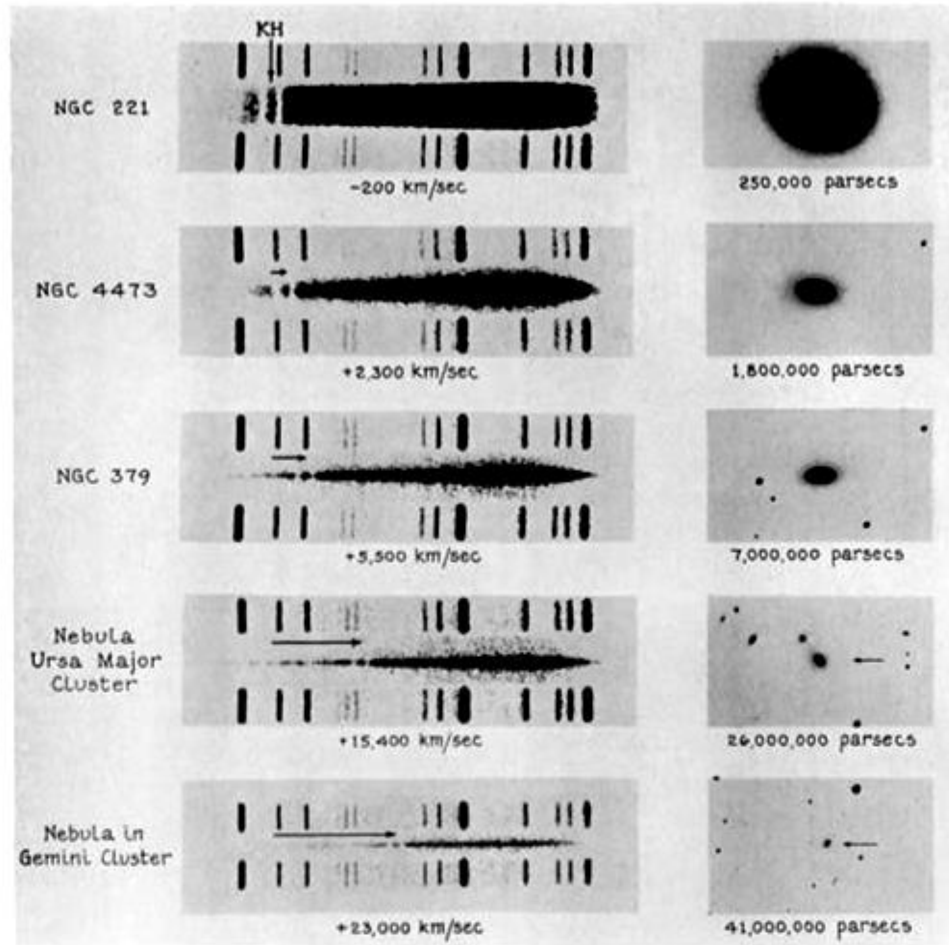

RED-SHIFTS IN THE SPECTRA OF EXTRA-GALACTIC NEBULAE

Arrows above the spectra (enlarged twenty times from the original negatives) point to the H and K lines of calcium and show the amounts these lines are displaced toward the red. The comparison spectra are of helium.

The direct photographs (on the same scale and with approximately the same exposure times) illustrate the decrease in size and brightness with increasing velocity or red-shift.

NGC 4473 is a member of the Virgo Cluster; NGC 379 of a group in Pisces.

Standard Candles:

Cepheids, RR-Lyraes, R-giants, Globular clusters, Novae etc.

M-m => Distance

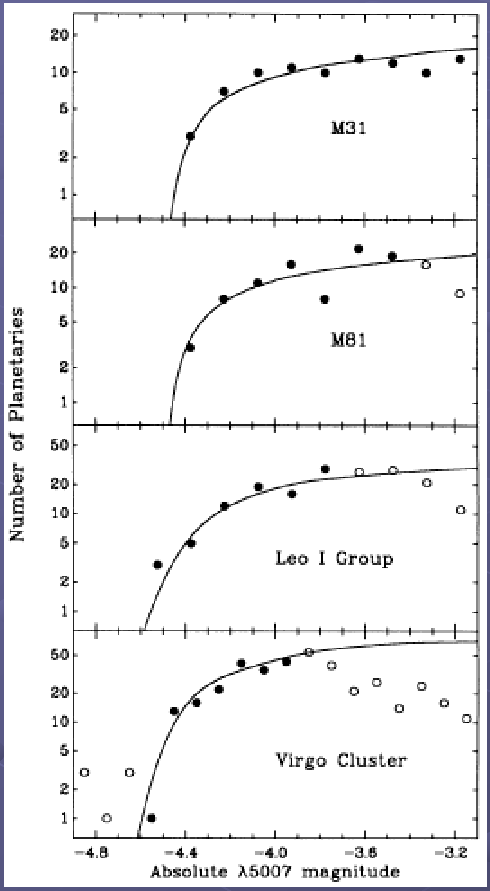

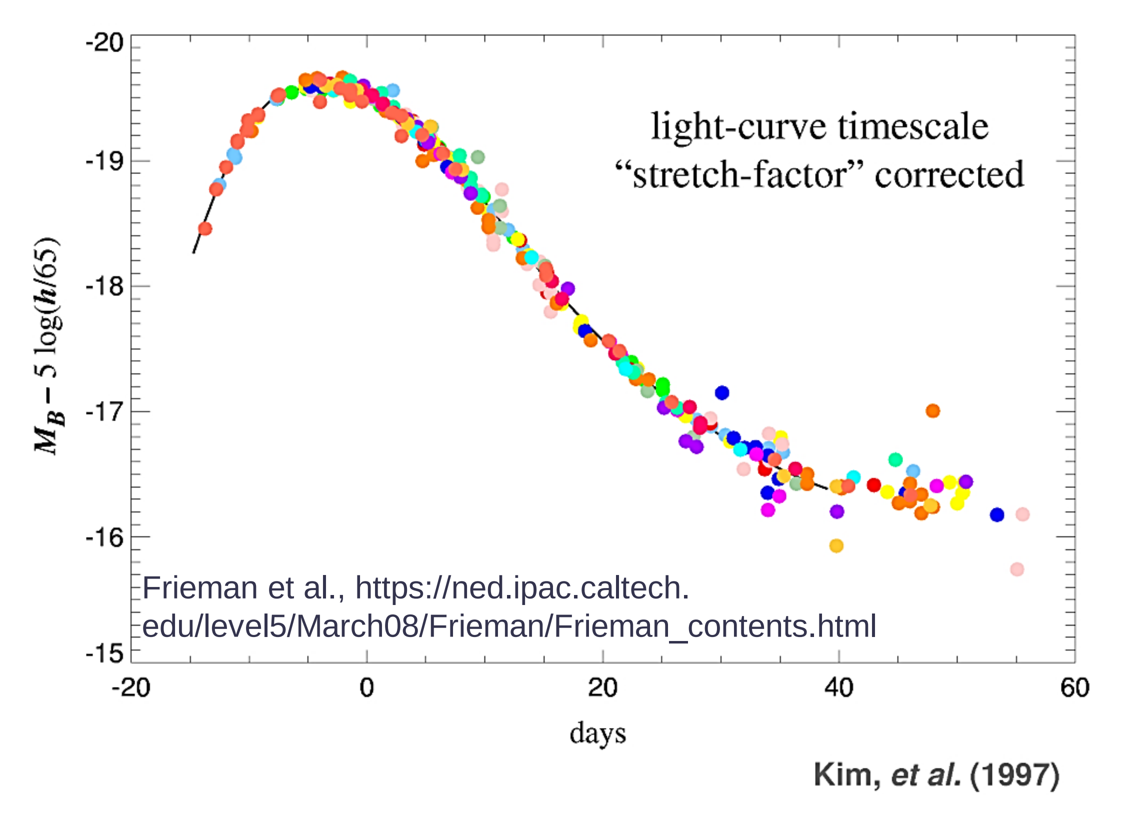

Planetary Nebula Luminosity Function: PNLF distances do not depend strongly on the properties of the underlying stellar population.

SN *Ia:* the light curves are identical.

The Tully-Fisher Relation, for disc galaxies

(A&A **54**, 661, 1977)

For self-gravitating systems:

$$\mathcal{M} = \frac{k}{G} W^2 R$$

$\mathcal{M}$ — the mass;

W — characterization of the motions in the body (in units of speed), dominated by rotation in the case of a disk galaxy;

R — linear size;

G — universal gravitational constant;

k — dimensionless constant (~1) that depends on the geometry of the system.

If M/L is the mass-to-luminosity ratio and $L \sim ld^2$ then TF relation is

$$L \sim W^{\alpha}$$

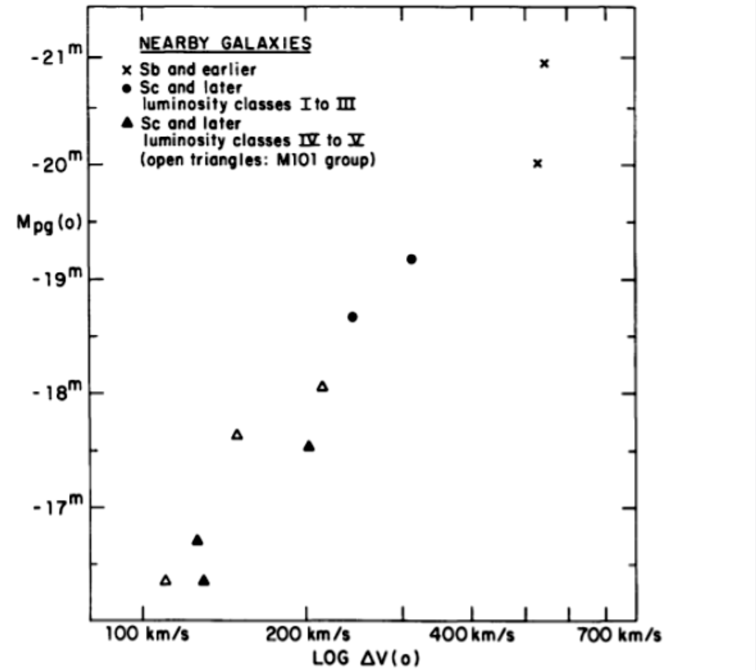

Fig. 1. Absolute magnitude – global profile width relation for nearby galaxies with previously well-determined distances. Crosses are M31 and M81, dots are M33 and NGC 2403, filled triangles are smaller systems in the M81 group and open triangles are smaller systems in the M101 group

More, α varies:

α =3.0 in B band (λ=4000 Å),

α =3.2 in I band (λ =8000 Å),

α =4.2 in H band (λ =12000 Å)

Faber–Jackson relation for elliptical galaxies

(ApJ, **204**, 668, 1976)

The Faber–Jackson relation: from theory: $L \sim \sigma^4$

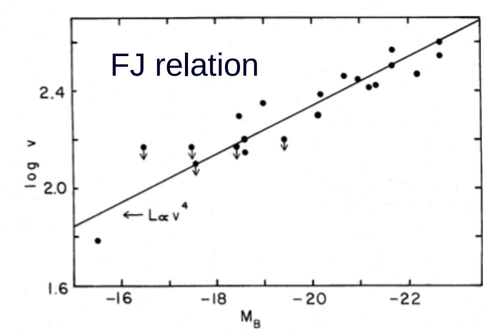

FIG. 16.—Line-of-sight velocity dispersions versus absolute magnitude from Table 1. The point with smallest velocity corresponds to M32, for which the velocity dispersion (60 km s^{-1}) was taken from Richstone and Sargent (1972).

In reality $L \sim \sigma^\alpha$ (α can be from 3.1 for the less massive galaxies to 15 for the more massive ones.

Modification of FJ relation:
Fundamental plane

FP is the relationship between 3 parameters: the effective radius, average surface brightness and central velocity dispersion of normal elliptical galaxies

FP relationship can be used as D_n–σ_0 correlation.

The two planes are inclined by about 11°. M_V=-23^m.04 (Gudehus, D. ApJ, **382**, 1, 1991)

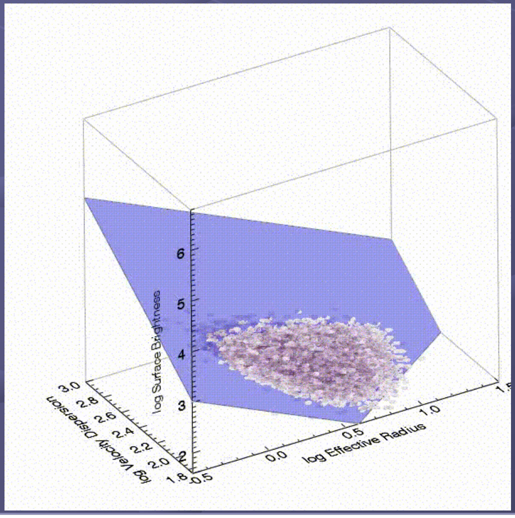

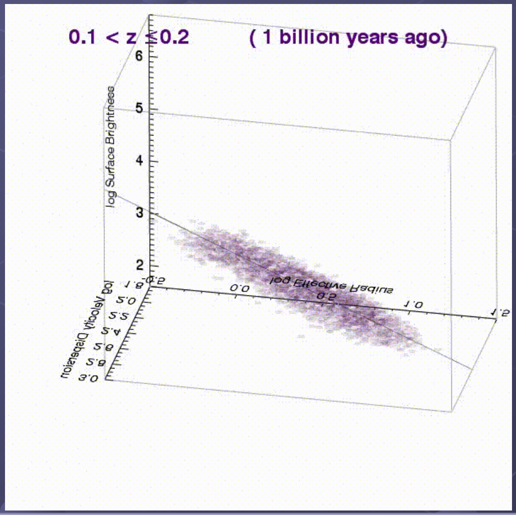

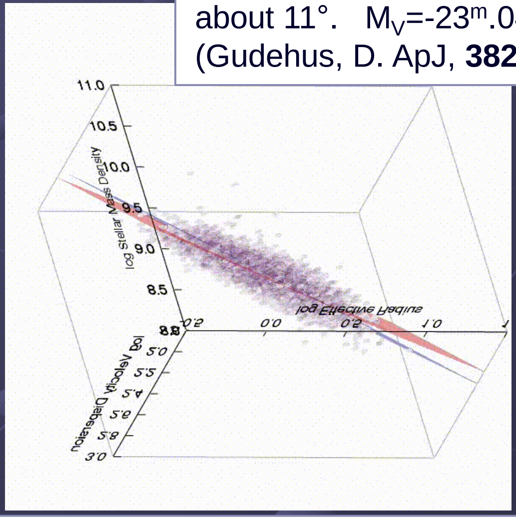

3-D Movies of the Fundamental Plane and Mass Fundamental Plane Courtesy: Rachel Bezanson

Open image

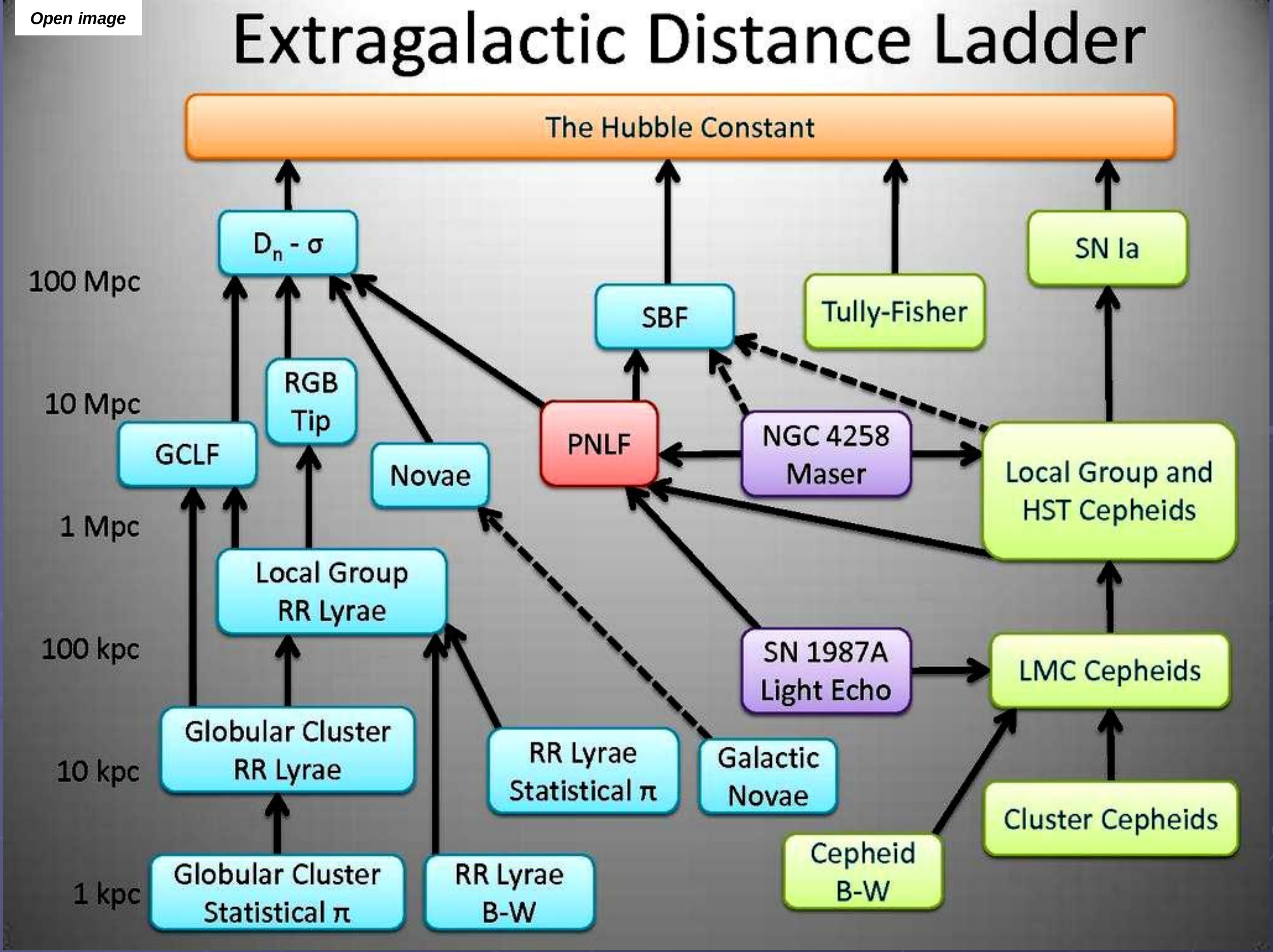

Green: applicable to star-forming galaxies. Blue: applicable to Population II galaxies. Purple Geometric distance technique. Red: PNLF is applicable to all populations of the Virgo Supercluster. Solid lines: Well calibrated ladder step. Dashed lines: Uncertain calibration ladder step.

What does mean "to measure distance"? How fare is it?

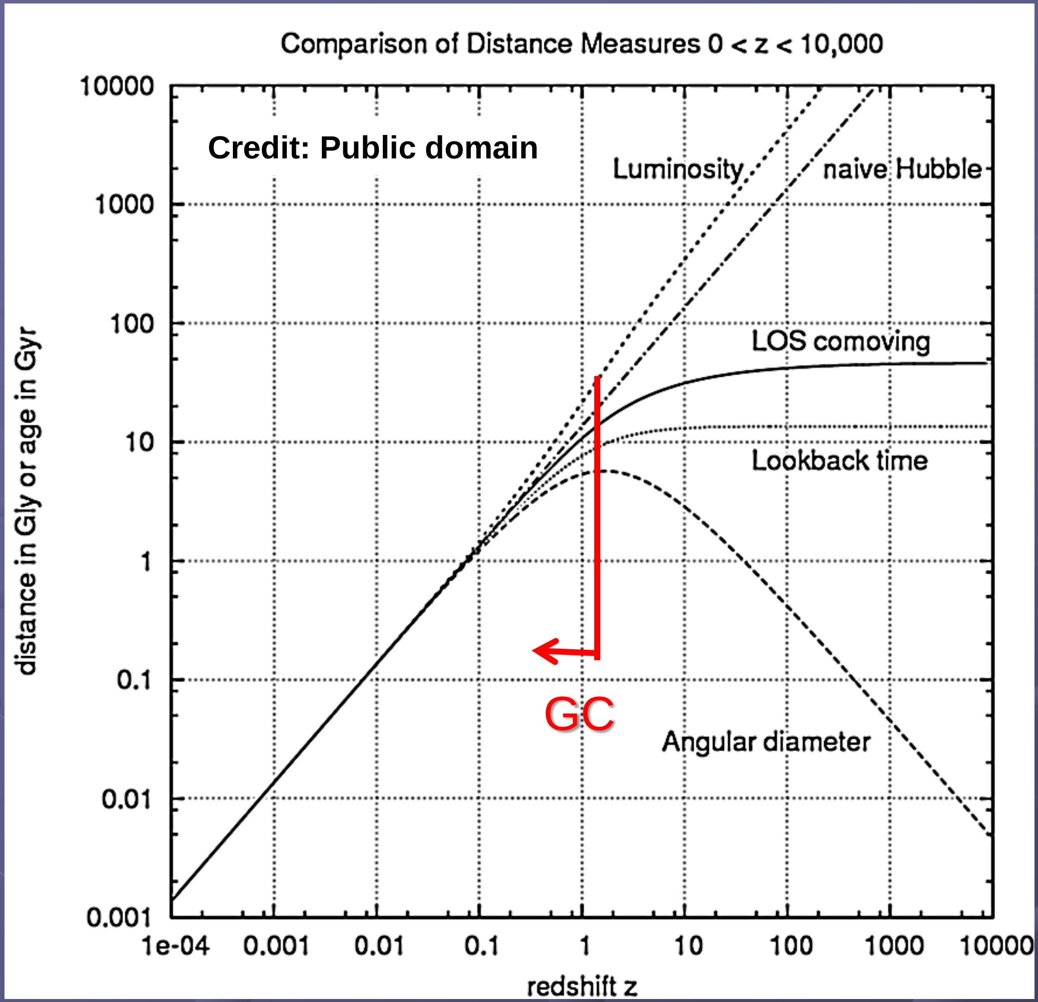

H_0= 72 km/s/Mpc, Ω_Λ=0.732, Ω_{matter}=0.266, $\Omega_{radiation}$ =0.266/3454 and, and Ω_k chosen so that the sum of Omega parameters is one.

The proper distance roughly corresponds to where a distant object would be at a specific moment of cosmological time, which can change over time due to the expansion of the universe.

The comoving distance between fundamental observers (moving with the Hubble flow) does not change with time.

Comoving distance and proper distance are defined to be equal at the present time (the scale factor is equal to 1. At other times, the scale factor differs from 1. The Universe's expansion results in the proper distance changing, while the comoving distance is unchanged by this expansion..

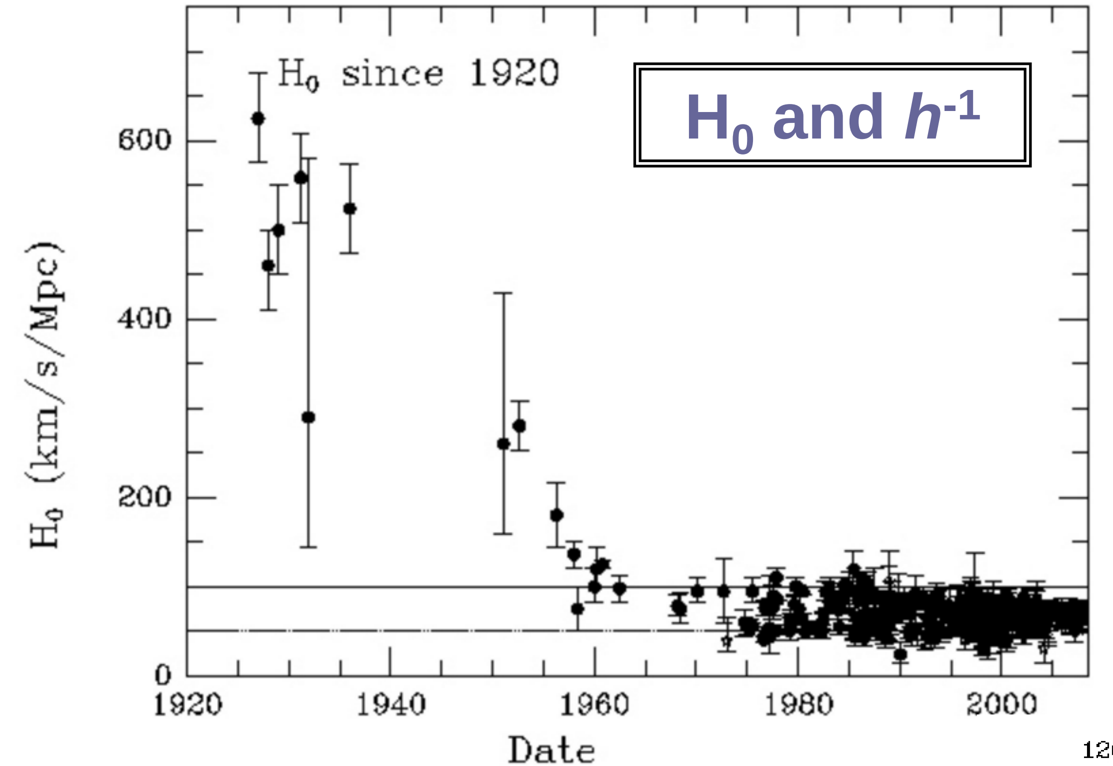

H_0 and h^{-1}

The evolution of our knowledge of the Hubble Constant, since it was first determined by Lemaitre, Robertson and Hubble in the late 1920's. Lundmark data is not shown.

H_0 value can be powerful constraint on the cosmological models.

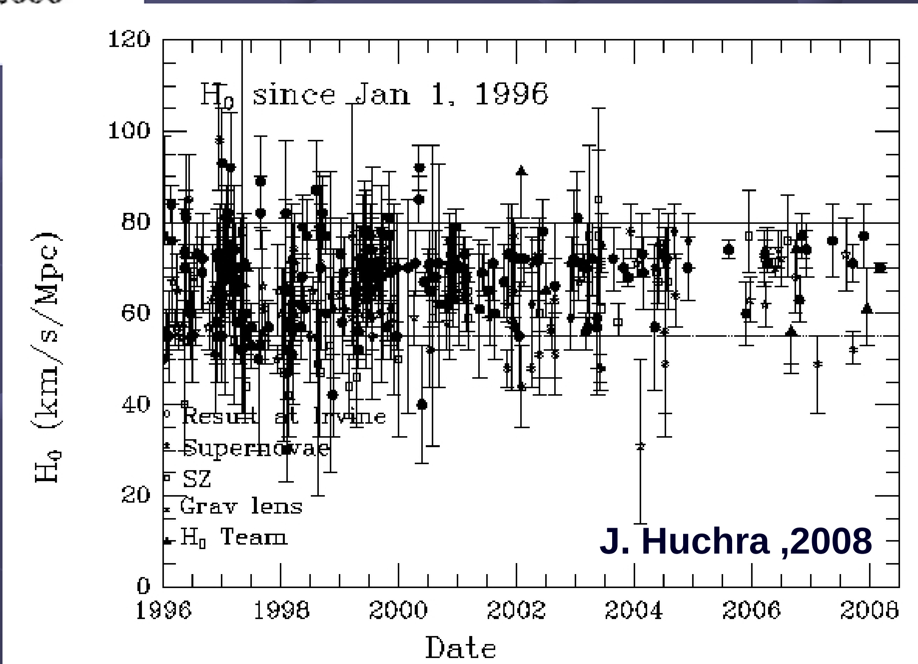

https://www.cfa.harvard.edu/~dfabricant/huchra/hubble/

The modern situation with H_0 is analyzed by Freedman (arxiv:1706.02739).

The blue and red shaded regions show the evolution of the uncertainties in H_0 values. At present measurements disagree is greater than 3-σ.

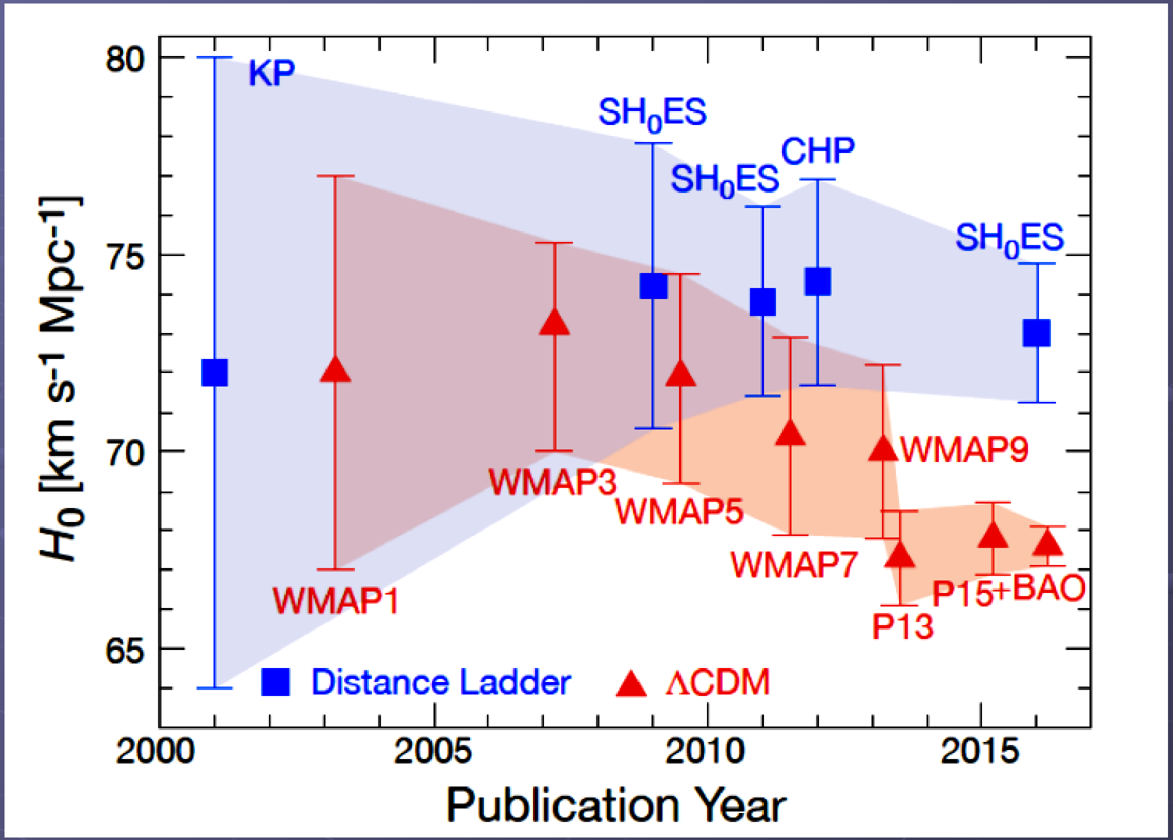

At present we have values:

72 km/s/Mpc (Freedman et al. 2012; Humphreys et al. 2013; Riess et al. 2016; Bonvin et al. 2017)

and (over 3-σ discrepant)

68 km/s/Mpc (baryon acoustic oscillations in combination with SNe Ia, Aubourg et al. 2015; Planck Collaboration 2016)

NED-D redshift-independent extragalactic distance methods

Standard Candles

AGN time lag
(BL Lac Luminosity)
Black Hole
Blue Supergiant
(BCG)
Stars (all variants)
Gamma-Ray Burst (GRB)
Globular Clusters
HII Luminosity Function
(HII LF)
Planetary Nebula
Luminosity Function
(PNLF)
Quasar spectrum
SNIa
Type II Supernovae,
Radio (SNII radio)

Total 43 SC

Standard Rulers

CO ring diameter
Dwarf Galaxy Diameter
Eclipsing Binary
Globular Cluster Radii (GC
radius)
Grav. Stability Gas. Disk
Gravitational Lenses
HII Region Diameters (HII)
Jet Proper Motion
Masers
Orbital Mechanics
Proper Motion
Ring Diameter
Type II Supernovae,
(Optical)

Total 13 SR

Secondary Methods

Diameter
Dwarf Ellipticals
Faber-Jackson (FP)
GC K vs. (J-K)
GeV TeV ratio
Globular Cluster (GC FP)
H I + optical distribution
IRAS
Magnitude
Mass Model
Radio Brightness
Tully Estimate
Tully-Fisher

Total 19

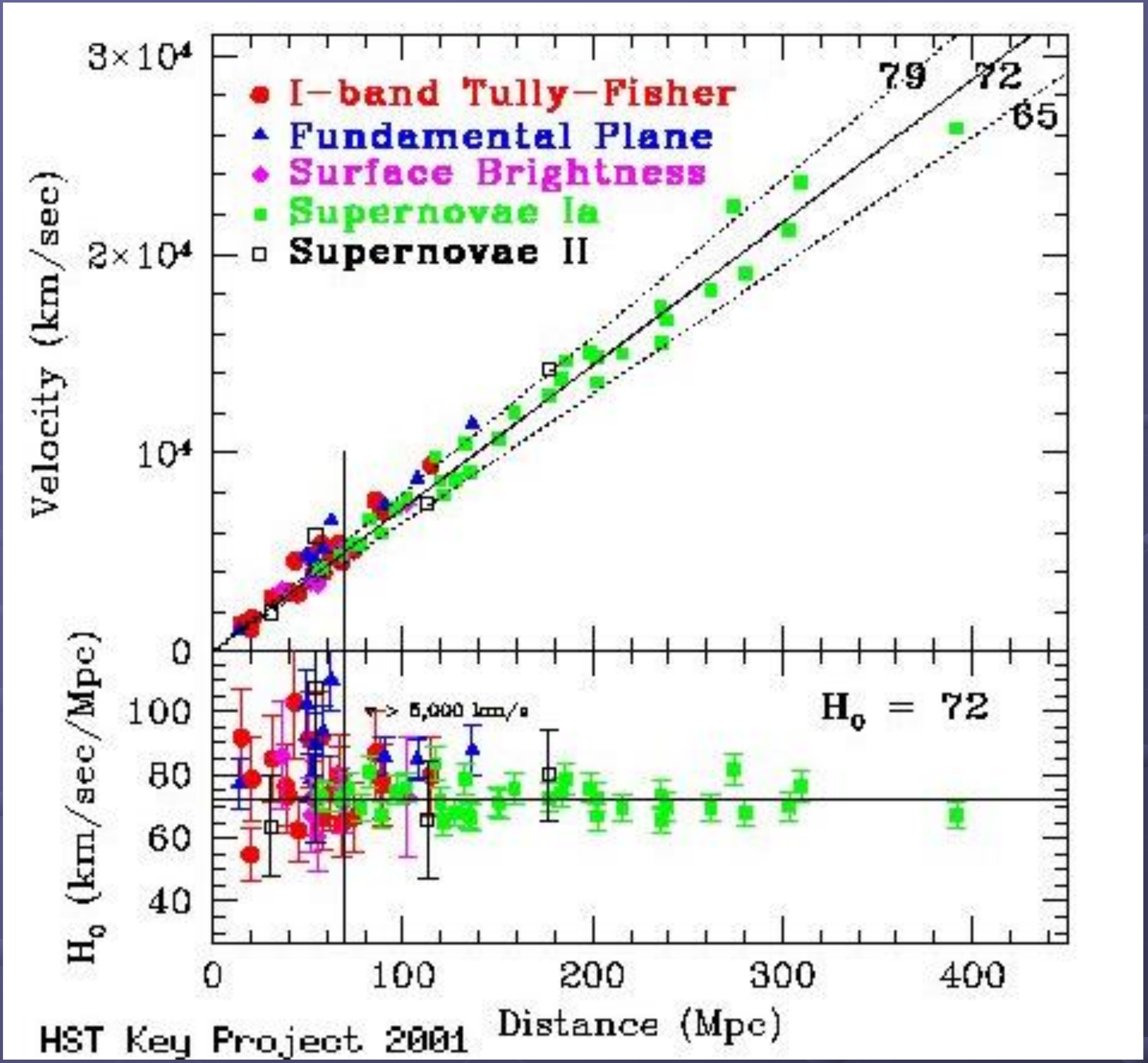

Freedman et al, 2001. Value of H_0 as a function of distance.
https://ned.ipac.caltech.edu/level5/Sept01/Freedman/Freedman_contents.html

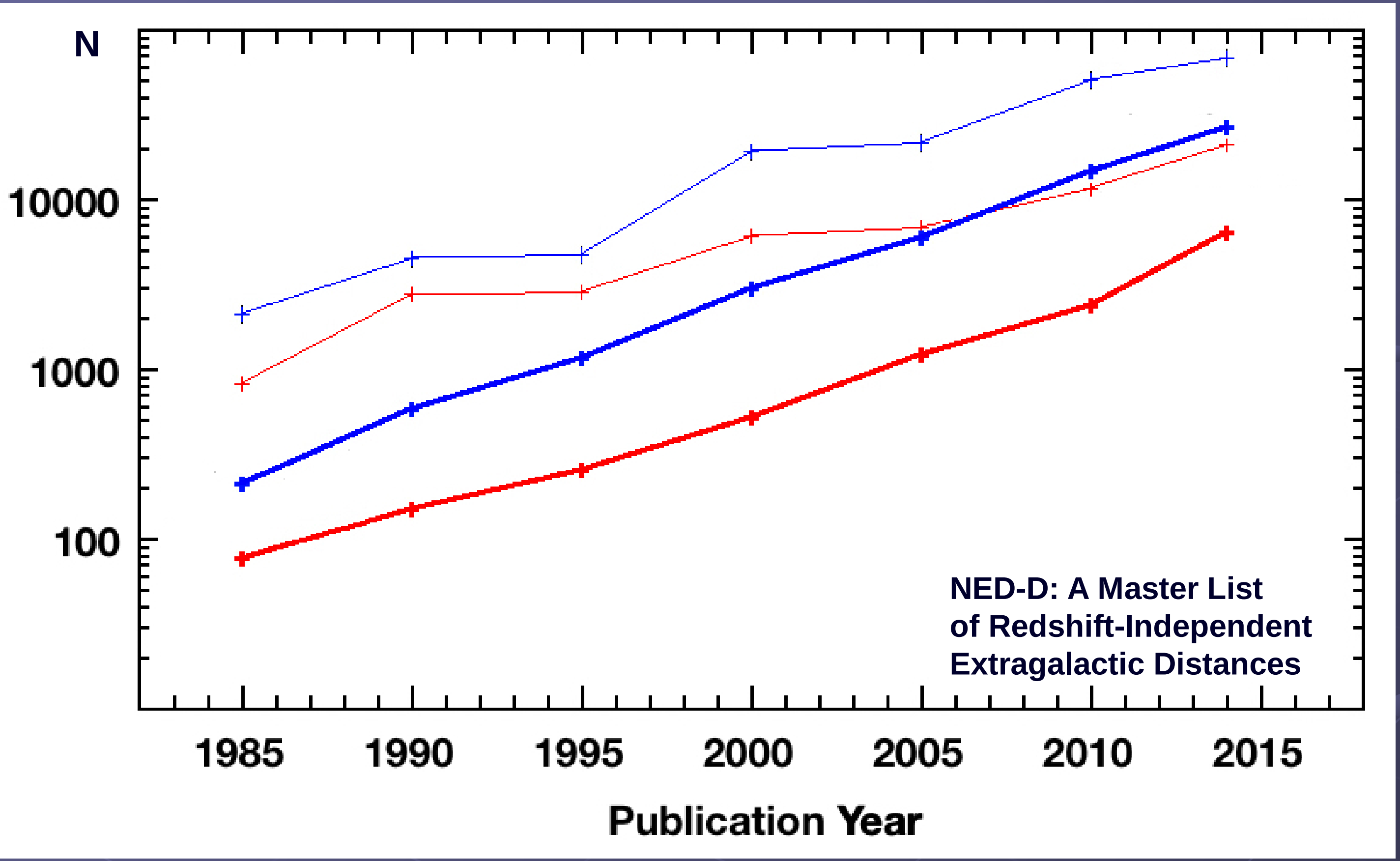

Growth in the number of individual redshift-independent distance estimates (blue), and the galaxies with such estimates (red), is shown for both primary indicators (thick lines) and secondary indicators (thin lines). Cumulative totals are shown for the end of each five-year period, except the most recent period which is current through 2014.

Modern situation

Wide-field digitized surveys and Automatic Procedure: objective search galaxy "overdense" regions

Pencil-beam observations (deep fields)

Red shift surveys

X-ray surveys

Numerical simulations!

Mock catalogues

Total area on sky ~ 4300 deg²

250,000 galaxies in total,

Mean redshift <z> ~ 0.1

Blue

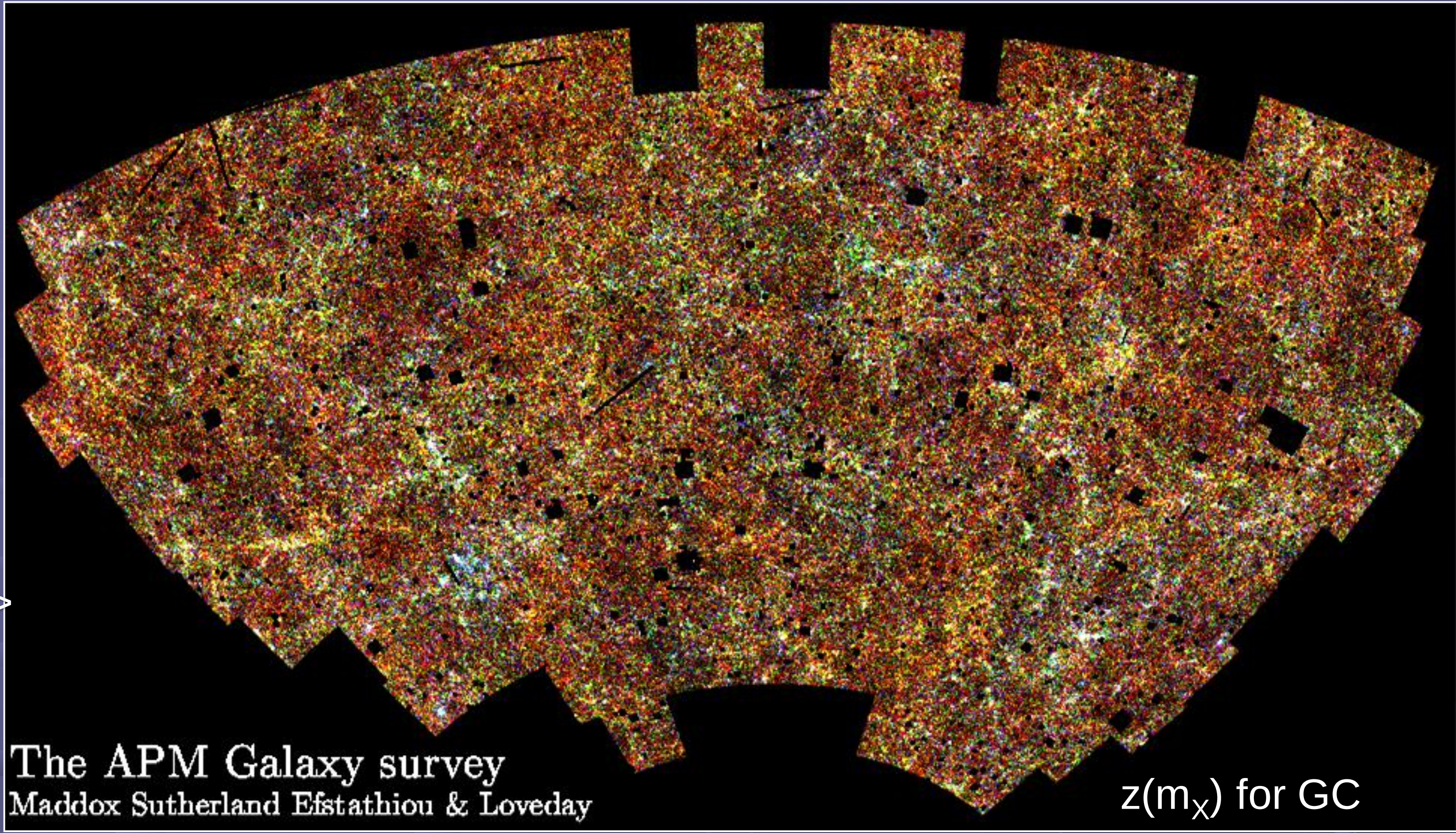

APM (Automatic Plate Measuring Machine). Main effort : scanning of UK Schmidt plates The first objective catalogue of clusters: Dalton G.B., Croft R.A.C., Efstathiou G. et al., *Mon. Not. R. Astron. Soc.* **271** L47 (1994)

z for galaxy clusters is estimated according to m_{10} value

Last 2*D* optical search for clusters: The Muenster Red Sky Survey. It covers an area of about 5000 deg^2 on the southern hemisphere. The catalogue includes 5.5 millions <u>confirmed</u> galaxies and is complete till to r_F=18^m.3 (Ungruhe, 1999). It's a result of scanning of 217 plates of Southern Sky Atlas R (ESO) by PDS 2020GM$_{plus}$ and automated recognition of galaxies with careful control.

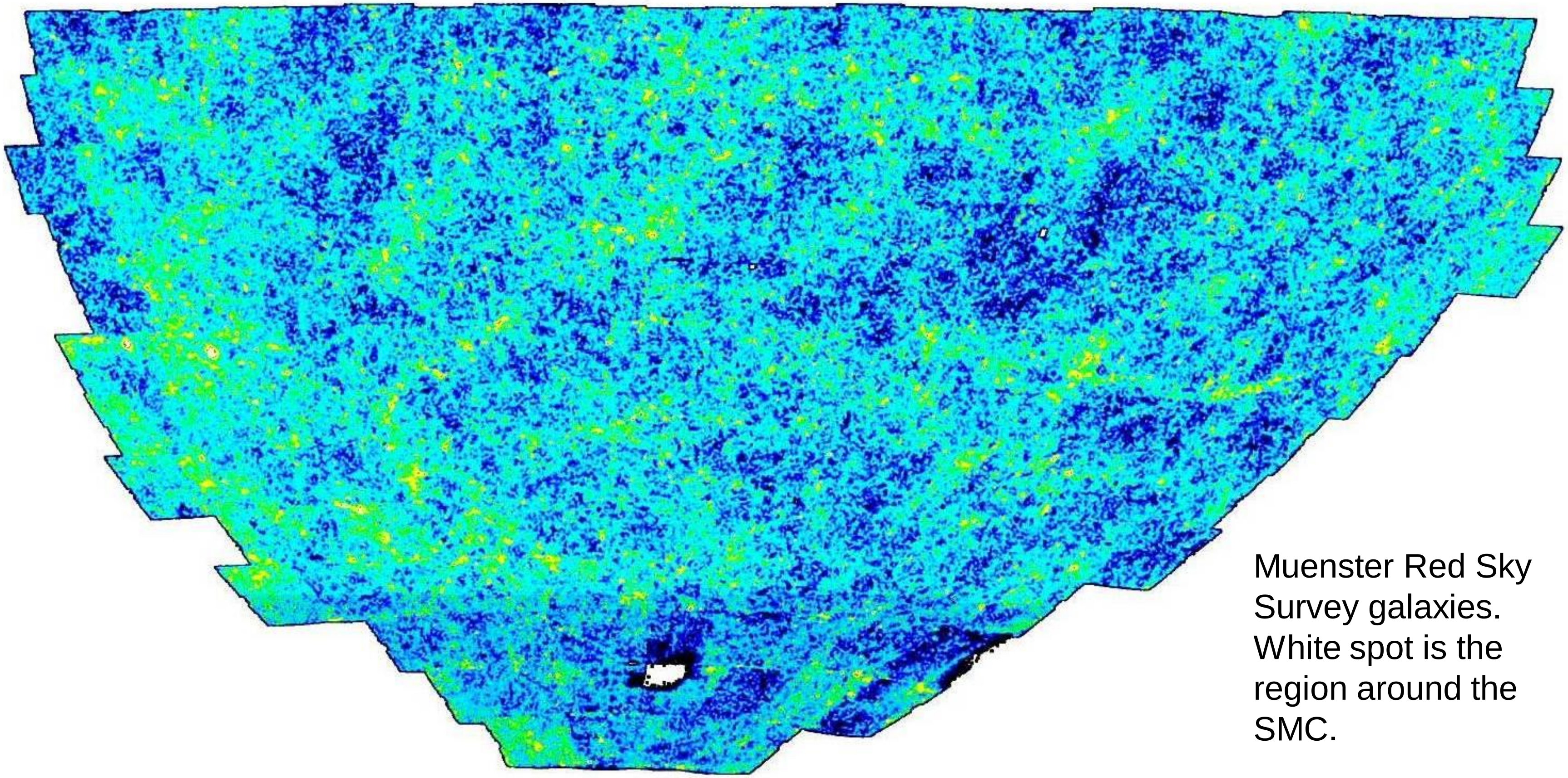

Muenster Red Sky Survey galaxies. White spot is the region around the SMC.

Galaxy clusters of MRSS (Panko & Flin, 2006)

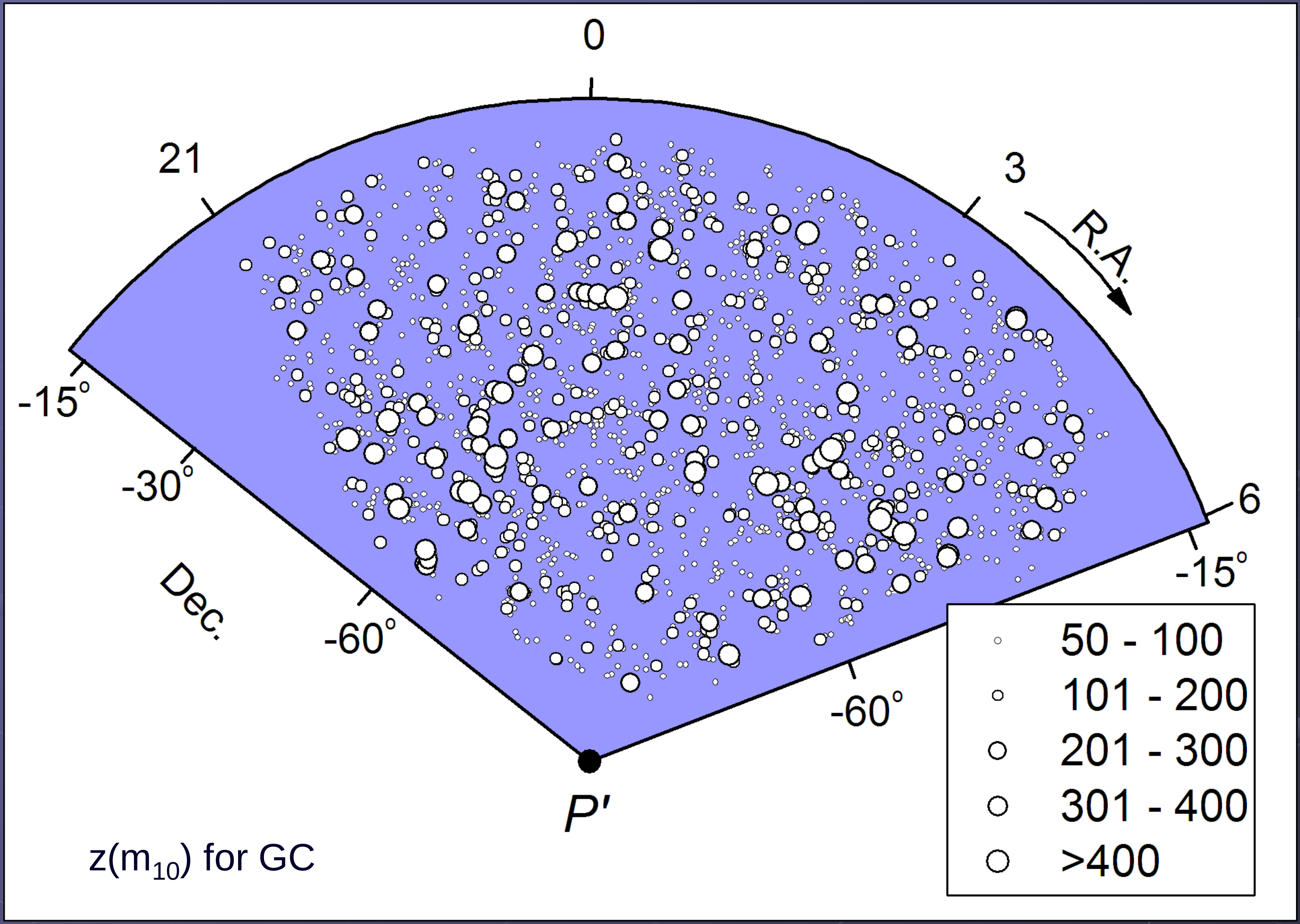

The data set allows to trace the development of galaxy clusters evolution changes. z galaxy clusters is estimated according to m_{10} value

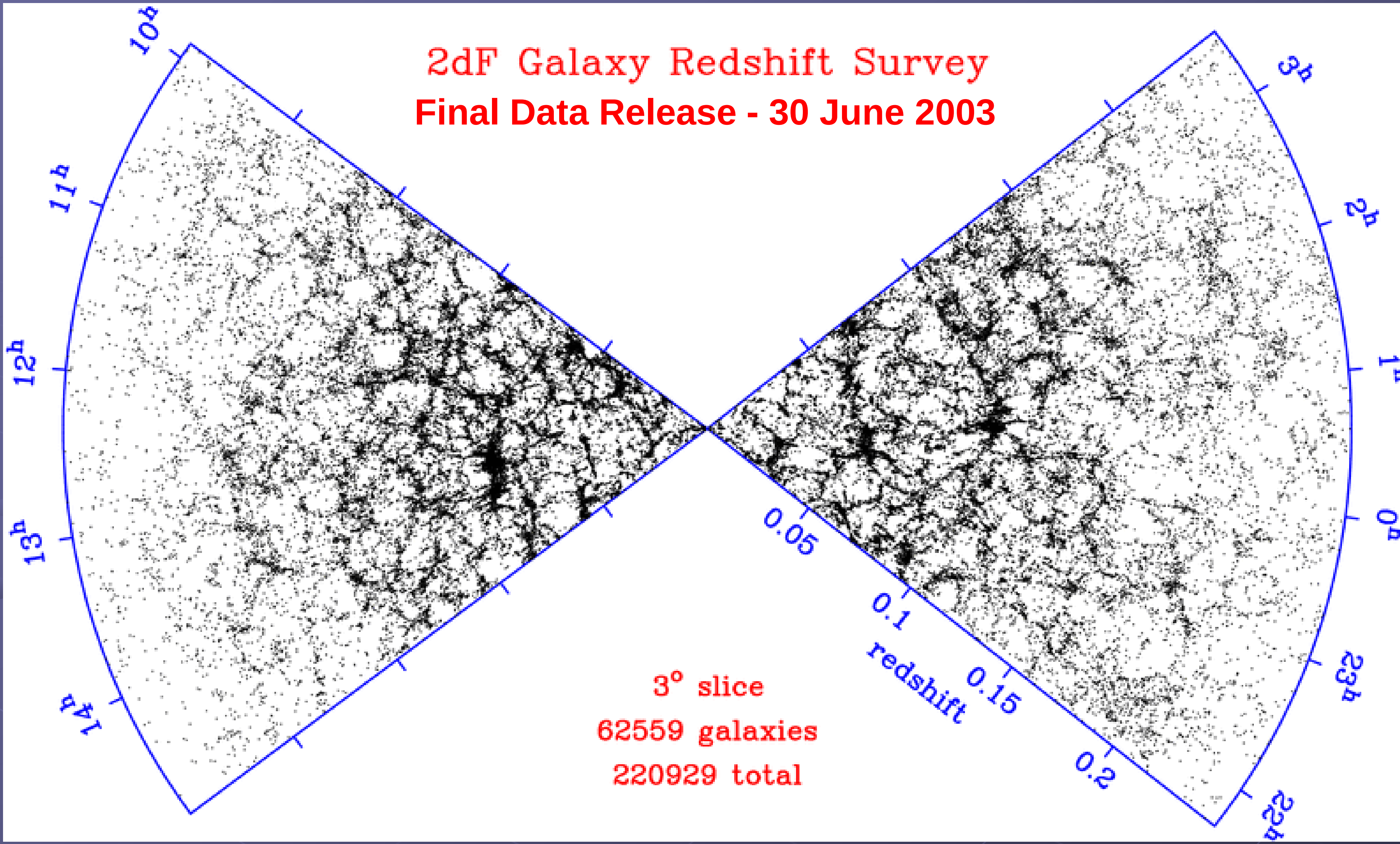

2dF Galaxy Redshift Survey
Final Data Release - 30 June 2003
3° slice
62559 galaxies
220929 total
redshift
0.05
0.1
0.15
0.2
10h
11h
12h
13h
14h
3h
2h
1h
0h
23h
22h

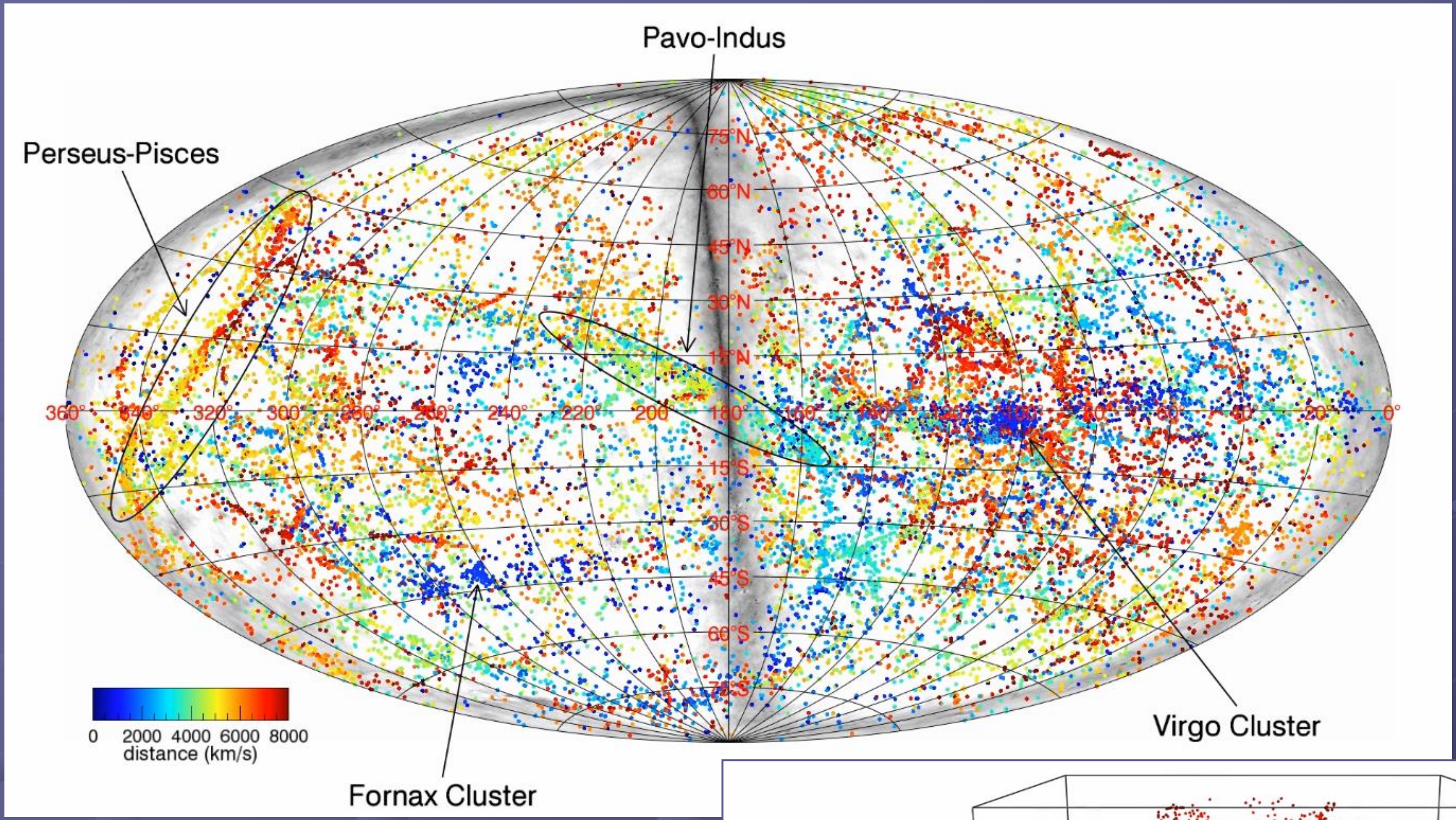

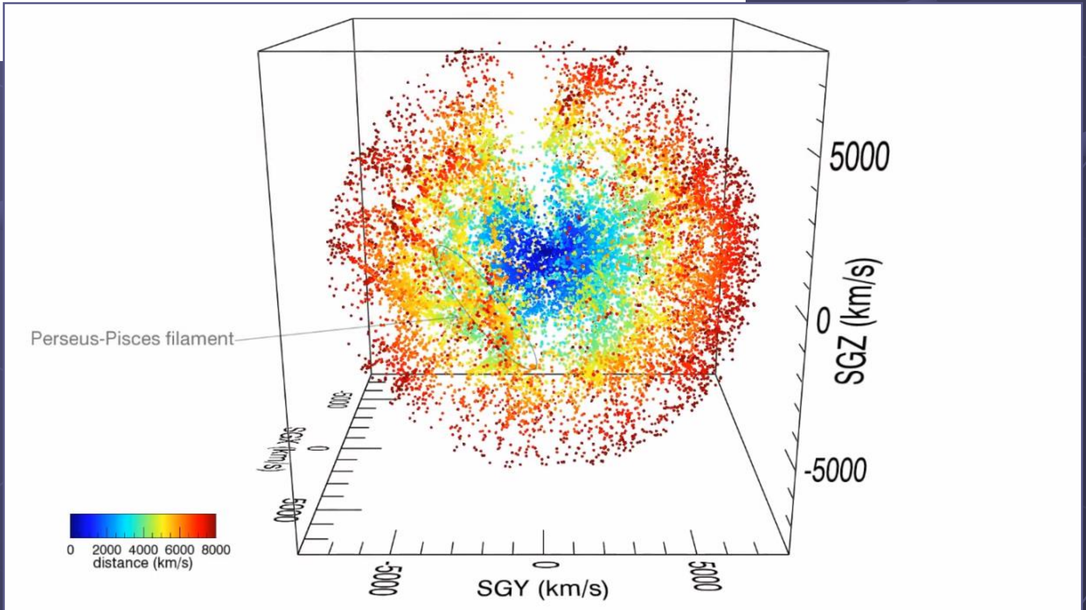

Cosmic-flows-3

Courtesy H. Courtois et al.

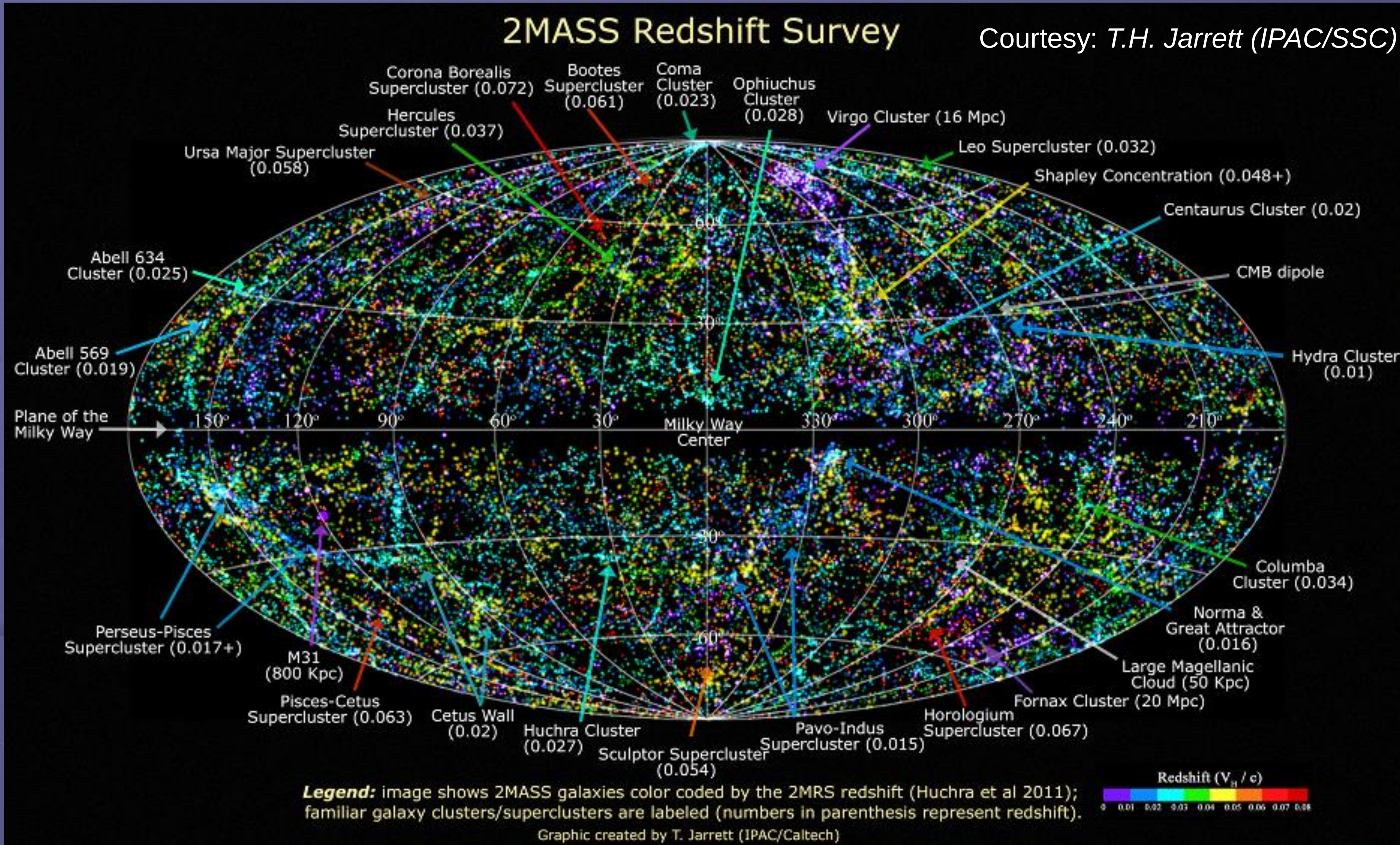

The Infrared Local Universe: 2MASS Redshift Survey. Measured redshifts of 44 000 galaxies. Colors coded by galaxy distances: violet ones are nearest (0 < z < 0.01), red ones are distant (0.08 < z < 0.09). Crook et al. in 2007 identified groups and clusters in the complete $11^m.25$, mag limited 2MASS (*ApJ*, **655**, 790).

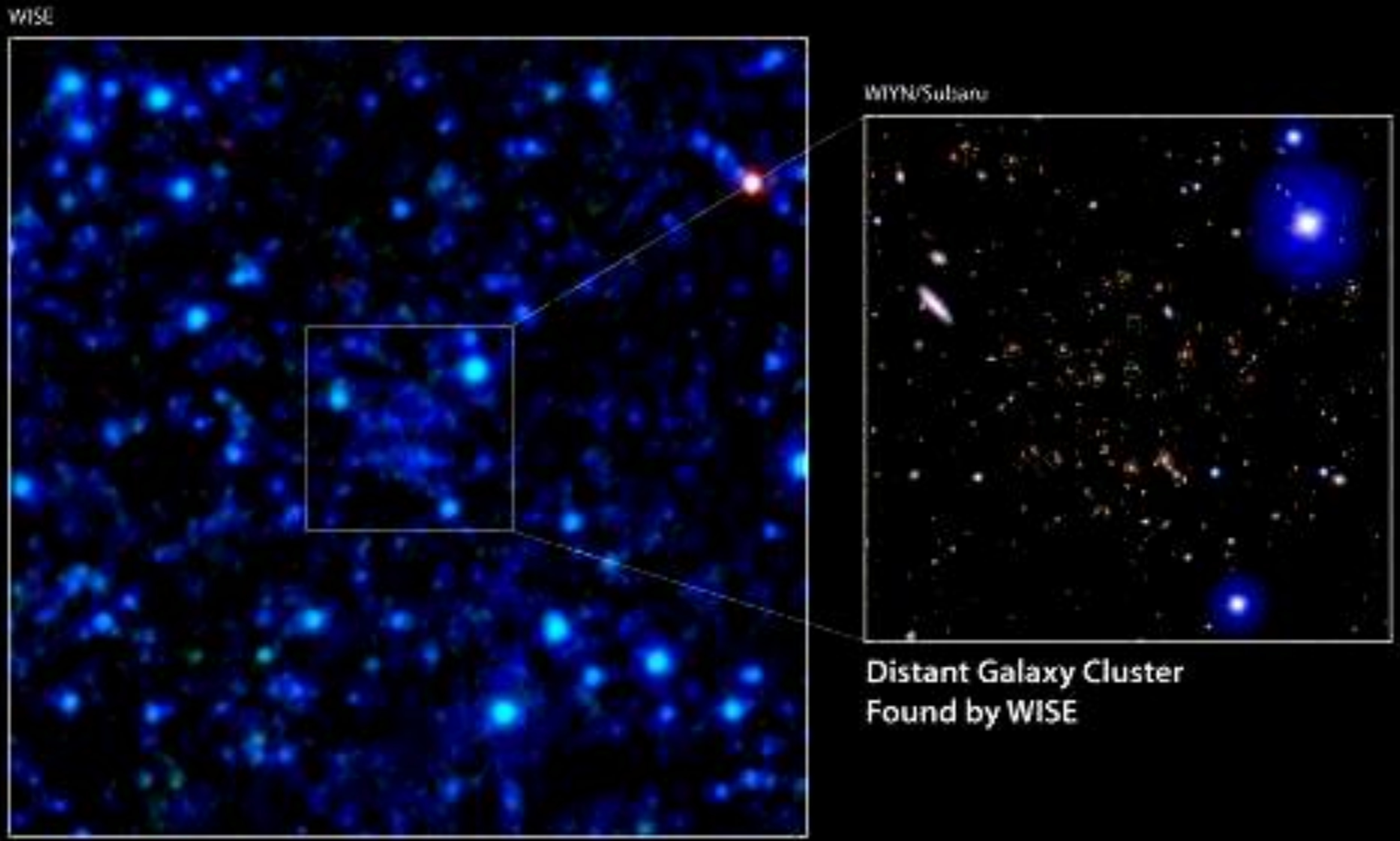

Image credit: NASA/JPL-Caltech/UCLA/WIYN/Subaru

A galaxy cluster 7.7 Gy away has been discovered using infrared data from NASA's Wide-field Infrared Survey Explorer (WISE).

SDSS-IV: Current Surveys (2014-2020)
Data Release 14

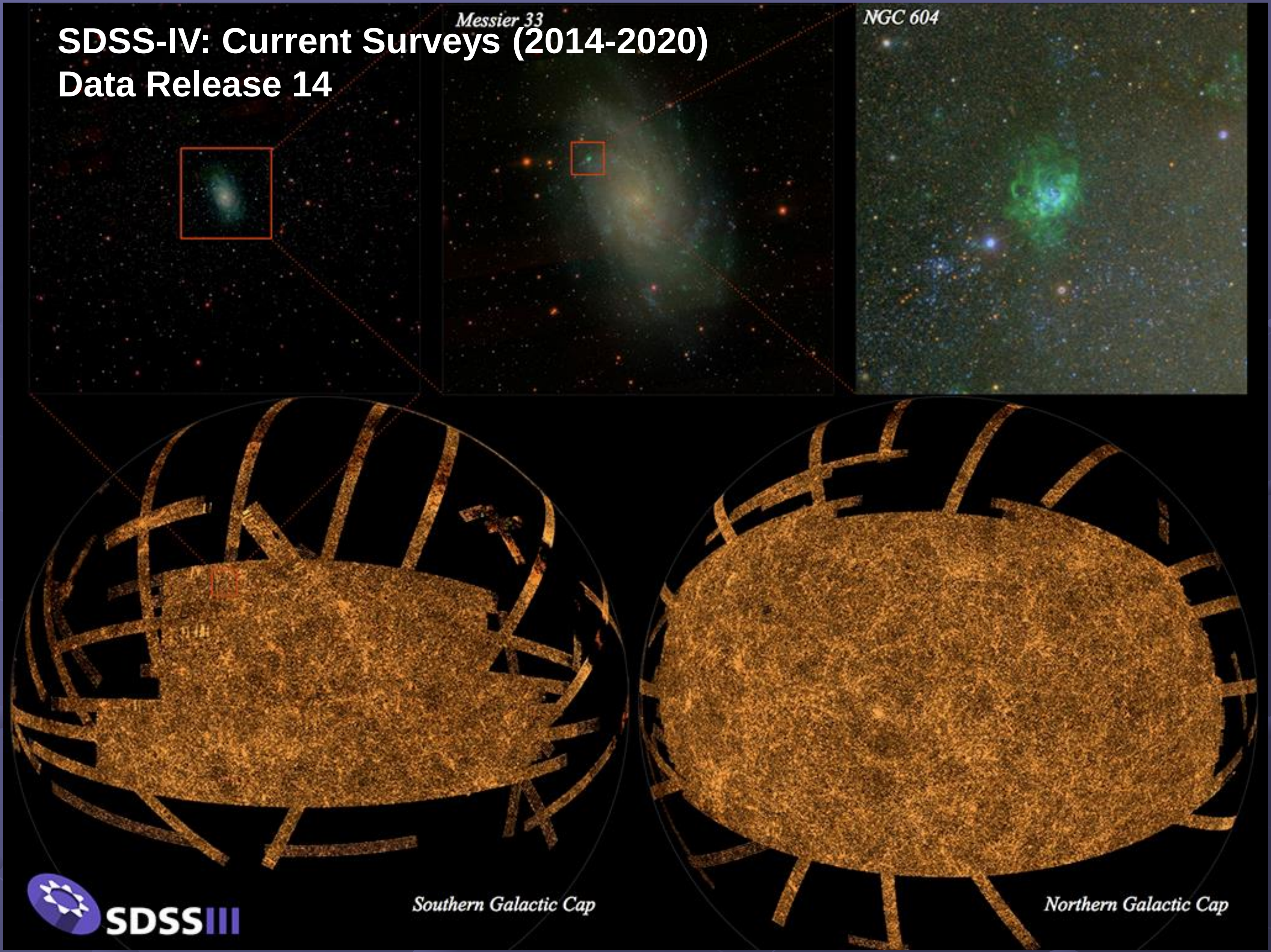

Galaxy distribution, SDSS

We can see "overdense" regions

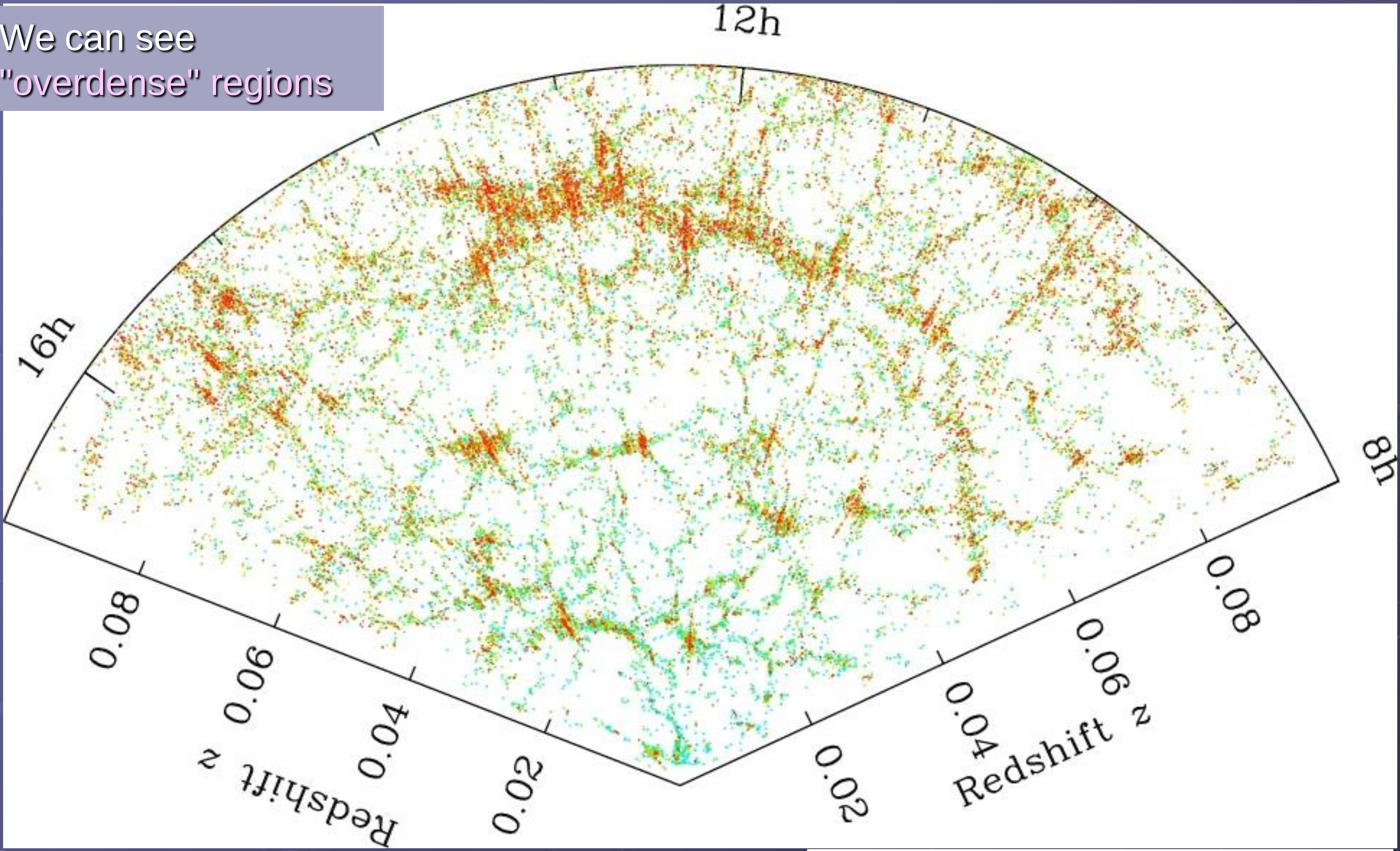

Credit: M. Blanton and the SDSS.

The four principal constituents of clusters include:

- Galaxies;
- Intracluster Stars; } vis
- Hot Gas/ Intra cluster medium, ICM; } baryon
- Dark Matter.

Clusters continue to grow (and form), even today.

Methods of Identification of clusters

- Overdensity regions in surveys;
- X-ray Identification of rich clusters;
- SZ (Sunyaev-Zeldovich) effect;
- Weak Gravitational Lensing;
- Color Search for Red Galaxies

The physics of the principal constituents of clusters

- Galaxies

  ~10^2 large galaxies;

  >10^3 total galaxies

  Typical speeds ~10^3 km/s – allows to estimate the mass of cluster

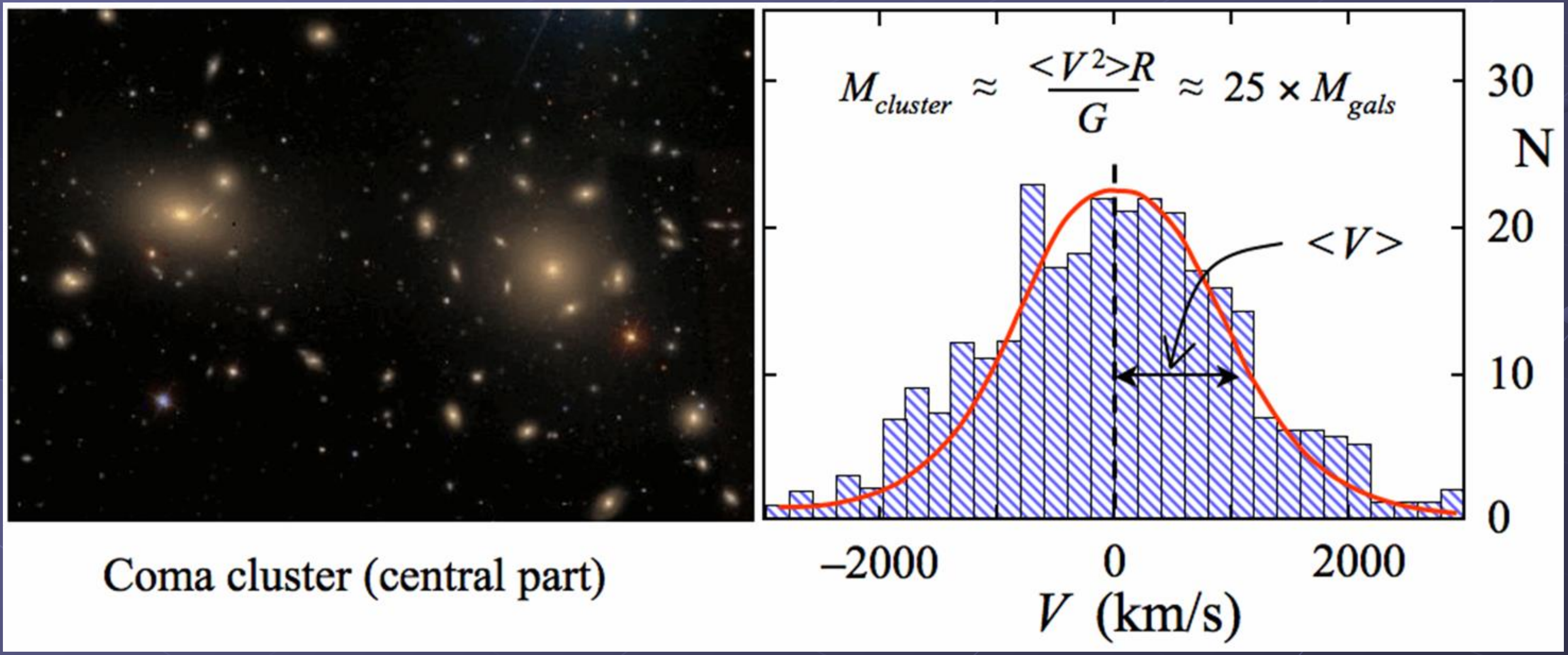

Coma cluster (central part)

The ensemble of thousands galaxies inside the cluster one can study statistically: luminosity function, mass function

Luminosity Functions

The luminosity function (*LF*) of galaxies in a cluster gives the number distribution of the luminosities of the galaxies. The integrated luminosity function $N(L)$ is the number of galaxies with luminosities greater than L, while the differential *LF* $(L)dL$ is the number of galaxies with luminosities in the range L to $L + dL$. Obviously, $n(L) \equiv -dN(L)/dL$. *LF* are often defined in terms of galaxy magnitudes $m \sim -2.5 \log_{10}(L)$; and $N(\leq m)$ is the number of galaxies in a cluster brighter than magnitude m. ≡

Sure, *LF* depends from Habble mix in cluster.

The Luminosity function contains information about :

- ✓ primordial density fluctuations;
- ✓ processes that destroy/create galaxies;
- ✓ processes that change one type of galaxy into another (eg mergers, stripping);
- ✓ processes that transform mass into light.

Real *LF* describes by Schechter function:

$$N(L)=N^*\Gamma(\alpha,L/L^*),$$

where L^* is a characteristic luminosity, $N^*\Gamma(\alpha,1)$, is the number of galaxies with $L > L^*$, $\Gamma(\alpha, x)$, is the incomplete gamma function, and $\alpha= 5/4$ for the faint end slope (Schechter,1976).

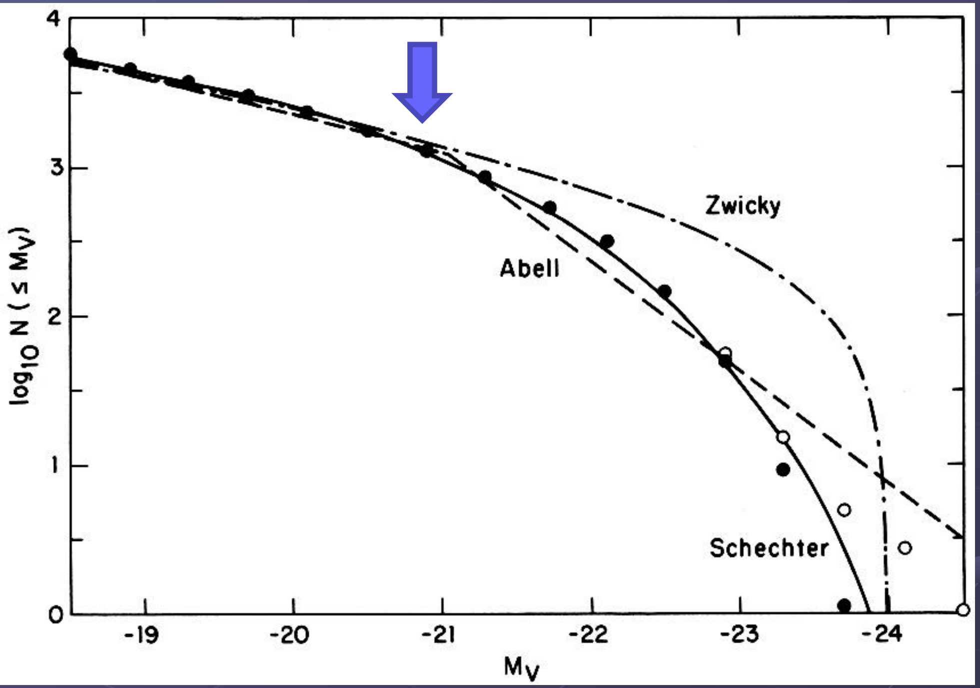

The Schechter function fits the observed distribution reasonably well from the faint
to the bright end, as long as the very brightest galaxies, the cD galaxies, are excluded.

Mass Functions

The observed mass function (*MF*), n(> M) of clusters of galaxies, which describes the number density of clusters above a threshold mass *M*, can be used as a critical test of theories of structure formation in the Universe. The richest, most massive clusters are thought to form from rare high peaks in the initial mass-density fluctuations; poorer clusters and groups form from smaller, more common fluctuations.

The observed cluster mass function in comparison with expectations from different *CDM* cosmologies using large-scale simulations (Bahcall and Cen, 1992). Observed *MF* is indeed a powerful discriminant among models.
A low-density CDM model, with Ω ~ 0.2-0.3 (with or without a cosmological constant), appears to fit well the observed cluster *MF*.

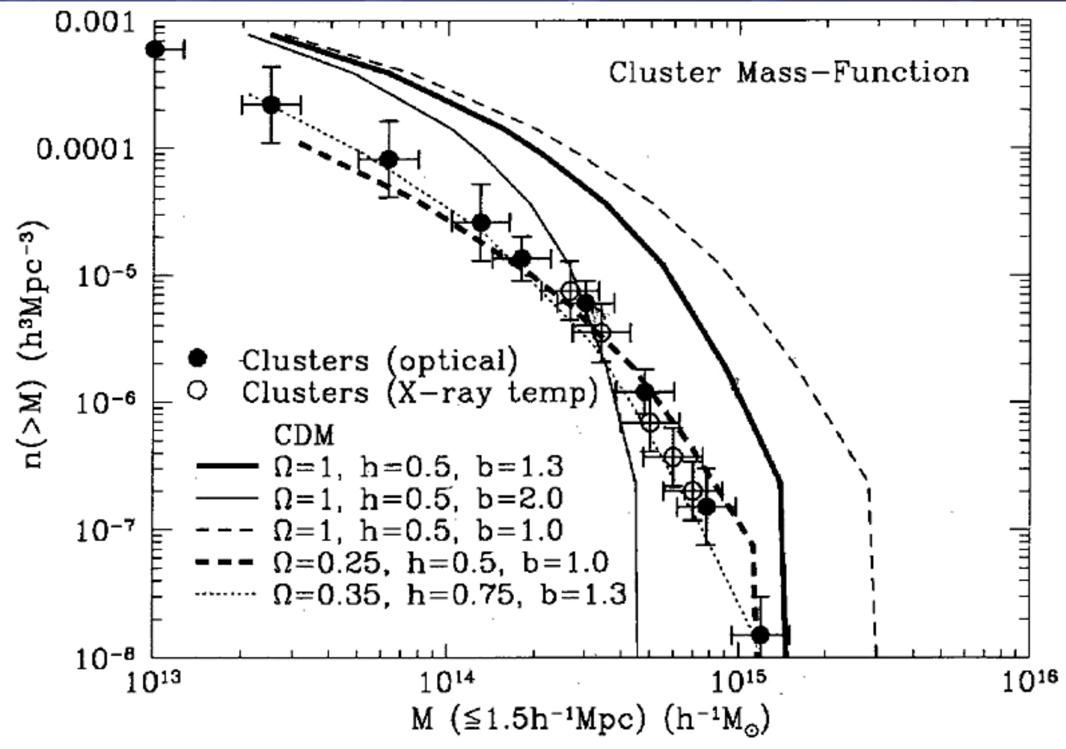

Bahcall, N. A., & Cen, R. 1992, *ApJ*, **398**, L81

Cluster Mass Function as cosmological probe

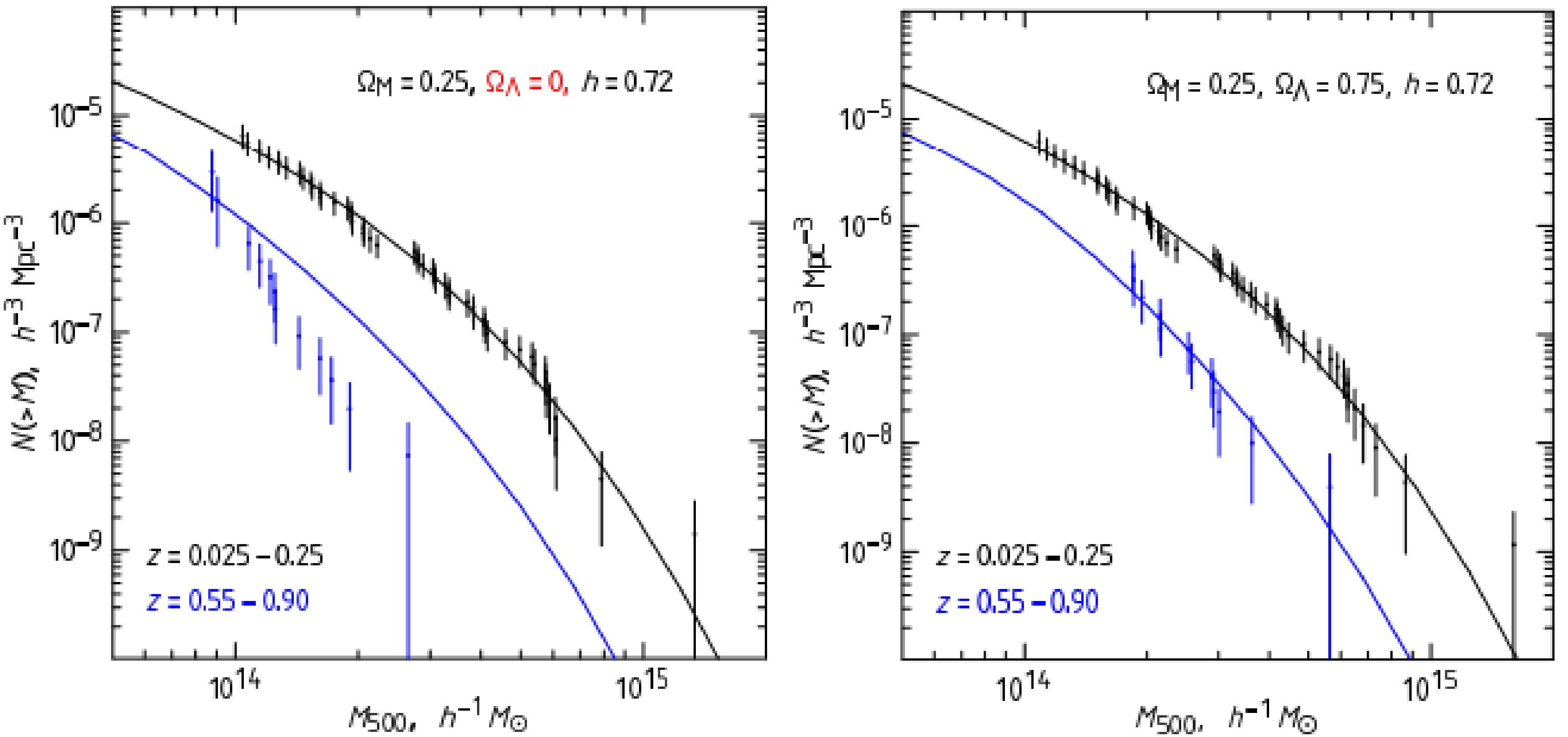

Example for the comparison of the observed cluster mass function with predictions from cosmological models. The data and the model are computed for $\Omega_\Lambda = 0$ in the left panel and for $\Omega_\Lambda = 0.75$ in the right one. The overall normalization is adjusted to $z = 0$.

From: Vikhlinin, A., Kravtsov, A. V., Burenin, R. A., et al. 2009, ApJ, 692, 1060

The physics of the principal constituents of clusters

- Intracluster Stars

very faint (~1% sky) diffuse light (distinct from c*D* halo light) comprises 10-50% total galaxy light (in rich clusters; much less in poor clusters) probably tidally stripped stars;

Wide angle view of most of the Virgo cluster from the DSS.

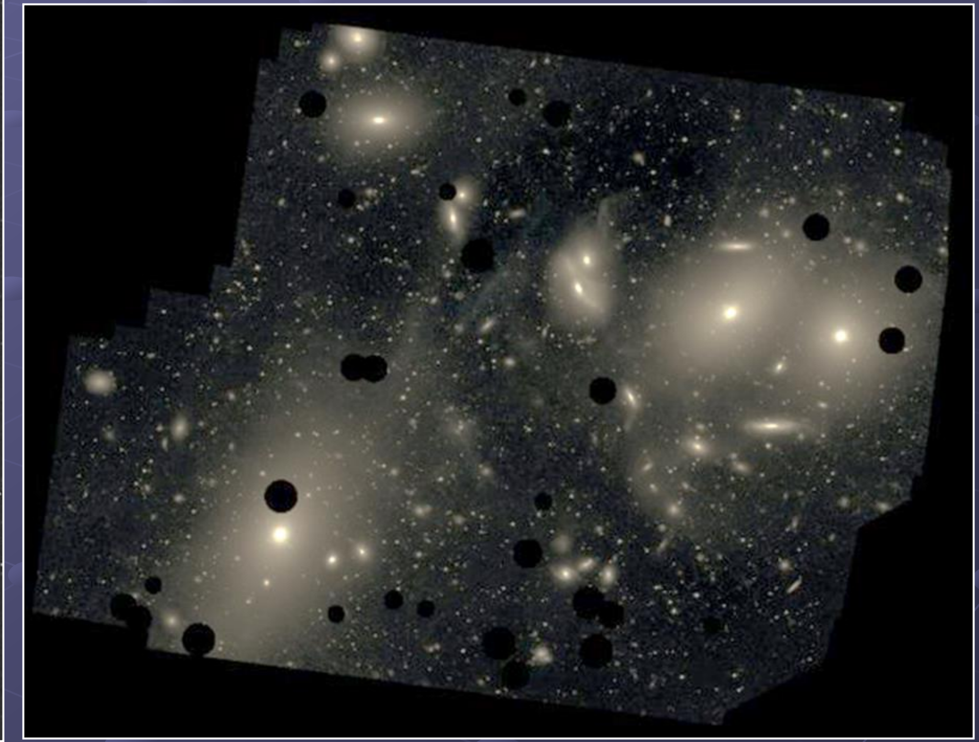

Deep image of Virgo by Chris Mihos et al, (2005) by Burrell Schmidt (bright stars removed). See also M. Doherty et al.: The M87 Halo and the Diffuse Light in the Virgo Core. A&A, 2009

The physics of the principal constituents of clusters

- <u>Dark Matter</u>

Dominates in the total mass:

$M_{DM} >\sim 4 \times M_{gas + gals}$

Taking into account

$M_{gas} \sim 5 \times M_{gals}$

$\boxed{M_{DM} > \sim 24 \times M_{gals}}$

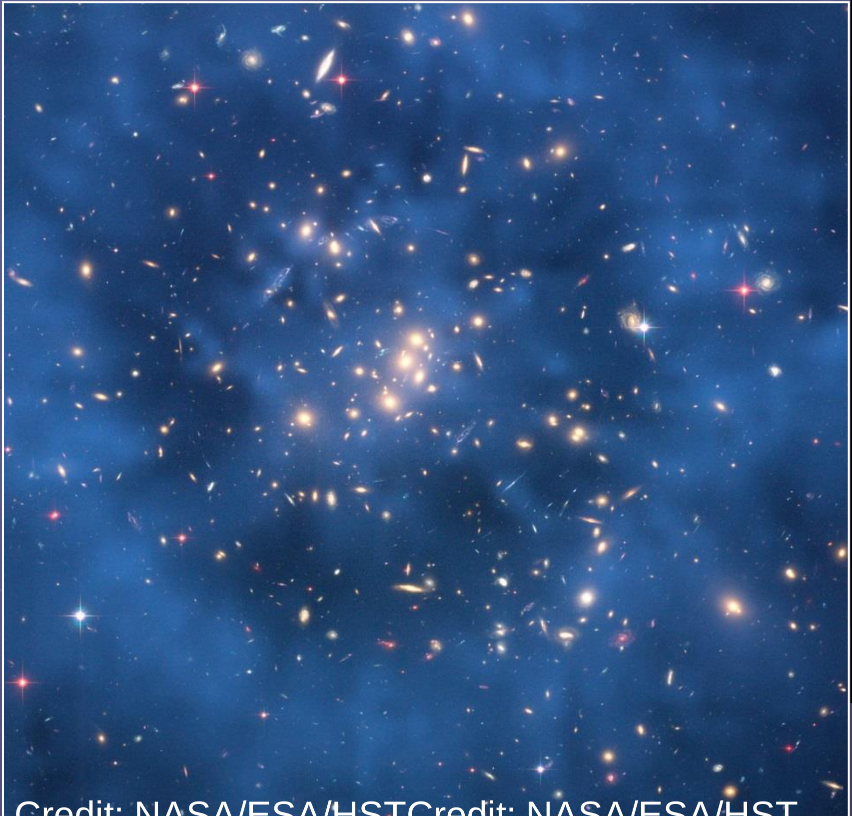

Credit: NASA/ESA/HSTCredit: NASA/ESA/HST

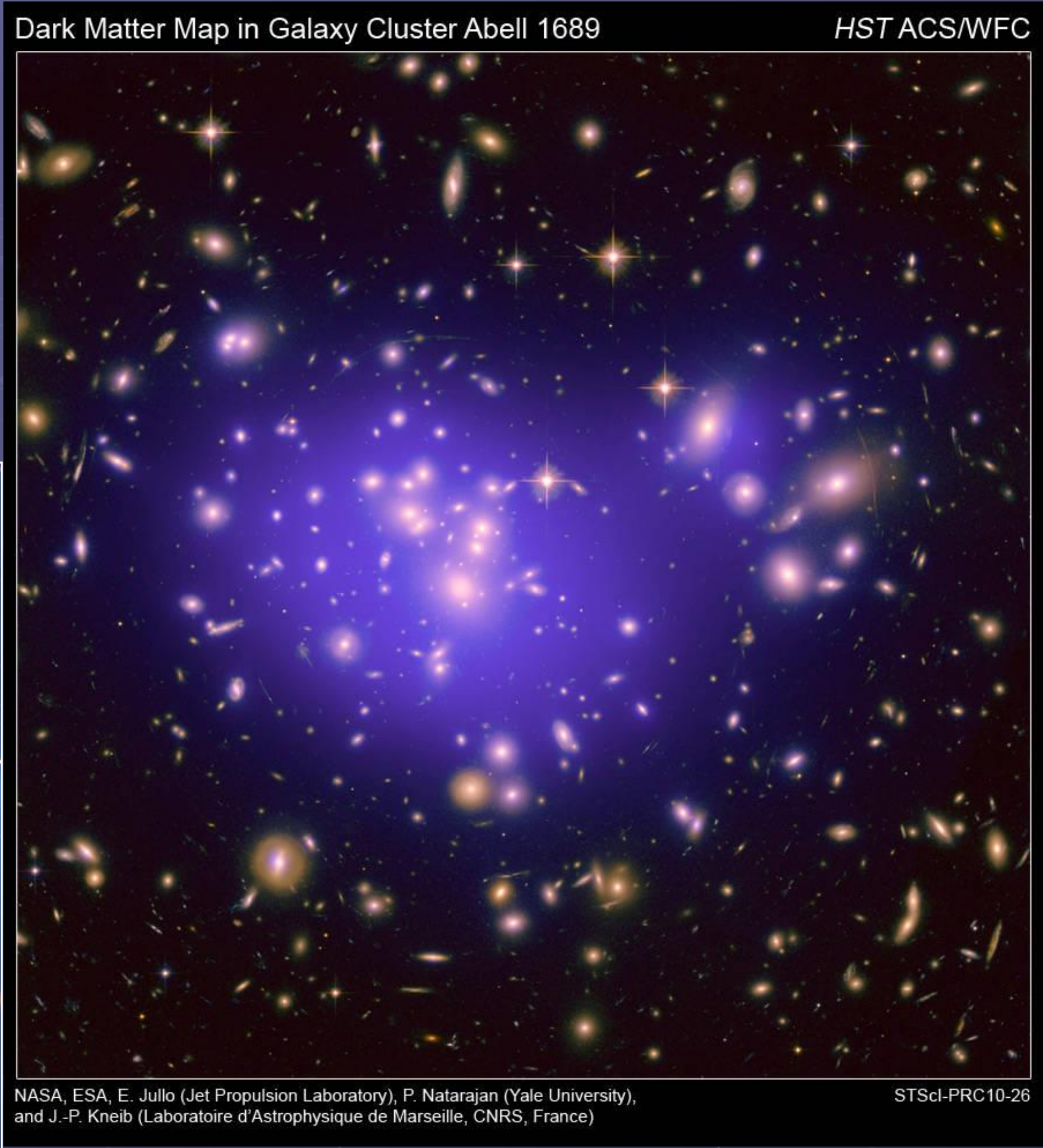

⇦ CL0024+17. The gravity map is superimposed on a Hubble image of the cluster.

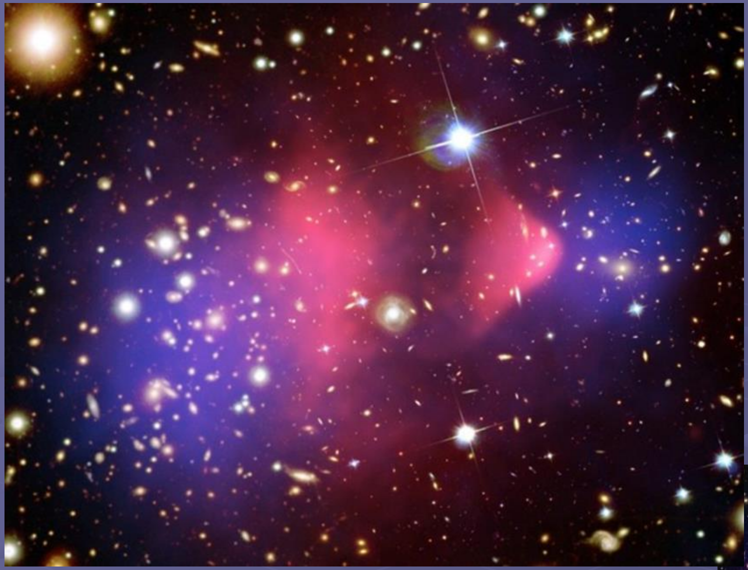

1E 0657-558 Bullet Cluster: composite image of X-ray (pink) and weak gravitational lensing (blue) of the famous Bullet Cluster of galaxies, z = 0.3

X-ray: NASA/CXC/CfA/ M.Markevitch et al.; Lensing Map: NASA/STScI; ESO WFI; Magellan/U.Arizona/ D.Clowe et al. Optical: NASA/STScI; Magellan/U.Arizona/D.Clowe et al. X-ray exposure time was 140 hours

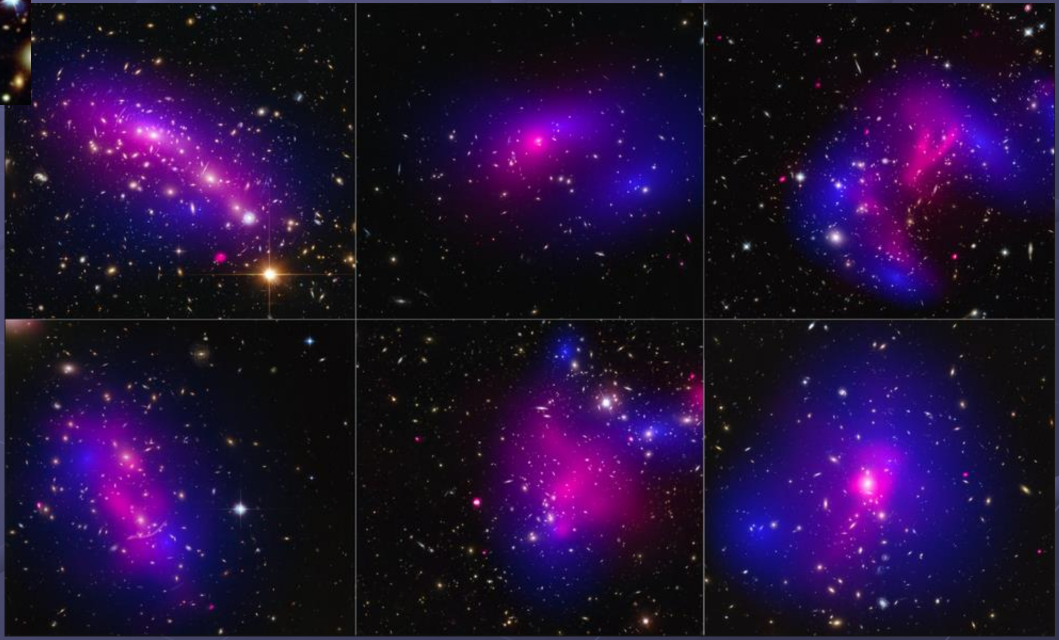

The images of six different galaxy clusters taken with NASA's Hubble Space Telescope and Chandra X-ray Observatory (pink) show dark matter (blue) in collided galaxy clusters. A total of 72 large cluster collisions were studied.

Credits: NASA and ESA

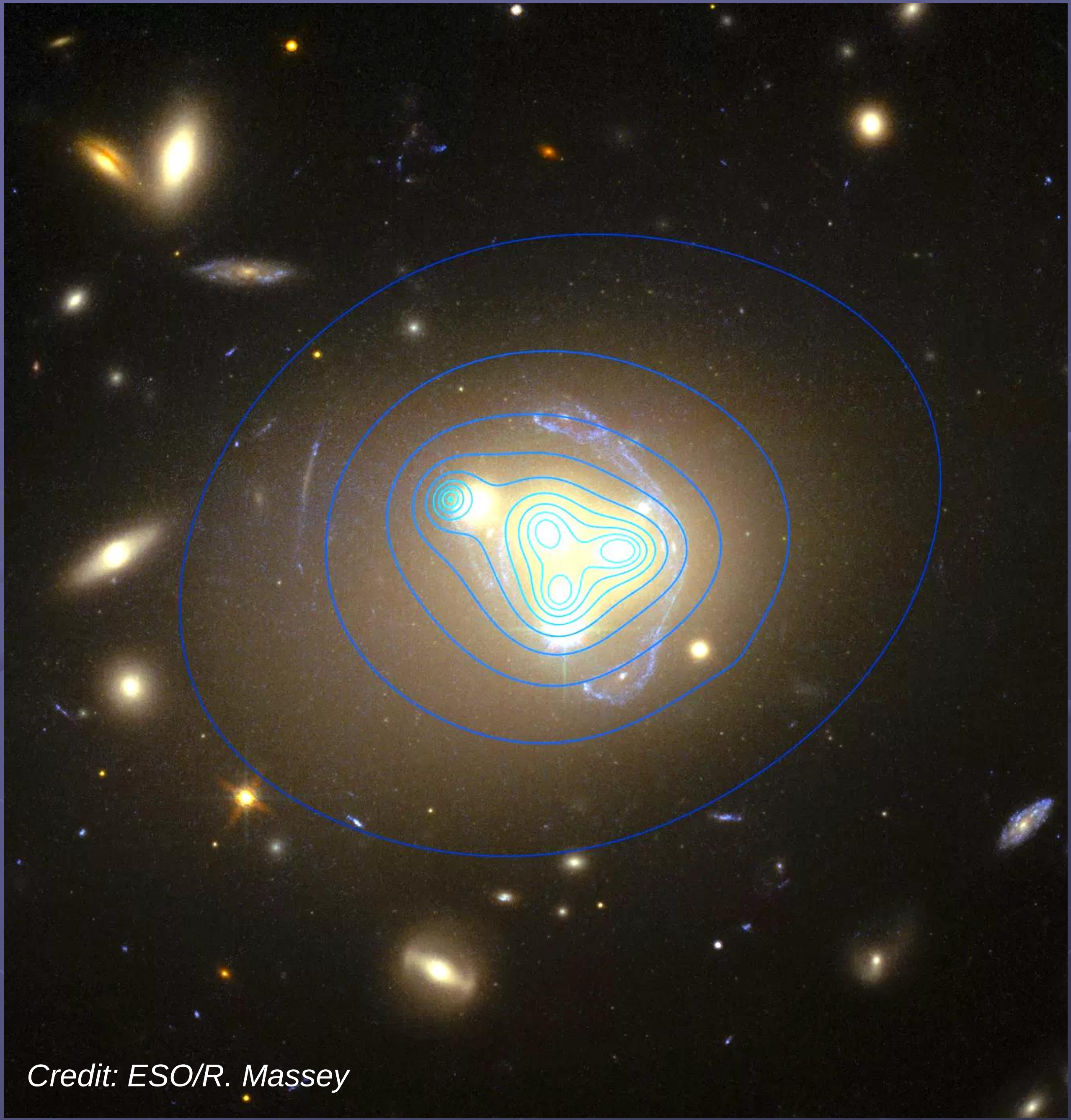

The distribution of dark matter in the galaxy cluster Abell 3827 (blue contour lines).

Observations of the central four merging galaxies have provided hints that the dark matter around one of the galaxies is not moving with the galaxy itself, possibly implying dark matter-dark matter interactions of an unknown nature are occurring.

The physics of the principal constituents of clusters

- Hot Gas -- Hydrostatic equilibrium (as first approximation)

  $T \sim 10^7 - 10^8 K$ (X-ray emitter)
  $n \sim 10^{-3} - 10^{-1} cm^{-3}$
  $L \sim 10^{43-46}$ erg/s $\sim 10^{-2} - 10^{-4} L_{opt}$
  $M_{gas} \sim 5 \times M_{gals}$
  $B \sim 0.1 - 10 \mu G$

  Gas metallicity $Z \sim 0.3 Z_{\odot}$ (enriched : not all primordial);

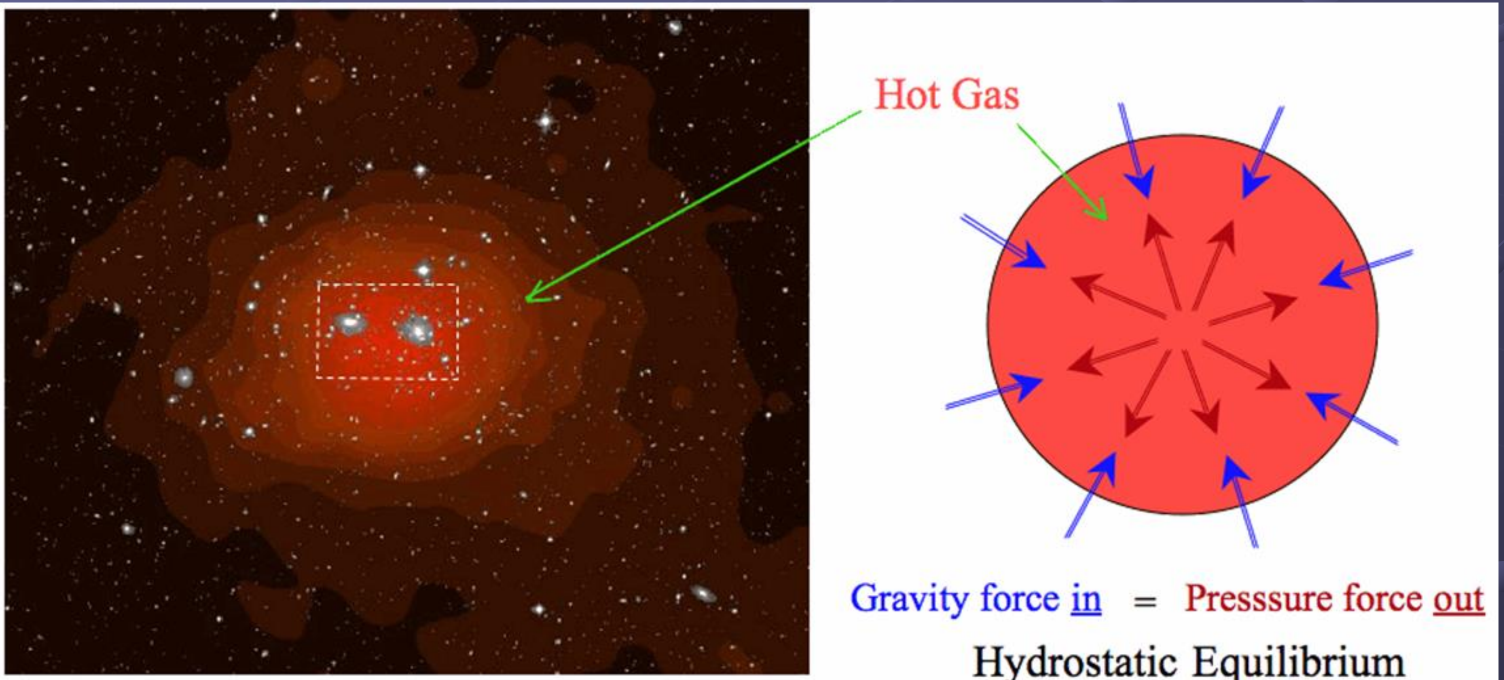

Coma cluster: X-ray (red), Optical (white)

The X-ray emission of a galaxy cluster is breaking Bremsstrahlung radiation produced in extremely hot intra-cluster gas by deceleration of an electron when deflected by an atomic nucleus.

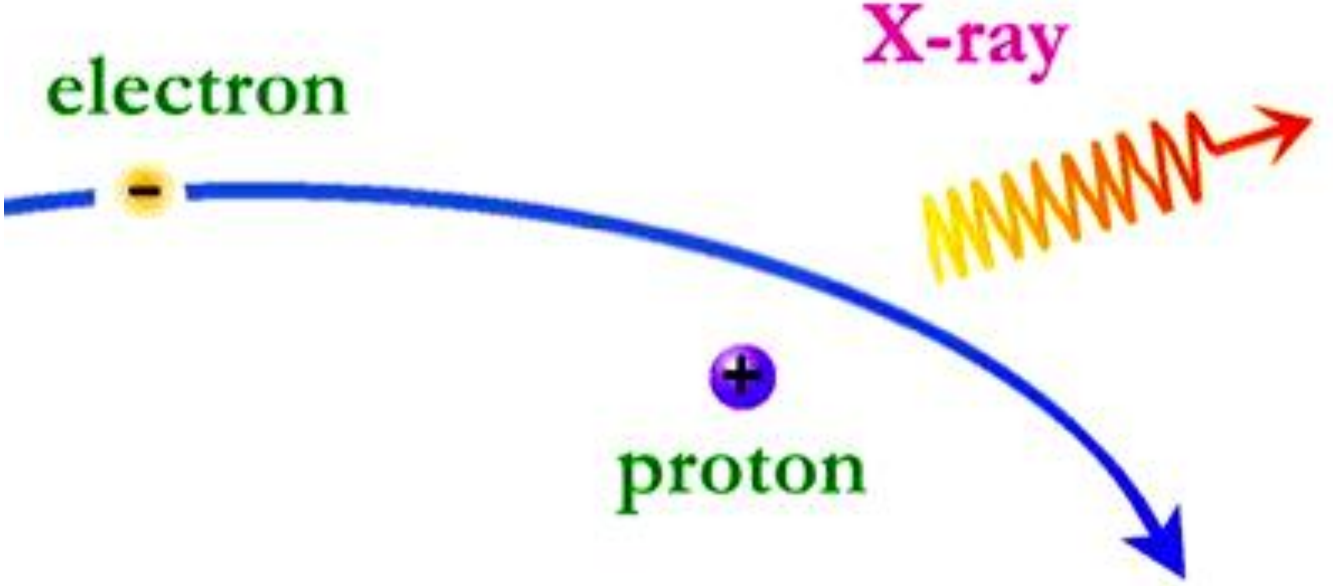

Image credit: Sarah H.R. Bank

With electron densities of $n_e \sim 10^{-4} - 10^{-1}\ cm^{-3}$ and temperatures of $T \sim 10^6 - 10^8$ K, the ICM radiates in X-rays predominantly through bremsstrahlung, 2-photons emission, photo- and dielectronic recombinations, and line emission due to collisional excitation processes. Except for the brightest emission lines in the cores of clusters, the gas is optically thin to such X-rays.

Extended X-ray emission from clusters of galaxies was first observed in the early 1970’s (G. M. Voit. astro-ph/0410173, 2004.)

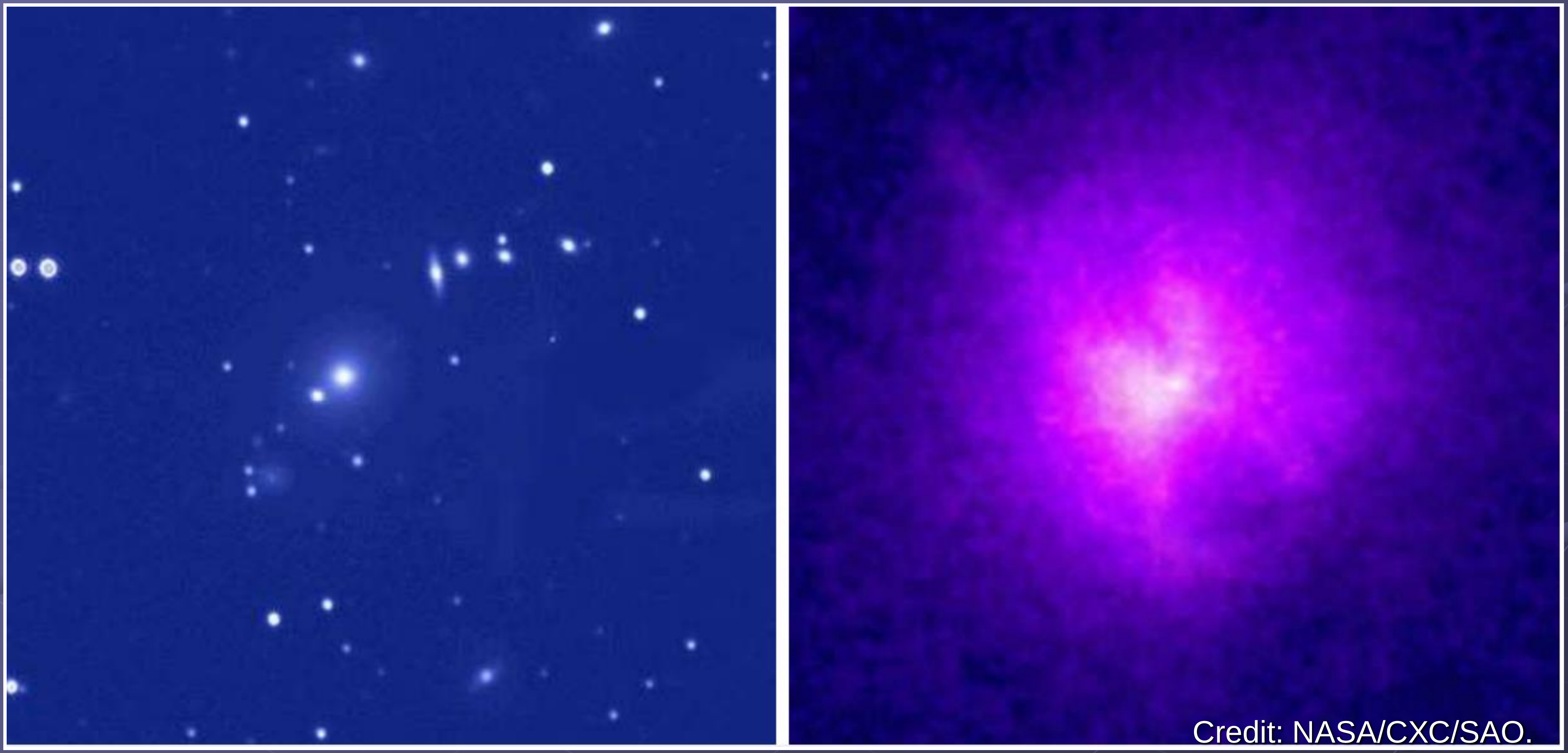

The Hydra A cluster of galaxies. Optical image from La Palma B.McNamara (left) and X-ray image from Chandra (right).

Morphology of Galaxy Clusters in Optic

Classification schemes of Galaxy Clusters based to one of several possible properties: viz shape, richness, lumpiness, Hubble mix, dominant galaxy types, etc.

Beginning approaches ware:

1)“rich” clusters vs. “poor” clusters (Abell richness classes)
Poor clusters include galaxy groups and clusters with 100’s of members. Rich clusters have 1000’s of members. Higher density of galaxies.

2) “regular” clusters vs. “irregular” clusters (Abell R vs. I)
R-clusters have spherical shapes. Tend to be the rich clusters.
I - clusters have irregular shapes. Tend to be the poor clusters.
IR and RI are intermediate types

3) Compact, Medium-Compact, Open (Zwicky)

Comparison of Regular and Irregular Clusters – different facets

Property	Regular Clusters	Irregular Clusters
Richness	Rich	Poor
Concentration	High concentration of members toward cluster center	No marked concentration to a unique cluster center; often two or more nuclei of concentration are present
Symmetry	Marked spherical symmetry	Little or no symmetry
Collisions	Numerous collisions and close encounters	Collisions and close encounters are relatively rare
Types of galaxies	Brightest galaxies are elliptical and/or S0 galaxies. Cluster often centered about one or two giant elliptical galaxies	All types of galaxies are usually present Late-type spirals and/or irregular galaxies present
Diameter (Mpc)	Order of 1 - 10	Order of 1 - 10
Subclustering	No	Often present.
V_r dispersion	Order of 10^3 km/sec	Order of 10^2 - 10^3 km/sec
Mass (from Virial Theorem)	Order of 10^{15} $M_\odot$	Order of 10^{12} - 10^{14} $M_\odot$
Examples	Coma cluster (A1656); Corona Borealis cluster (A2065)	Virgo cluster, Hercules cluster (A2151)

More: Bahcall N. arXiv:astro-ph/9611148.

Main classification schemes:

The Bautz-Morgan (BM) classification is based on brightness contrast between first- and second-ranked galaxies(*ApJ* **162**, L149,1970)
.

BM I single central dominant cD galaxy (A 2199)

BM II several bright galaxies between cD and gE (Coma)

BM III no dominant galaxy (eg Hercules)

Intermediate types are I-II and II-III

Some later Oemler (1974) recognised three types of cluster according to Hubble mix: "spiral rich" (eg Hercules);
"spiral poor" (eg Virgo); "cD" (eg Coma);

Lòpez-Cruz at al. introduced the definition of a cD cluster, the complement to this class is called a non-cD cluster.
(ApJ **194**, *1,1974. ApJ*, **475**, L97, 1997)

The Rood and Sastry (RS) classification is based on the projected distribution of the brightest 10 members.

cD - single dominant cD (elliptical) galaxy (A2029. A2199)

B - dominant binary, (Coma)

L - linear array of galaxies (Perseus)

C - single core of galaxies

F - flattened (IRAS 09104+4109)

I - irregular distribution (Hercules)

(*PASP* **83**, 313, 1971, *AJ* **87**, 7, 1982).

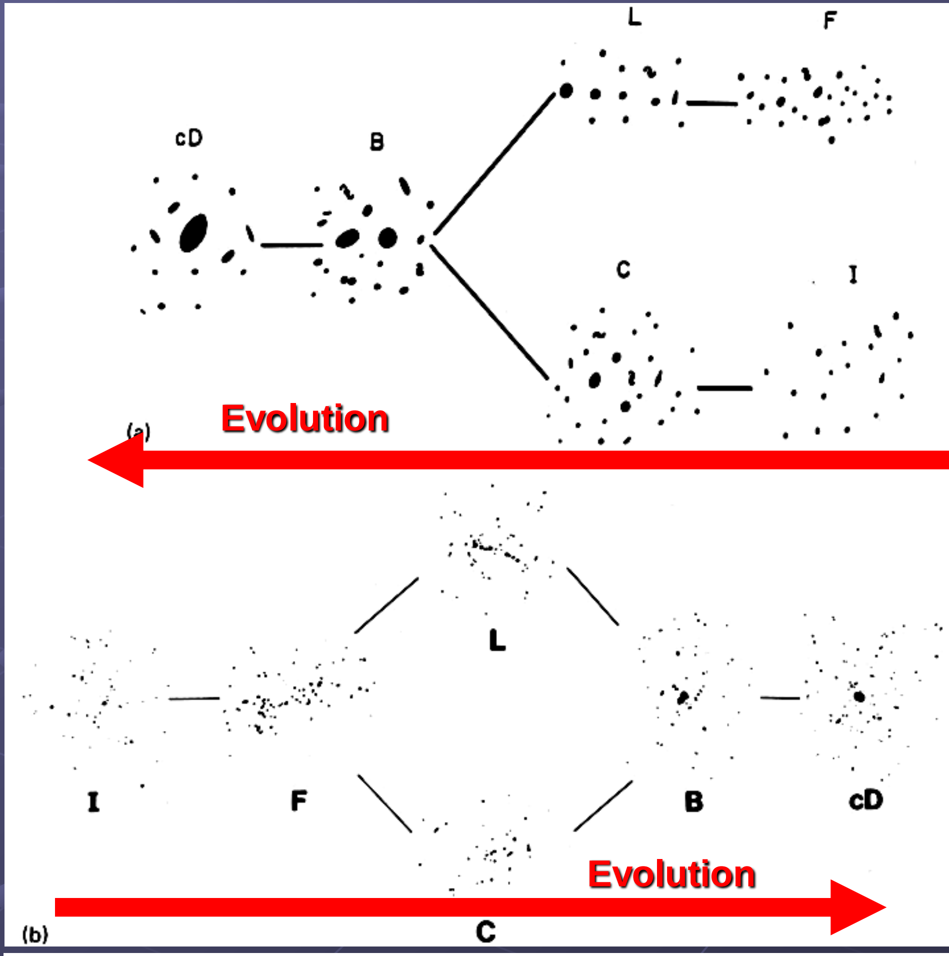

RS 1971“tuning-fork” (*a*) and revised R-S (*b*) cluster classification scheme (1982).

BM I, RS cD, R…

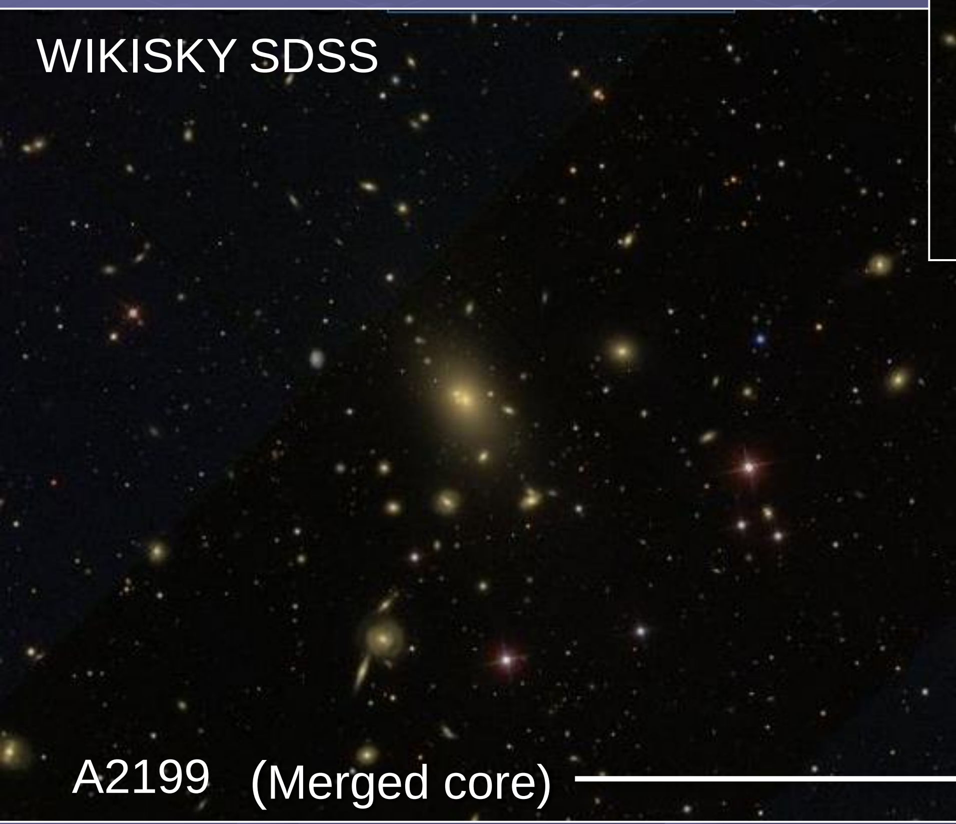

BM II, RS L…

WIKISKY SDSS

Galaxy cluster MACS J0416.1-2403, courtesy Hubble Frontier Fields

The Perseus Galaxy Cluster (Abell 426)

BM III, RS F

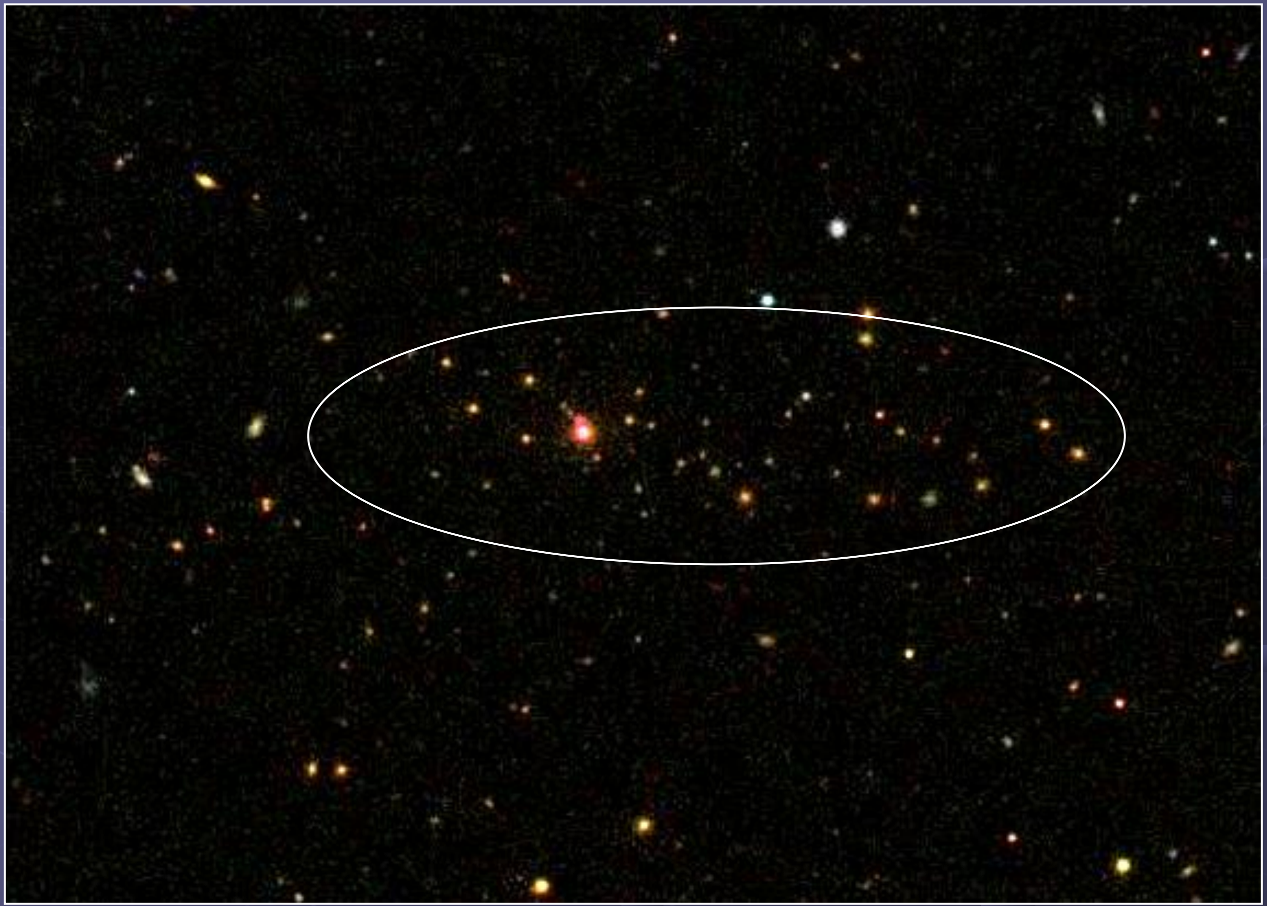

IRAS 09104+4109 WIKISKY SDSS

L

Types of clusters

C

Note a correlation between position angle for the major axes of the best-fit ellipse (black) and the direction of the preferred plane (red) in L and F clusters.

CL type was not found.

F

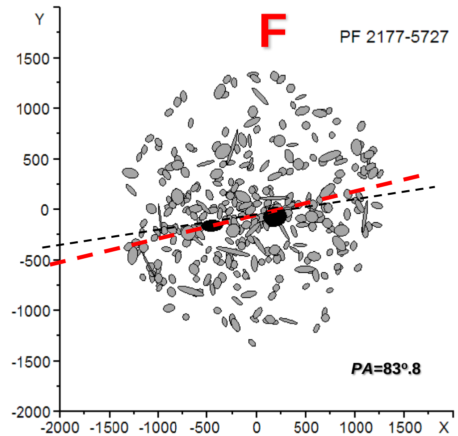

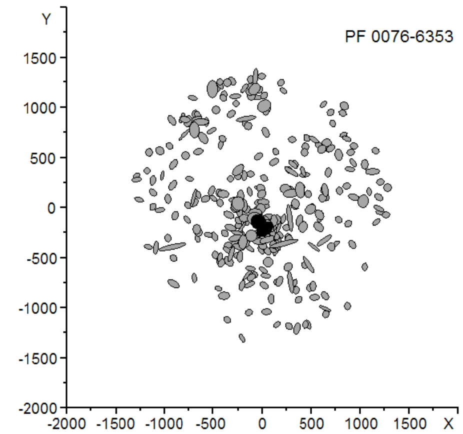

I

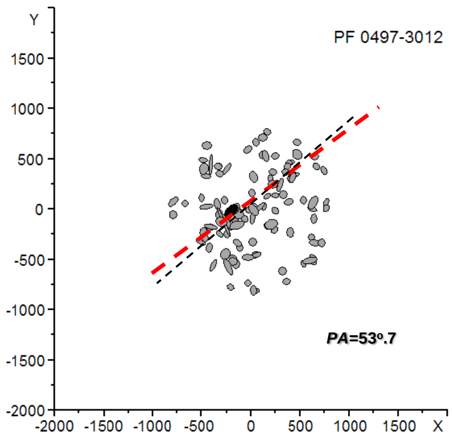

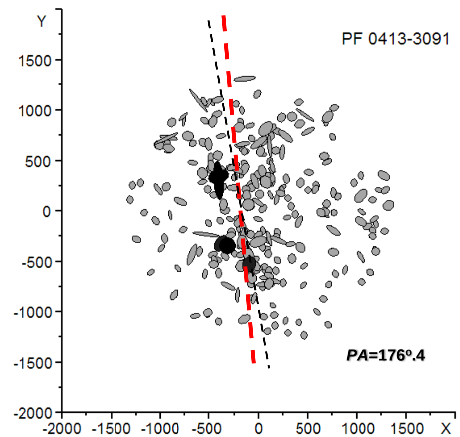

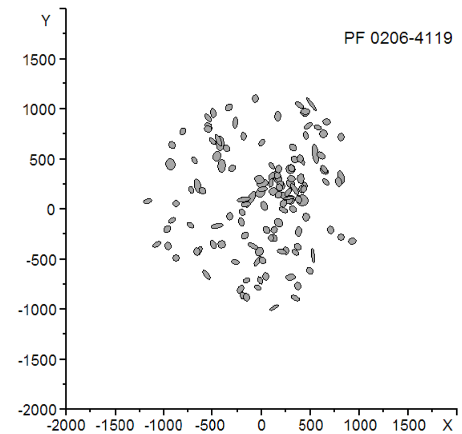

O

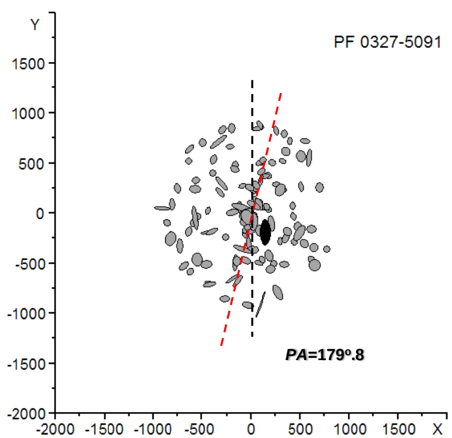

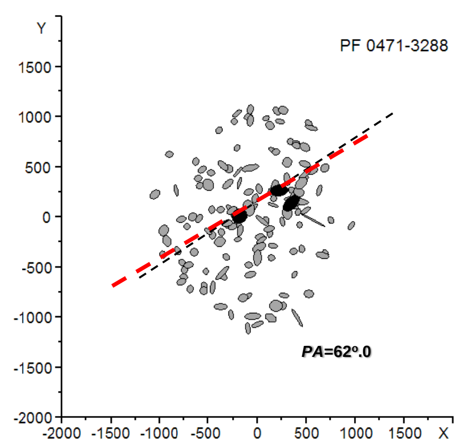

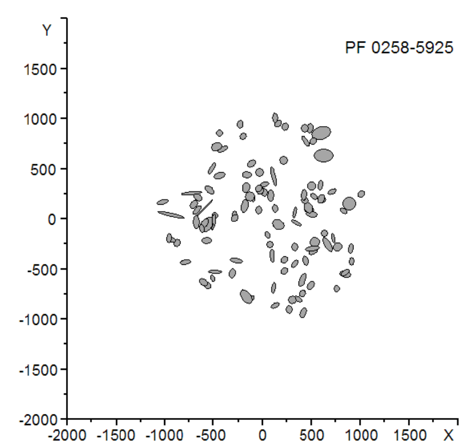

For study the PF Galaxy clusters (MRSS) one more scheme was proposed. Adapted morphological classes based on 3 parameters: concentration, the single of preference plane (flatness) and BG positions:

- concentration ***C*** – compact, ***I*** – intermediate and ***O*** – open;
- flatness ***L*** – line, ***F*** – flat and no sign of flatness (no symbol);
- using Bright Cluster Members role ***cD*** *and* ***BG;***
- other peculiarities are noted as ***P****.*

The parameters can be combined.

Property \ Cl ass	Regular	Intermediate	Irregular
Zwicky type	Compact	Medium-Compact	Open
Bautz-Morgan type	I, I-II, II	(II), II-III	(II-III), III
Rood- Sastry type	c*D*, B, (L,C)	(L), (F), (C)	(F), I
Lòpez-Cruz	c*D*	non-c*D*	non-c*D*
Symmetry	Spherical	Intermediate	No
Central concentration	High	Moderate	Very little
Central profile	Steep	Intermediate	Flat
Panko types	*C, (CF), CcD, CBG*	*I, IBG, IL, IF, IP*	*O, OBG, OL, OF, OP,*

Most evolved ⇨ Intermediate ⇨ Least evolved

From the distributions of the frequencies of clusters with different morphology one can see that concentration and flatness are independent morphological criteria. The frequencies of L and F types are similar in C-I-O subsets.

In contrast, the role of BCMs is strongly connected with cluster concentration: the number of cD clusters is greatest in C-type.

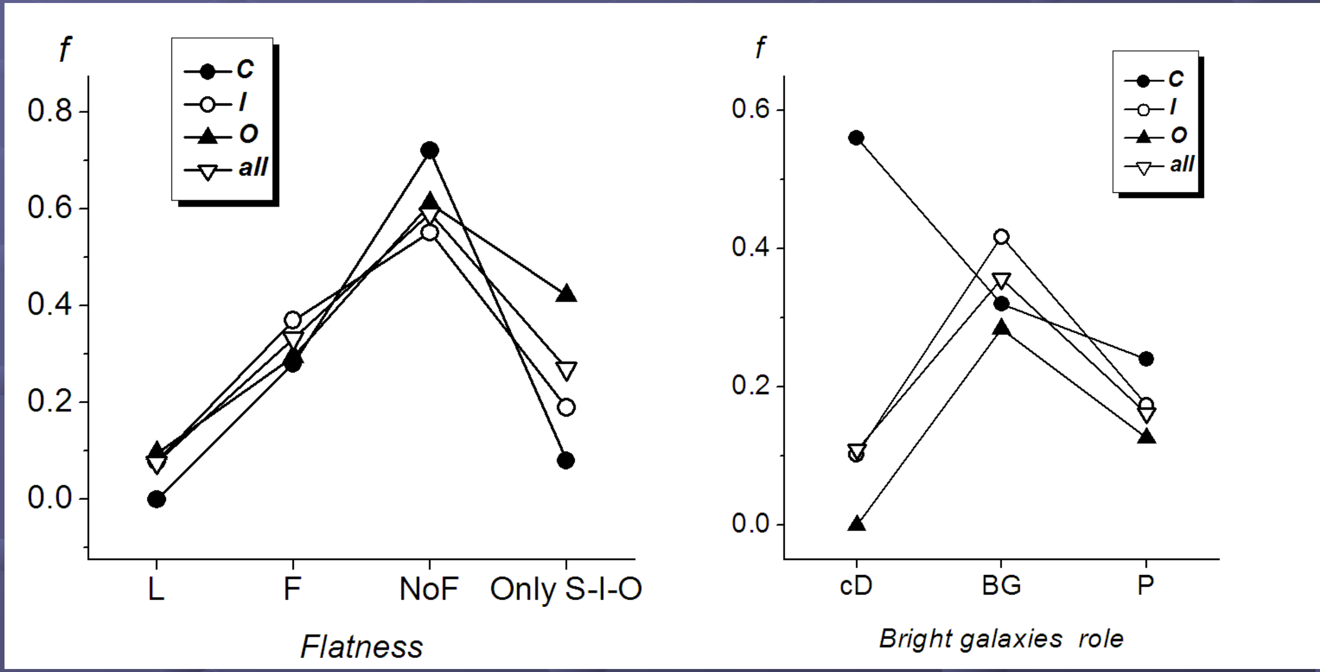

cD galaxies are anomalies in the galaxy population. The are:

- very luminous Elliptical galaxies ($L_{cD} \approx 10 \times L_G$), i.e. unusually bright;
- very large with an extended halo (50 - 100 h^{-1}kpc);
- there is alignment of cD galaxy and parent cluster;
- located at the spatial and velocity center of the cluster.;

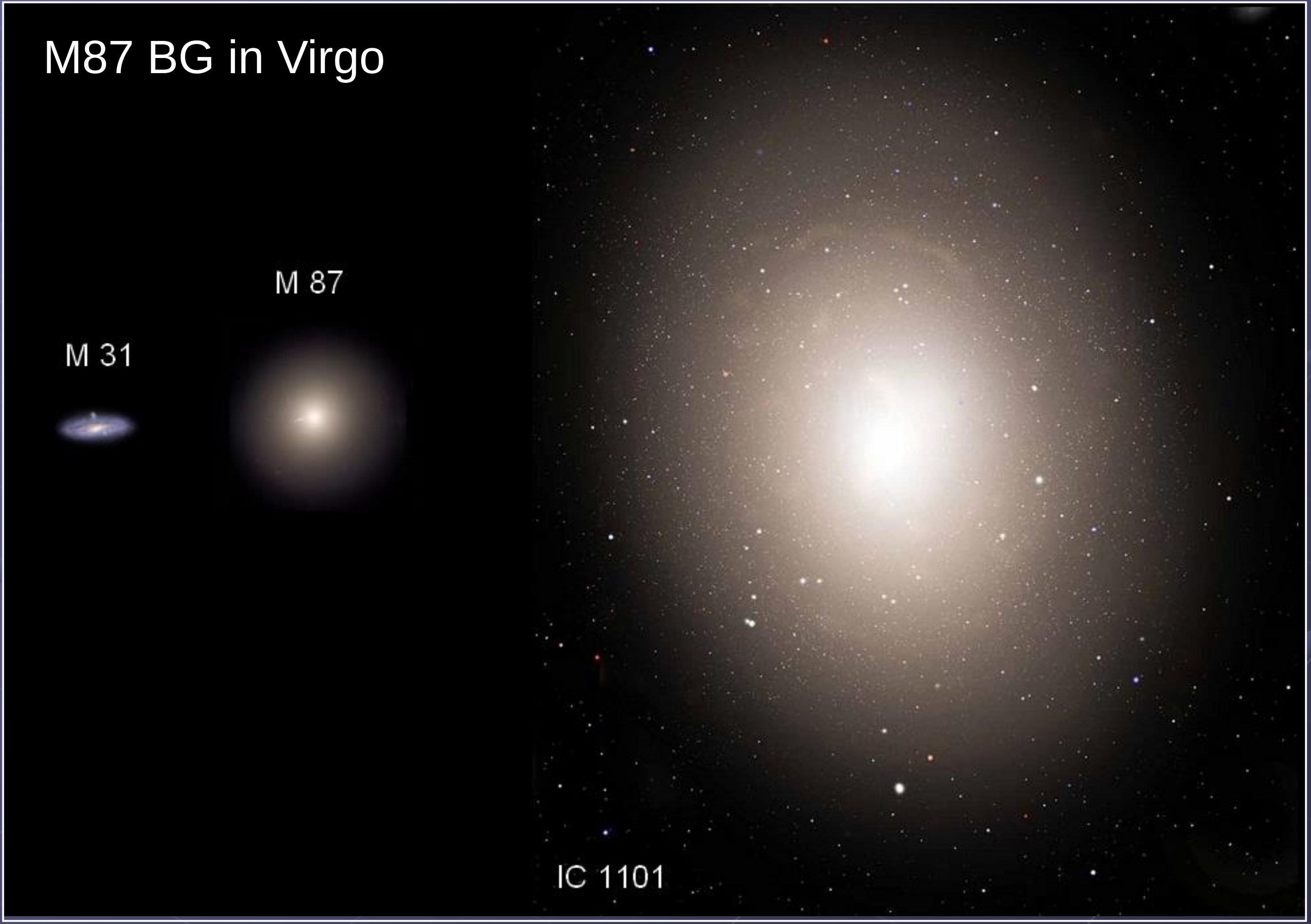

- Images often show double/triple merging nuclei within cDs.

File usage on Commons
Fernando de Gorocica

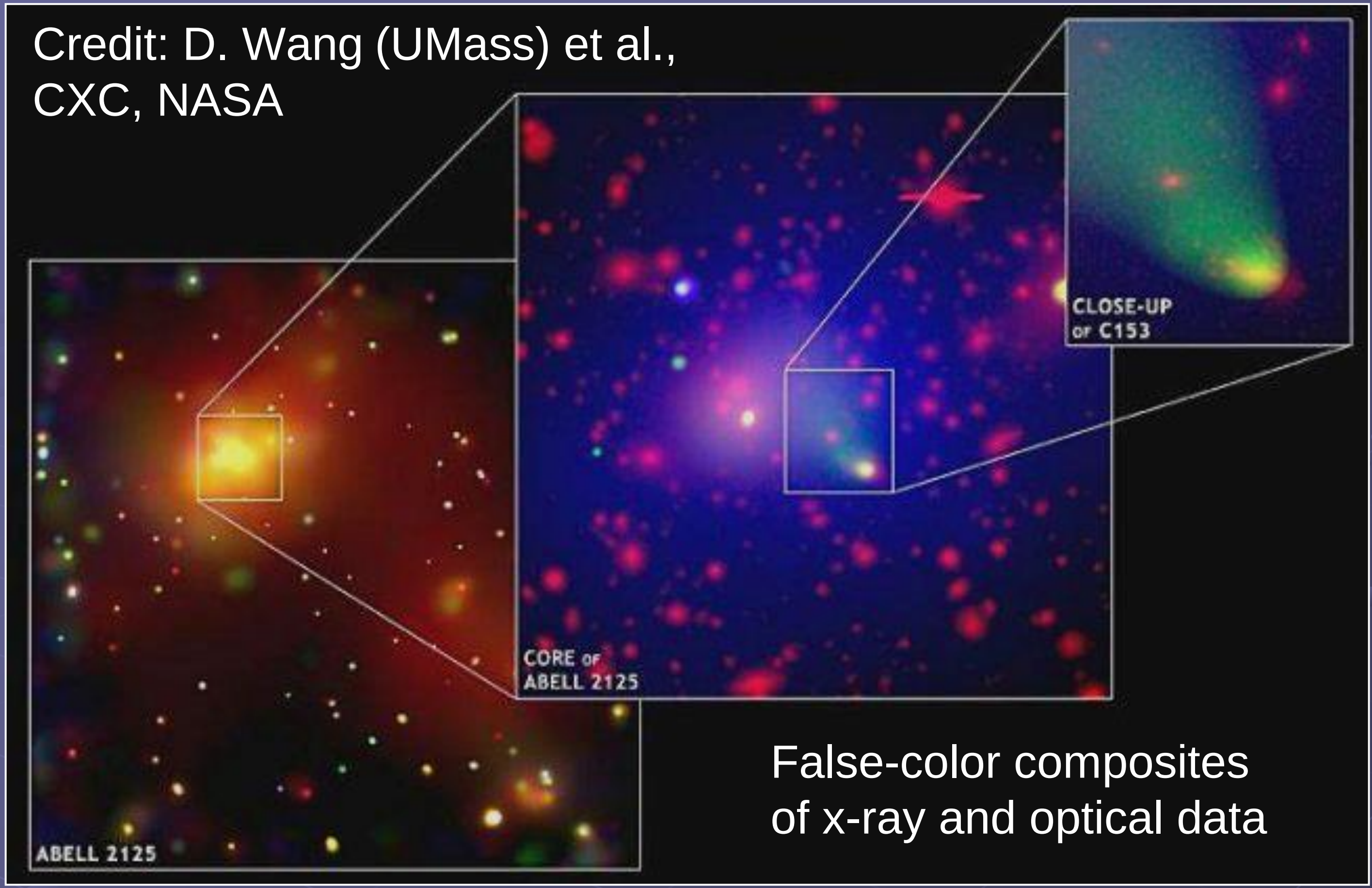

cD galaxies have a qualitative different formation history than other cluster galaxies. Their origin can be connected with mergers of cluster galaxies in the cluster core. A comet-like tail of glowing gas from galaxy C153, 200'000 light-years long, on the core of galaxy cluster Abell 2125 is the stage of "galactic cannibalism". The series of images illustrate a possible history of cD galaxies grow.

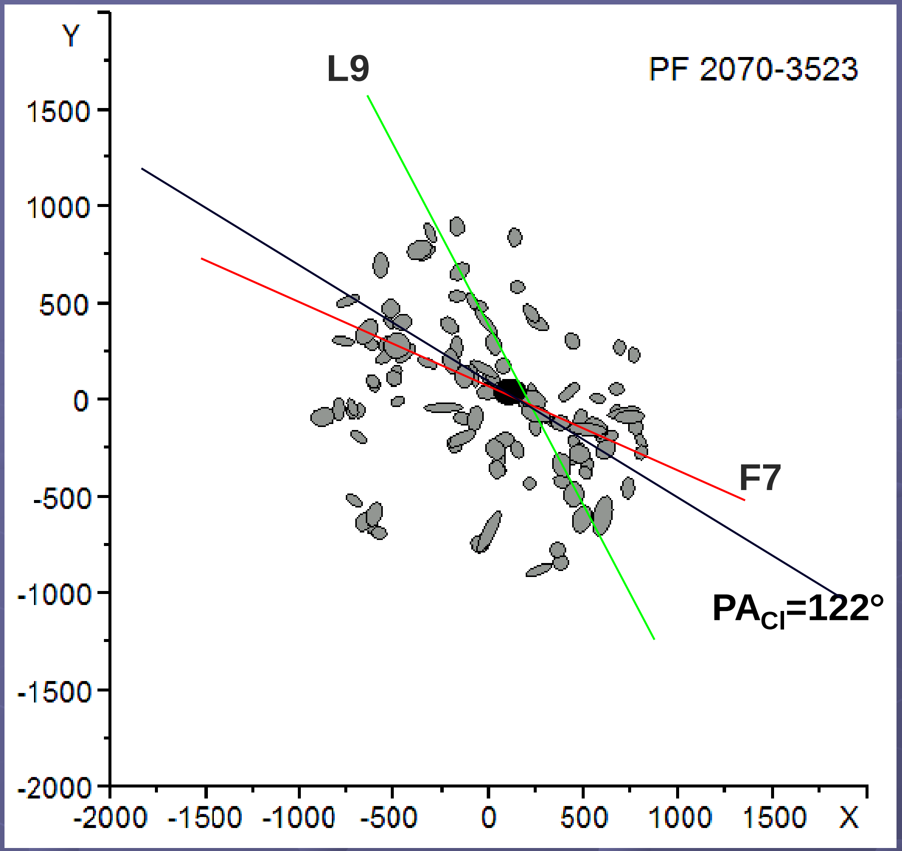

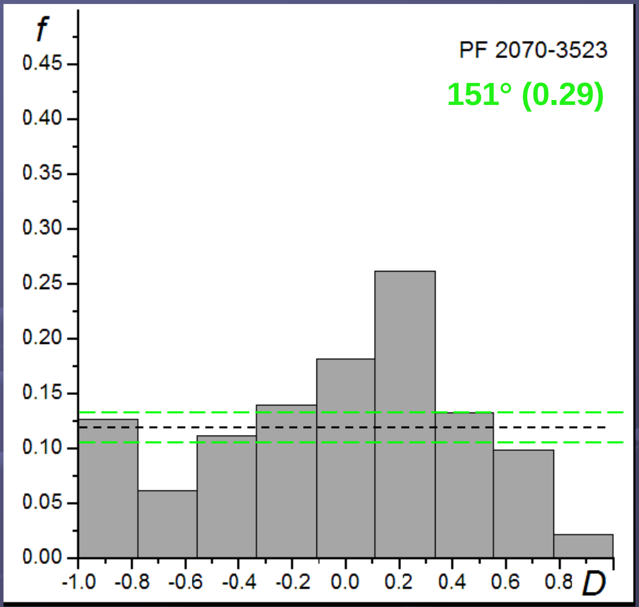

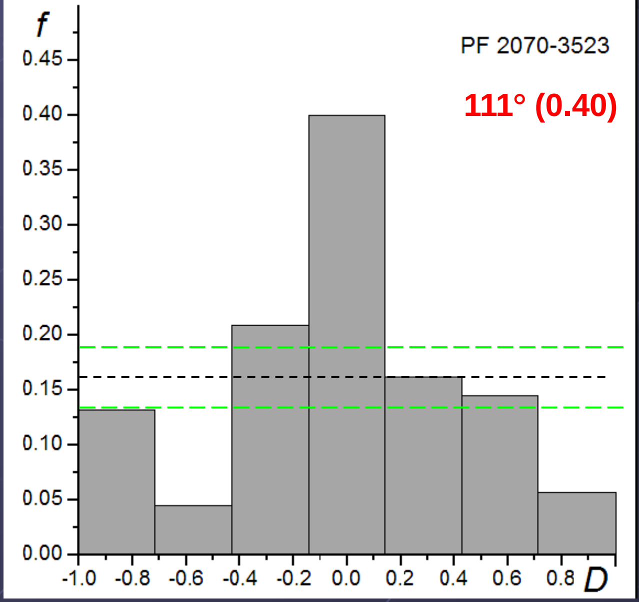

Cross F7xL9 (BG is placed on the cross) as example of substructures in the galaxy cluster

Cross:

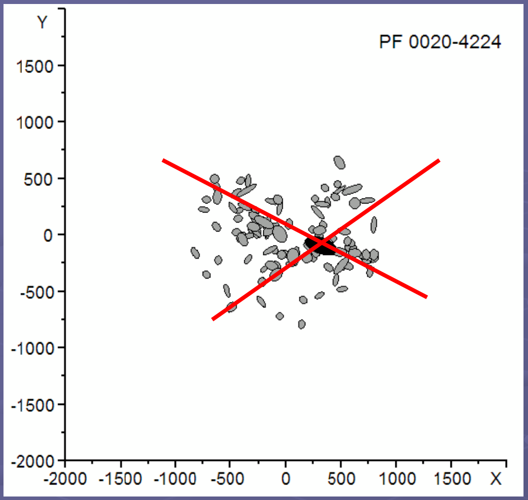

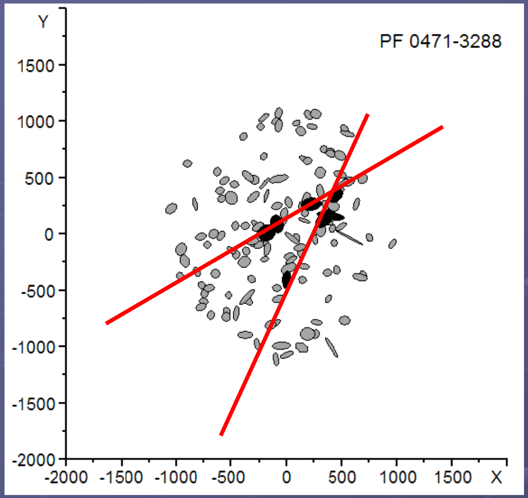

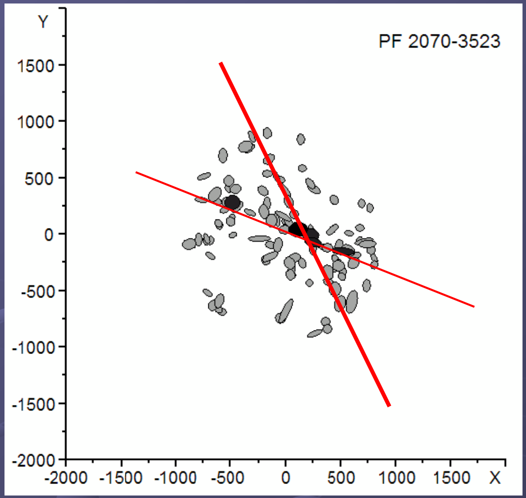

(Curved) bands:

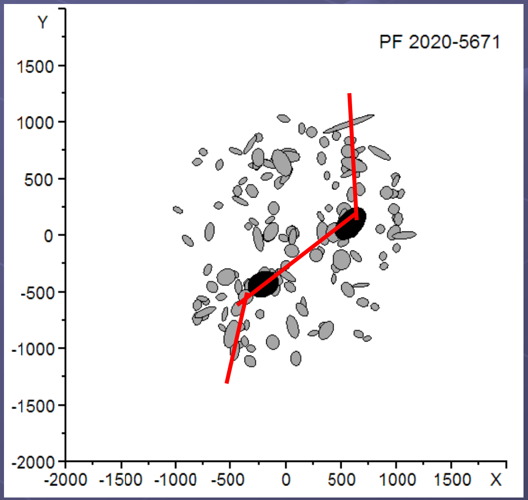

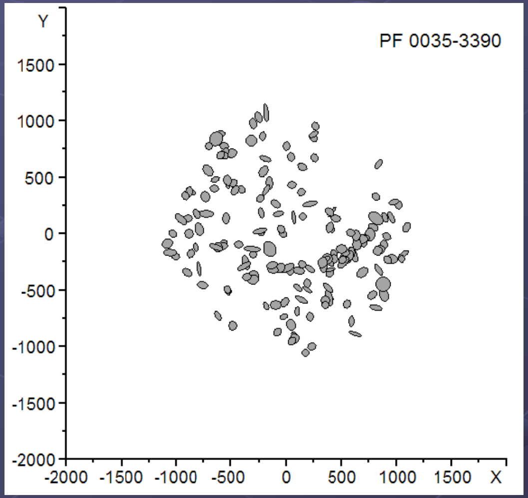

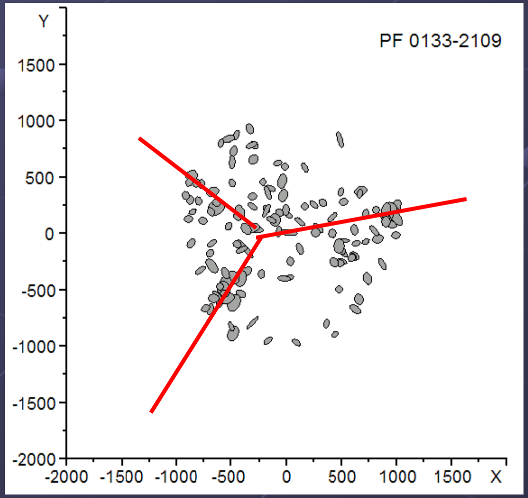

The comparison of X-ray image and optical map of PF 2187-1978 galaxy cluster (type C F BG)

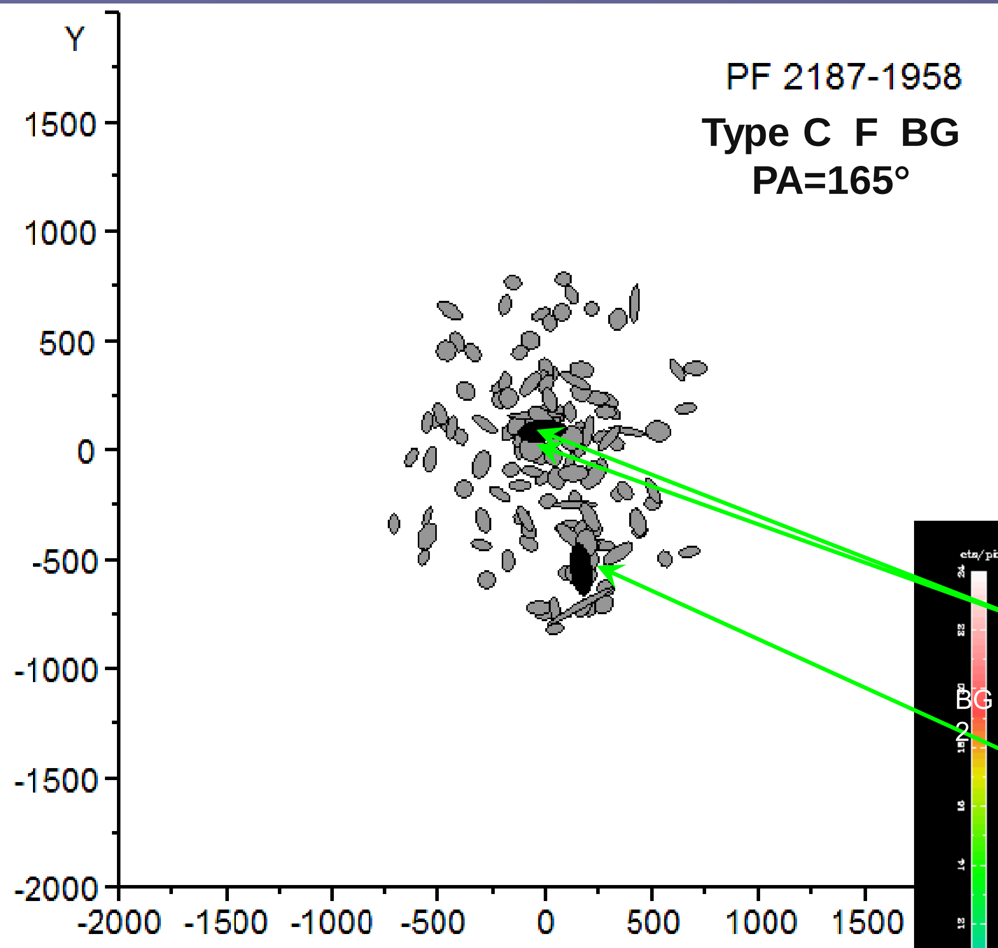

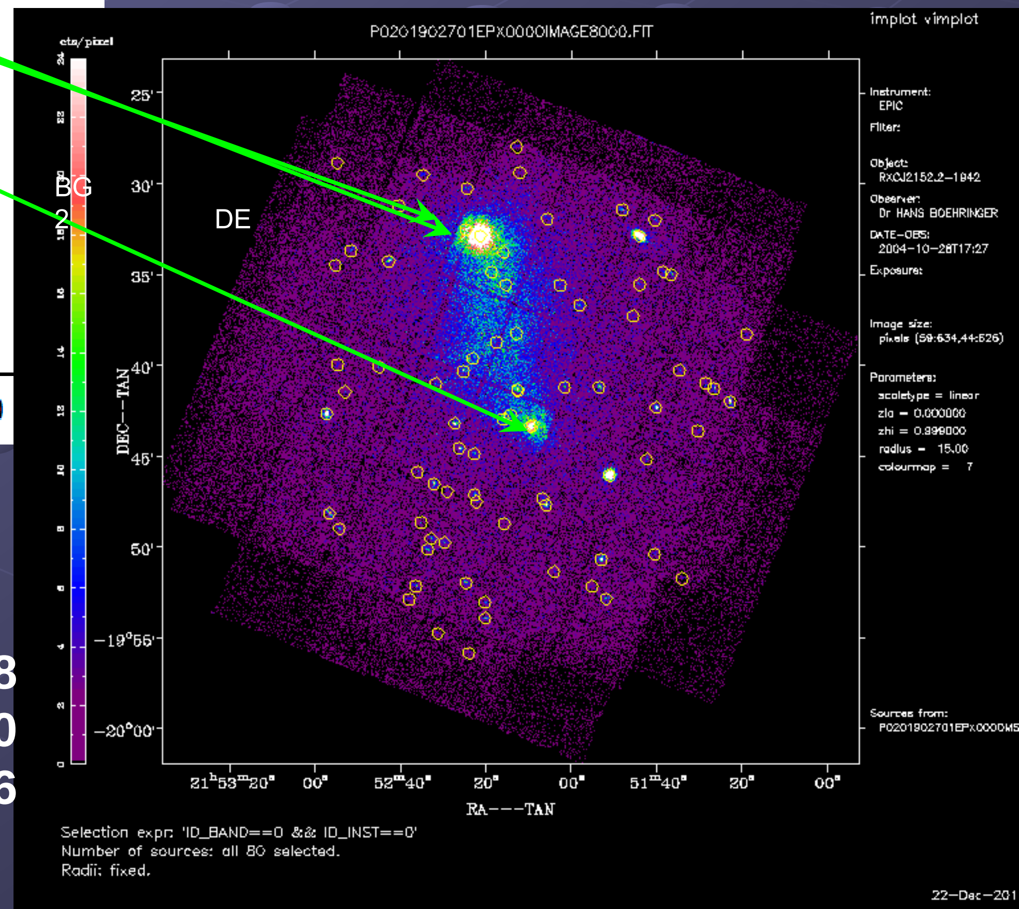

Brightest galaxies in PF2187-1958

m_F	m'_F	RA	Dec
14.87	14.79	$21^h\,52^m\,09^s.66$	-19°43′ 21″.8
15.10	15.03	$21^h\,52^m\,22^s.00$	-19°32′ 48″.0
15.15	15.07	$21^h\,52^m\,23^s.43$	-19°32′ 49″.6

Clusters are prolate or triaxial; richer clusters are less elongated, so C-I-O consecution with L-F marks divides clusters by shape and concentration.

The anisotropy in L or F clusters can be connected with dark matter filaments.

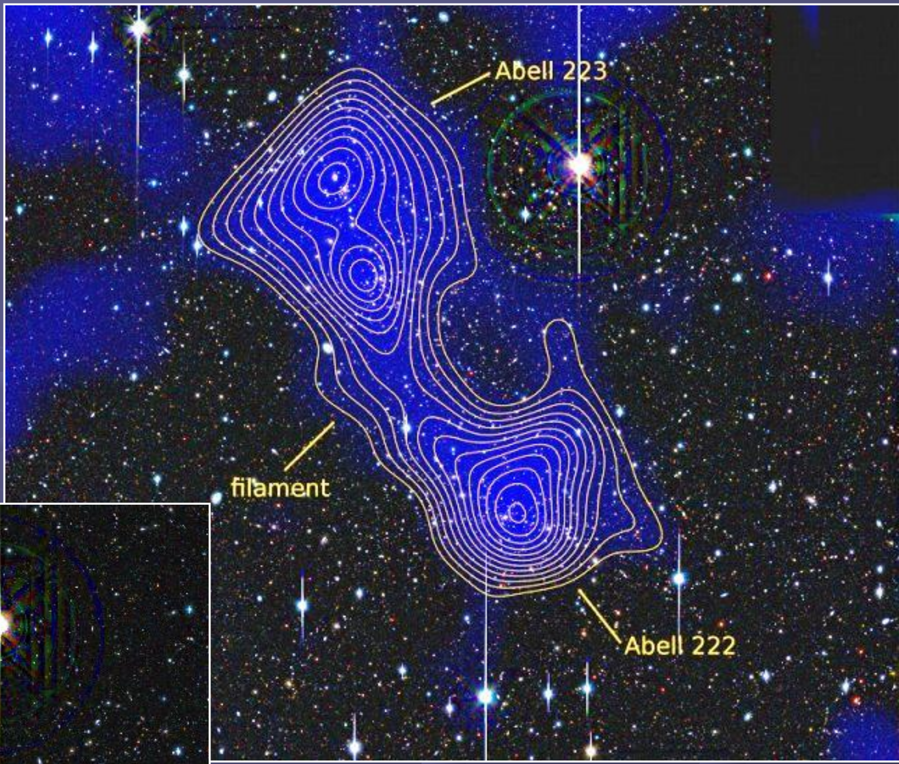

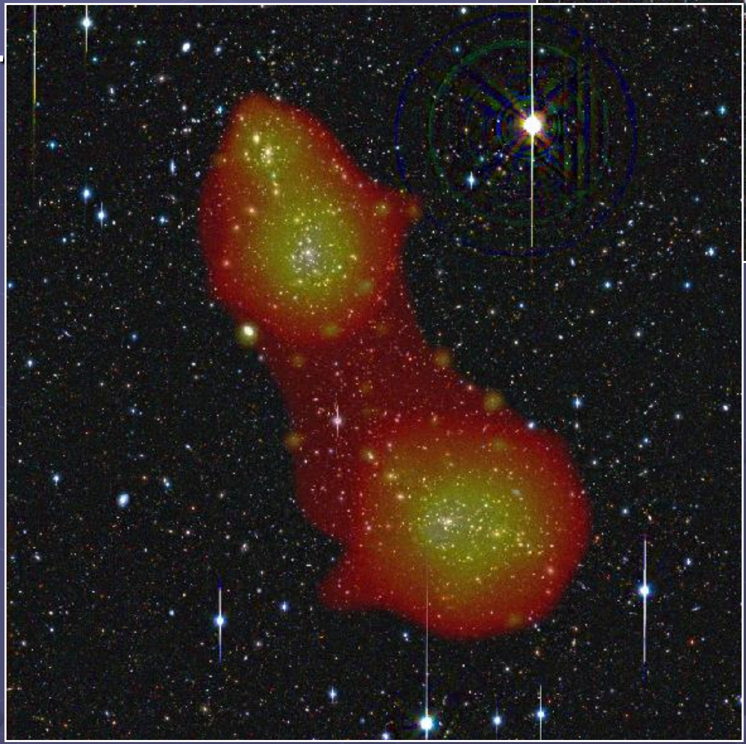

Jörg Dietrich et al. found the dark matter filaments (blue) in A222 and A223 clusters.
http://arxiv.org/abs/1207.0809

Composite optical/X-ray image with a filament of hot, low-density gas. *Jörg Dietrich*

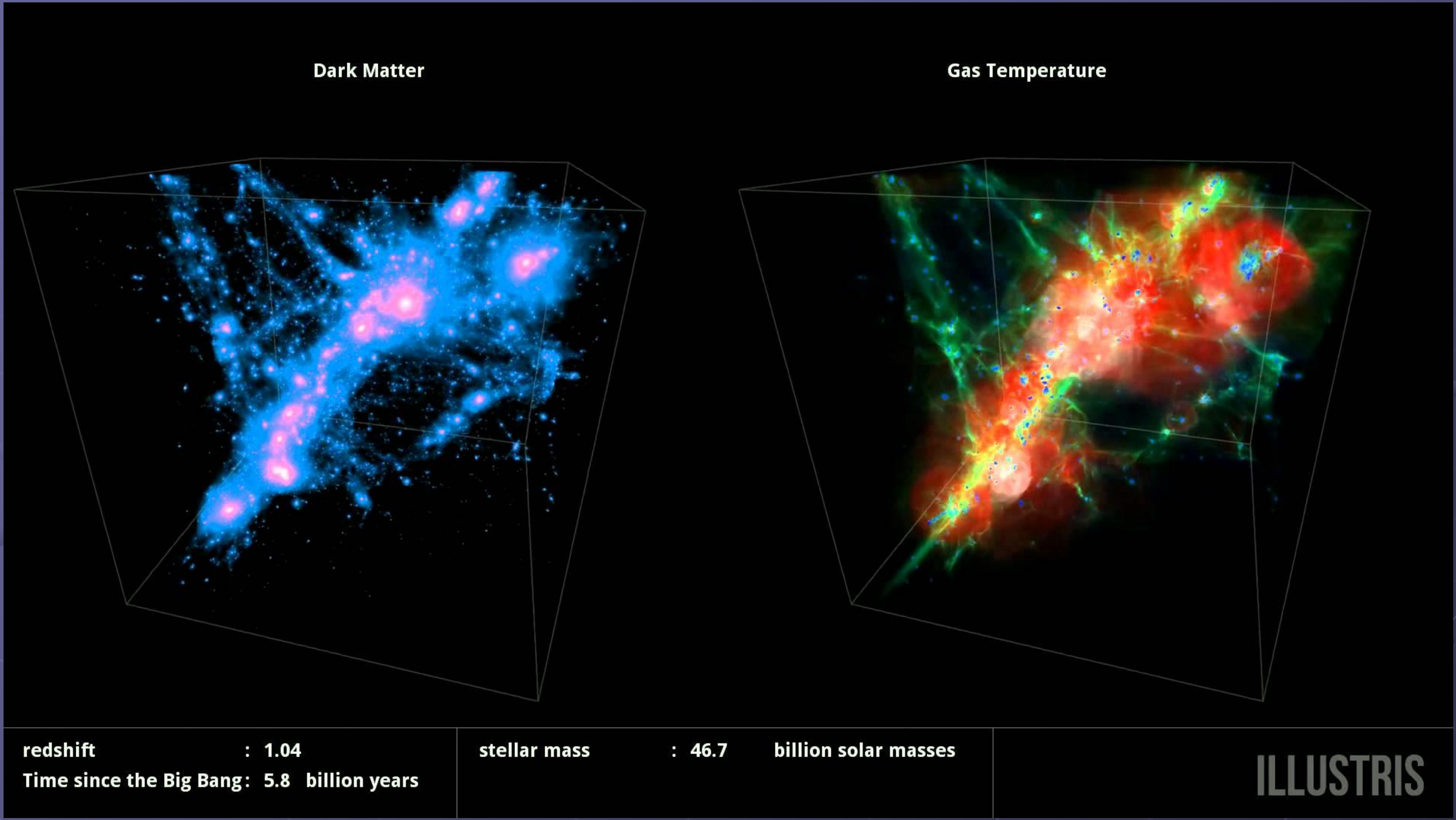
Dark Matter
Gas Temperature
redshift : 1.04
Time since the Big Bang : 5.8 billion years
stellar mass : 46.7 billion solar masses
ILLUSTRIS

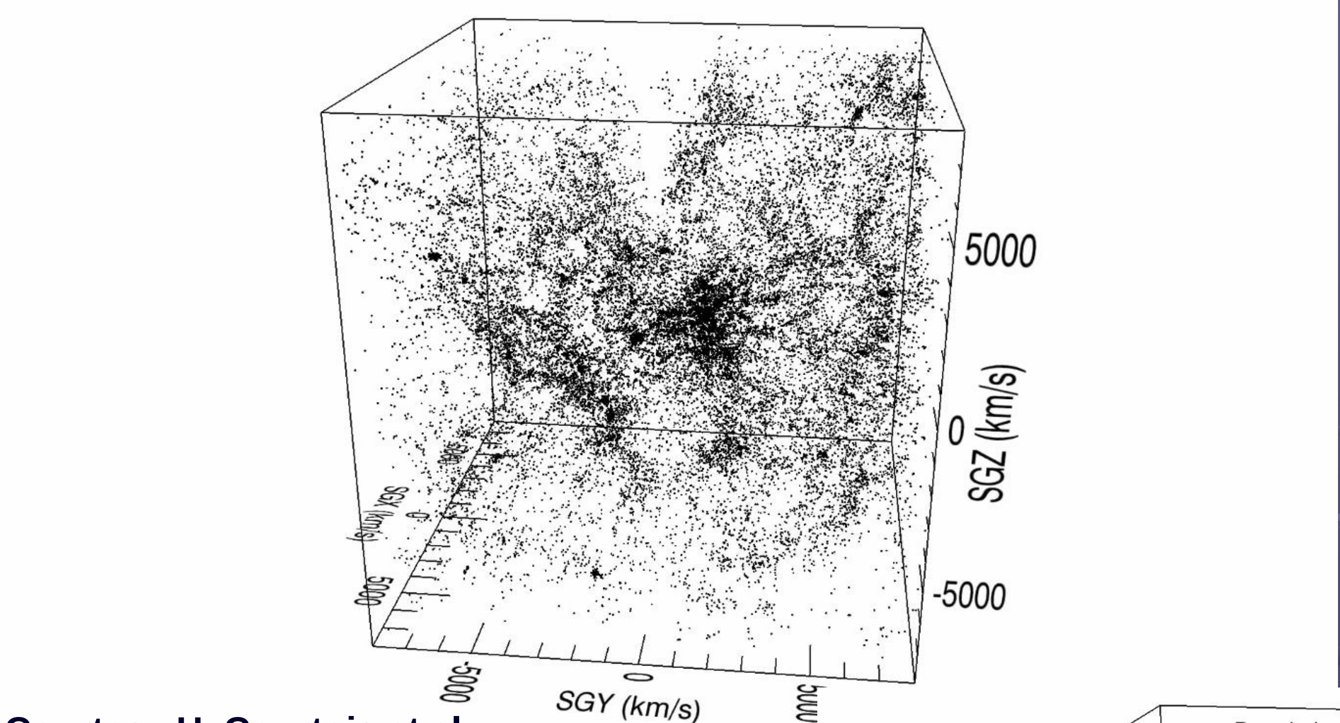

Courtesy H. Courtois et al.

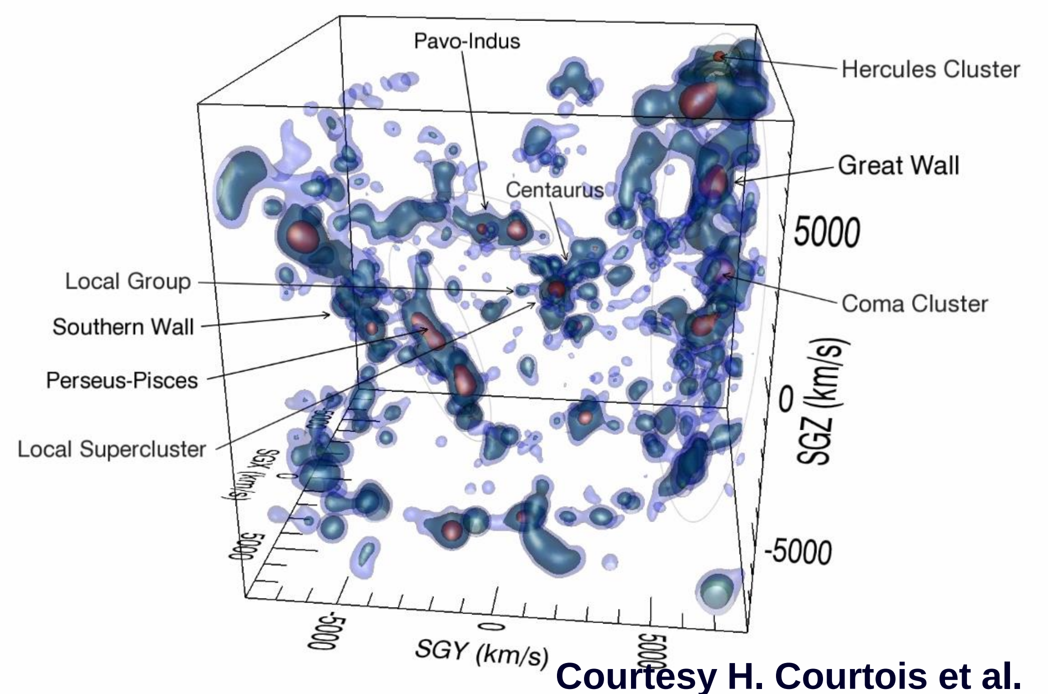

Courtesy H. Courtois et al.

https://vimeo.com/64868713

X-rays galaxy clusters

The most massive baryonic component of galaxy clusters is the “intracluster medium” (ICM), a diffuse, hot, weakly magnetized plasma that is most easily observed in the X-ray band.

Firstly the M87 in the Virgo cluster was detected as extragalactic X-ray source. The next ones were connected with the Perseus cluster and the Coma cluster.

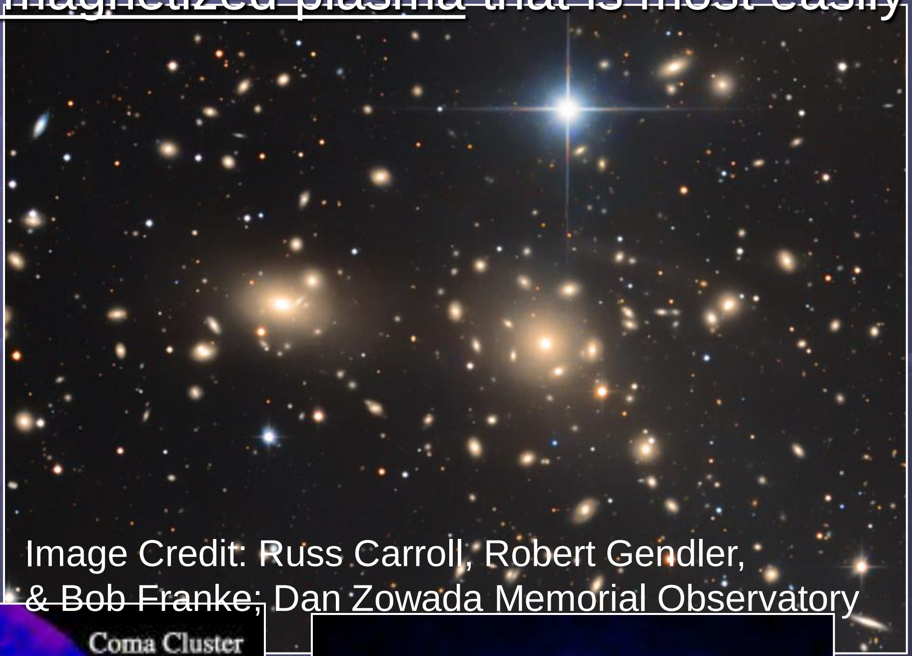

Image Credit: Russ Carroll, Robert Gendler, & Bob Franke; Dan Zowada Memorial Observatory

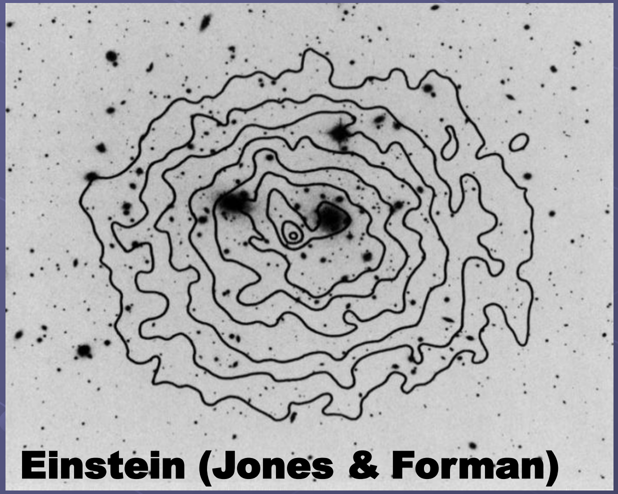

Einstein (Jones & Forman)

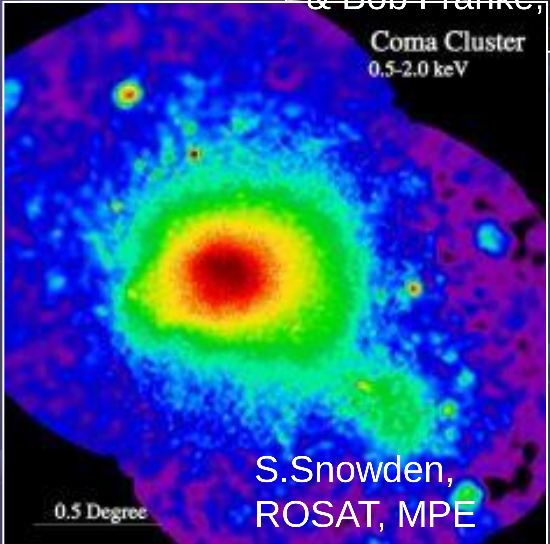

S.Snowden, ROSAT, MPE

Vikhlinin et al, 2001; CXC, SAO, NASA

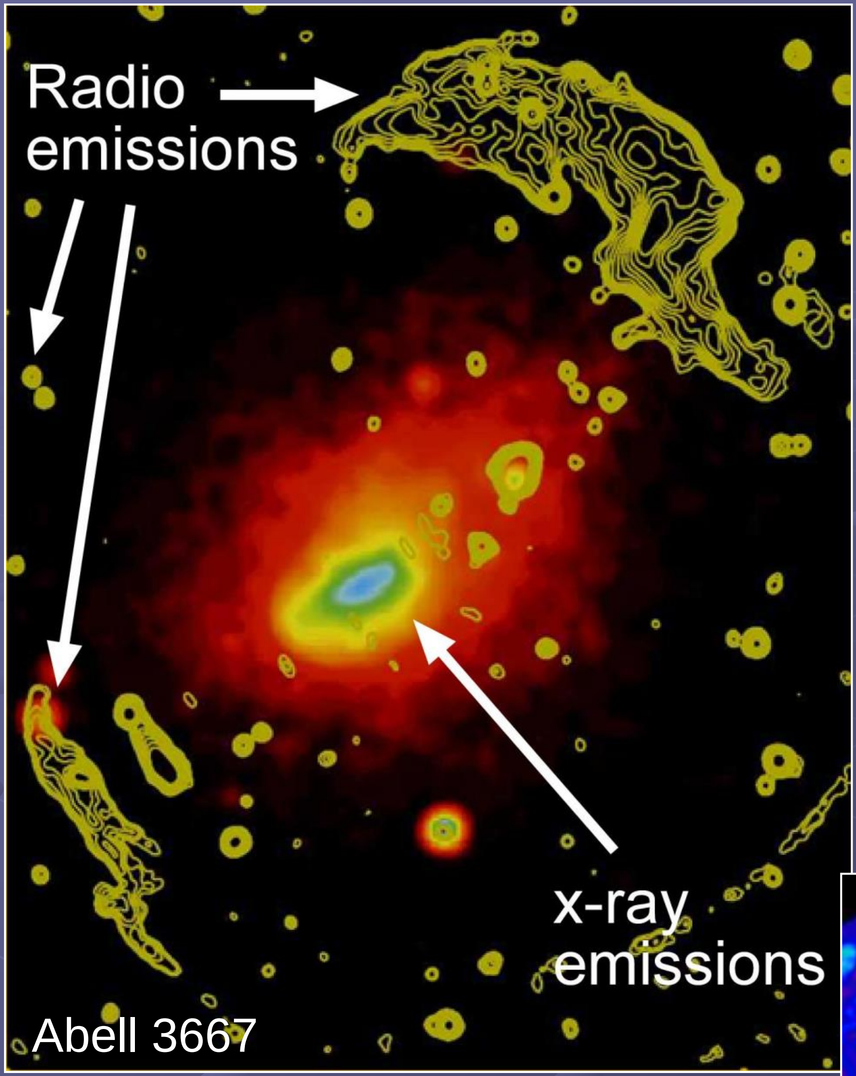

⇦ The hot gas and radio emission contours (yellow) produced by shock waves in A3667cluster.

Interaction.

Radio data: Australia Telescope Compact Array. X-ray data: ROSAT (PSPC). Composite image by Matteo Murgia, Istituto di Radioastronomia, Bologna, Italy.

X-ray and radio images ⇨ of Coma cluster.

No interaction

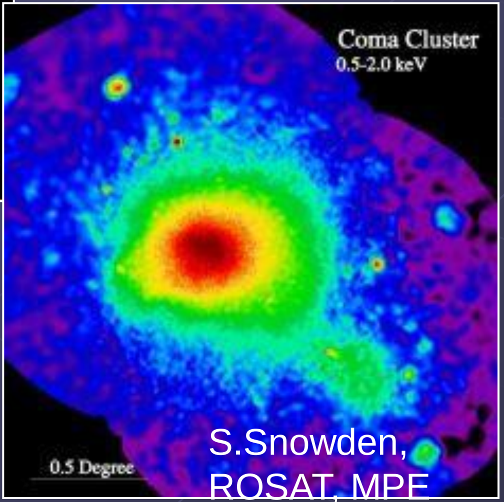

S.Snowden, ROSAT, MPE

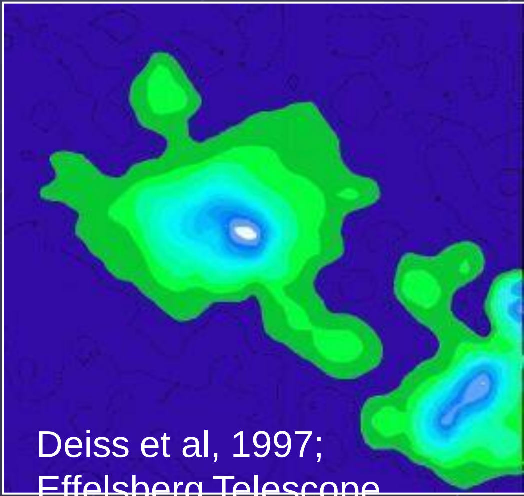

Deiss et al, 1997; Effelsberg Telescope

Hydra A galaxy cluster 30.10. 1999, 6 hours

(z= 0.54)

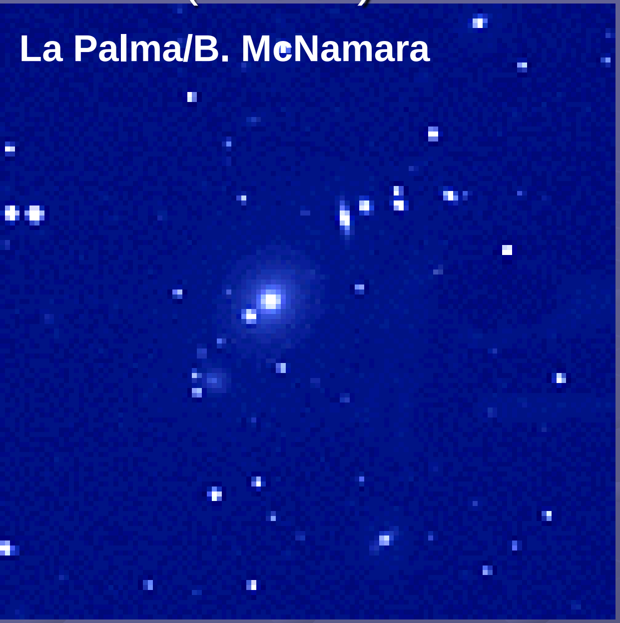

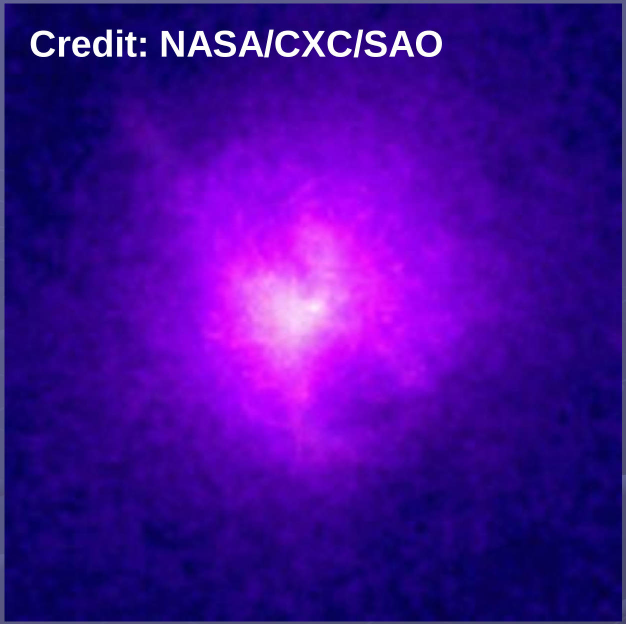

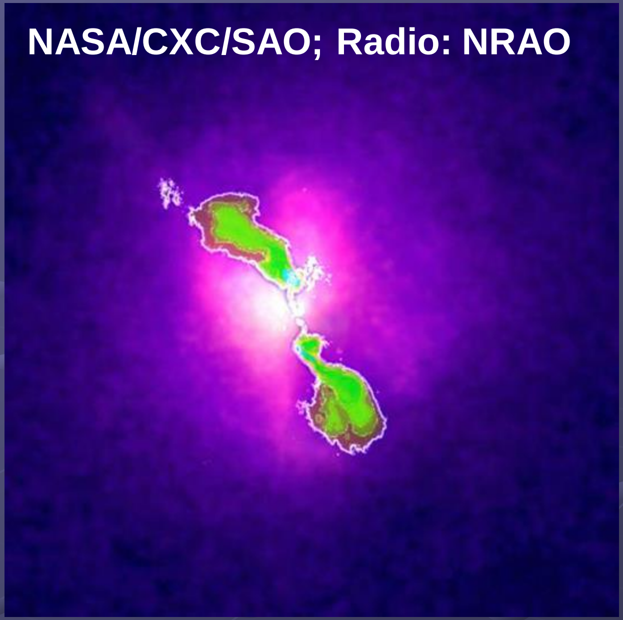

The Chandra image of Hydra A galaxy cluster displays for the first time long snake-like strands of 35 million degree gas extending away from the center of the cluster. These structures show that the inflow of cooling gas is deflected by magnetic fields produced by explosions from a central black hole.

Hya A is radiogalaxy near the center of the cluster. Optical observations show a few hundred galaxies in the cluster. Chandra X-ray observations reveal a large cloud of hot gas that extends throughout the cluster. The gas cloud is several million light years across and has a temperature of about 40 million degrees in the outer parts decreasing to about 35 million degrees in the inner region.

3C295 (Cl 1409+524)
z= 0.461

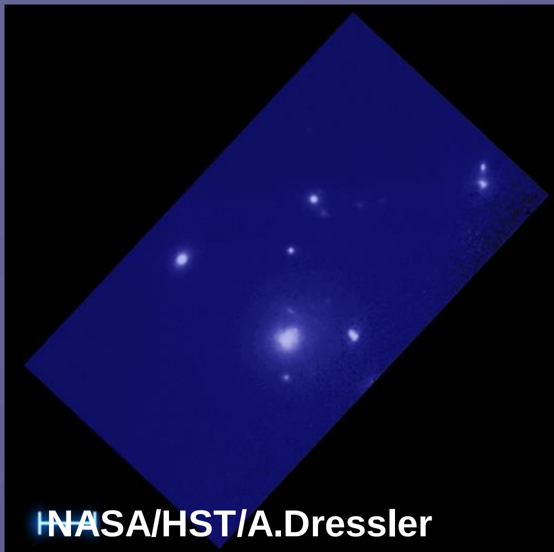
NASA/HST/A.Dressler


Credit: NASA/CXC/SAO

Radio: NRAO/AUI/NSF/ R.Perley & G.Taylor
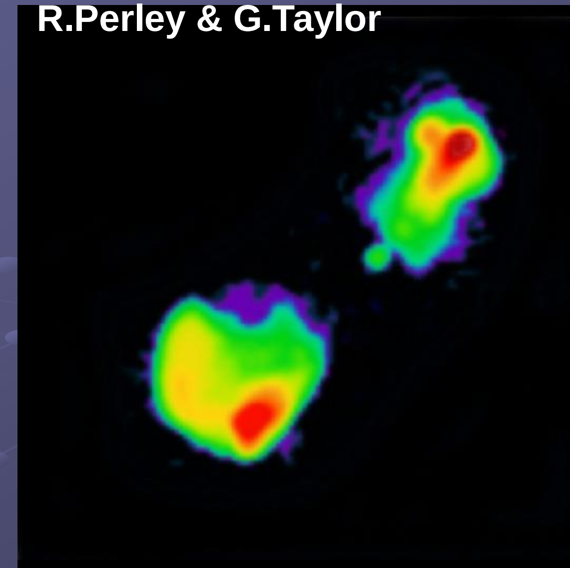

3C295 (Cl 1409+524) cluster is filled with a vast cloud of fifty million degree gas that radiates strongly in X rays. 3C295 was first discovered as a bright source of radio waves. The source of the radio emission was found to be a giant elliptical galaxy located in the center of the cluster of galaxies. Chandra discovered that this central galaxy is a strong, complex source of X-rays.

First: The Uhuru X-ray satellite
(lifetime: 12 Dec 1970 - March 1973),
which carried out the first X-ray sky survey.

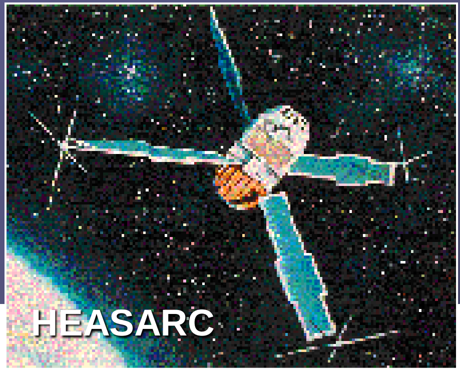

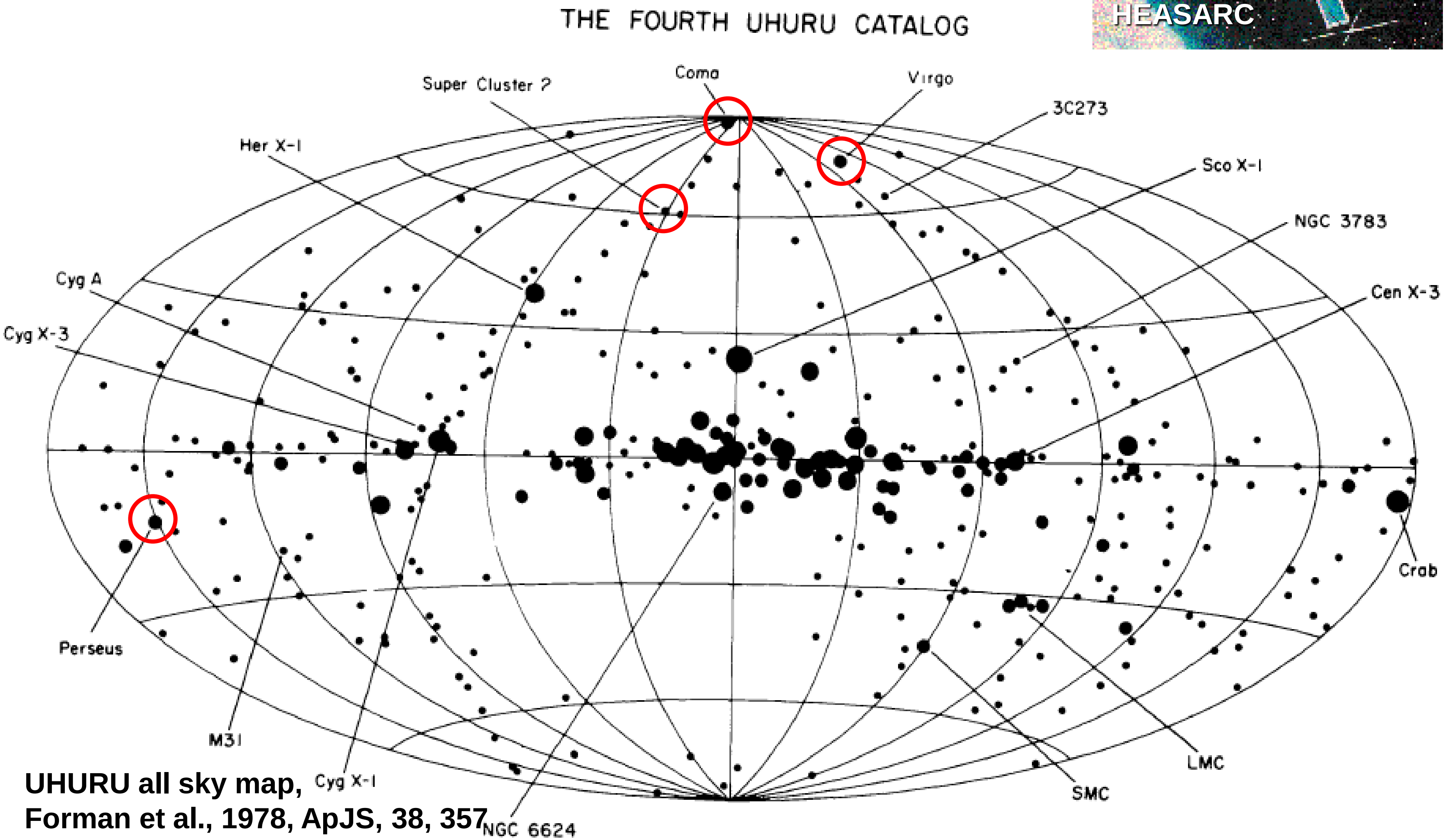

UHURU all sky map,
Forman et al., 1978, ApJS, 38, 357

Uhuru observations (energy range: 2-20 keV) established a number of properties of the X-ray sources associated with clusters:

1. The clusters of galaxies are the most common bright extragalactic X-ray sources.
2. The clusters of galaxies are extremely luminous in their X-ray emission, with luminosities approx 10^{43}-10^{45} ergs/s, and they have a wide range of luminosities. This makes clusters as a class the most luminous X-ray sources in the Universe, with the exception of quasars.
3. The X-ray sources associated with clusters are extended; the sizes found from the Uhuru data range from about 200 to 3000 kpc.
4. The clusters have X-ray spectra showing weak evidence for low energy photoabsorption, contrary to the spectra of the compact sources associated with the nuclei of galaxies.
5. The X-ray emission from clusters is constant in time.

Three results points suggest that the emission is truly diffuse

First:

Ariel-V (UK, USA), in X-ray spectrum of the Perseus Cluster detected 7 keV emission feature, correspond to Fe XXV and Fe XXVI transitions. It is provides strong evidence for the presence of hot plasma in the cluster (Mitchell at al., MNRAS, 1976, 175, 29).

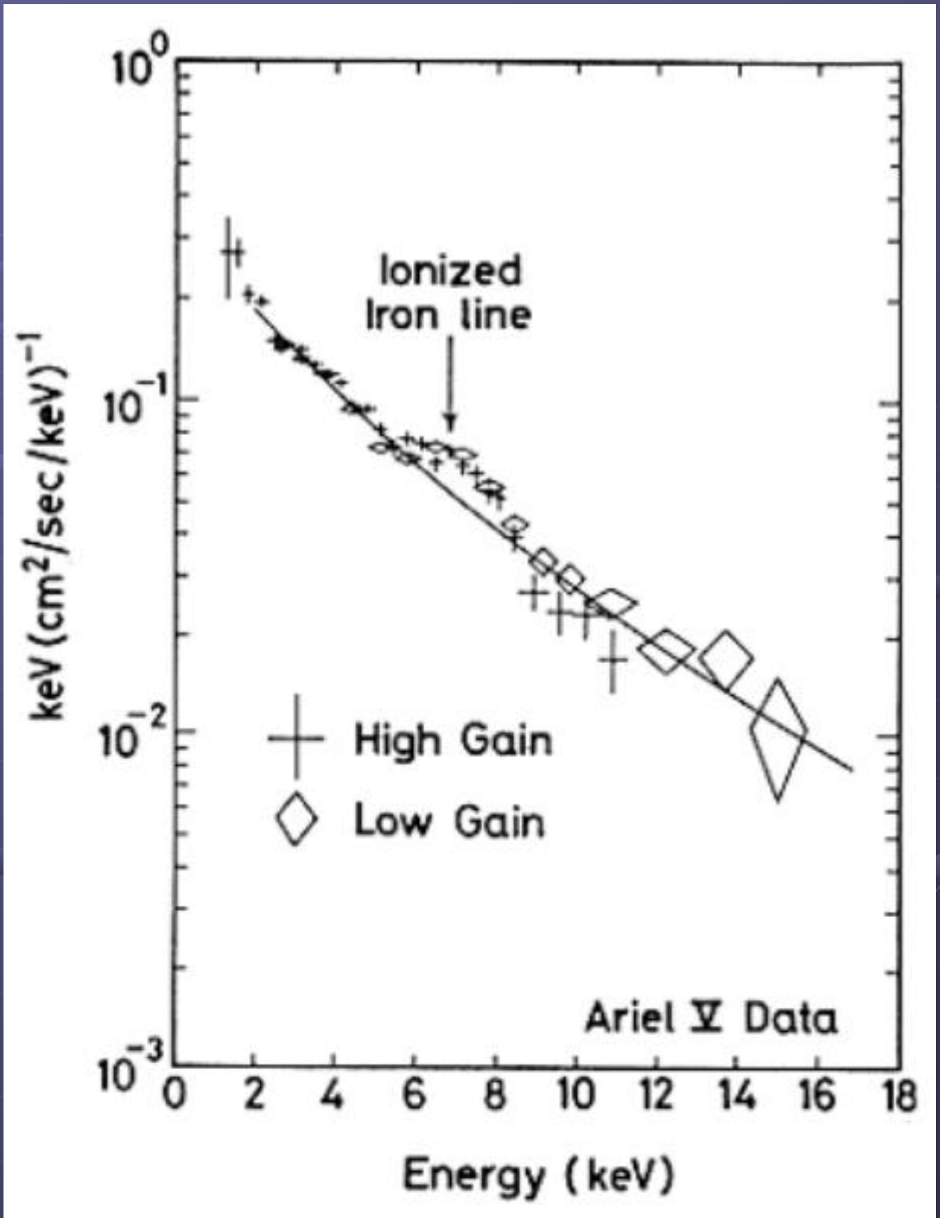

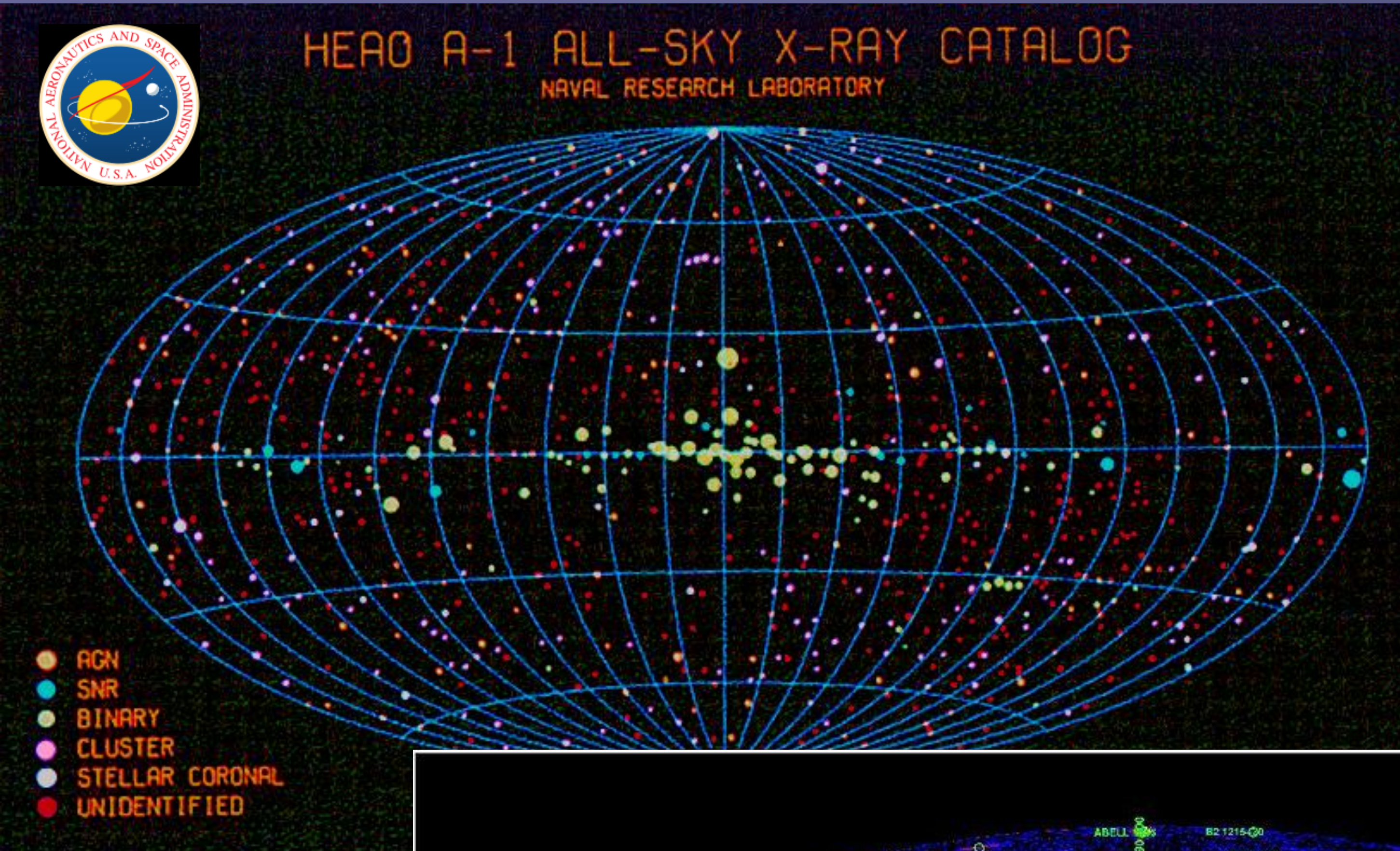

The next major advance in sensitivity came with the launch of the HEAO-1 X-ray observatory

Galactic ridge X-ray emission, measured by HEAO 1, (A2), 1977-1979

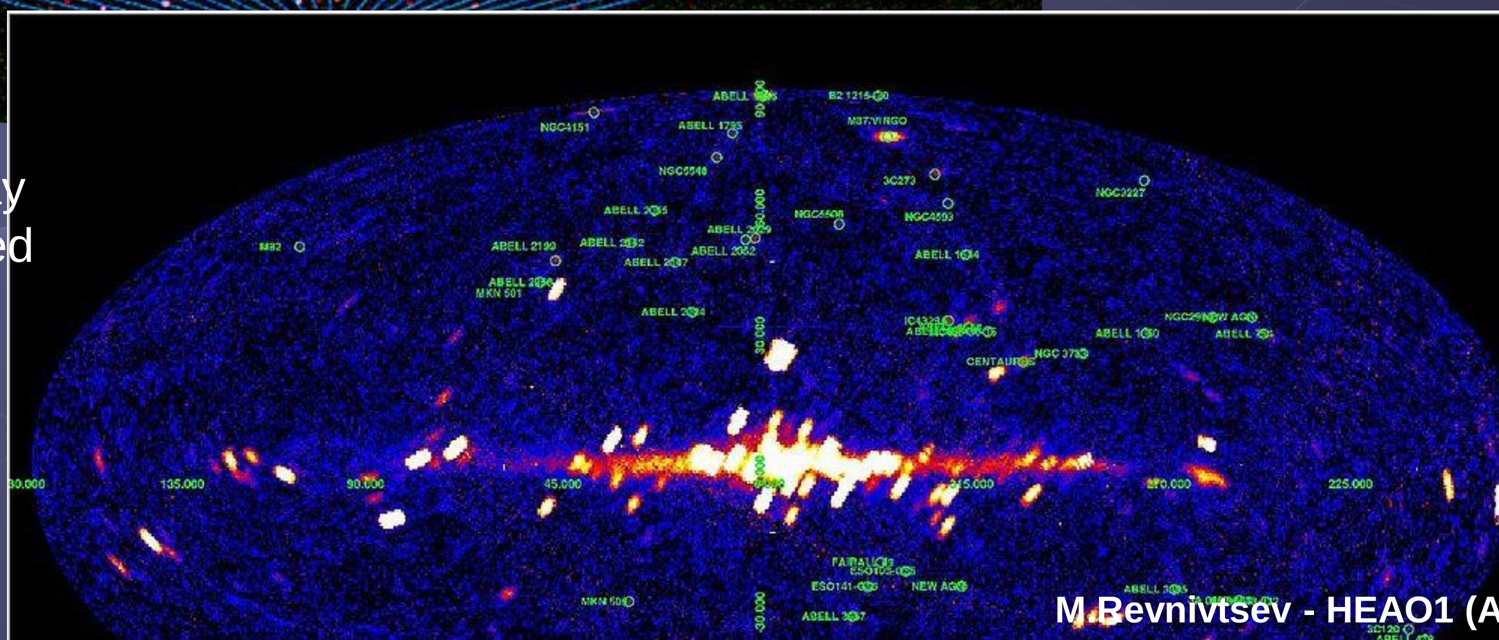

Einstein observatory (HEAO B, launched in 1978)
First imaging X-ray telescope +
spectrometer 500 mm-1 & 1000 mm-1,
energy resolution dE/E ~ 50.
Record angular resolution ~2 *arcsec* (better only
Chandra launched 1999).

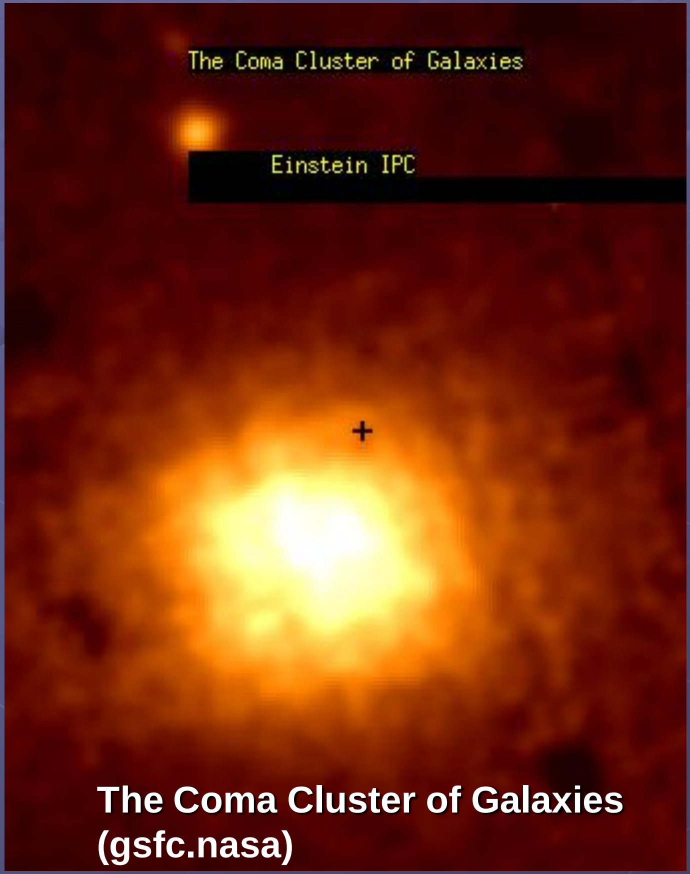

The Coma Cluster of Galaxies (gsfc.nasa)

Results:

- All-sky imaging survey in the 0.2-2.5 keV range.
- First study of the X-ray emitting gas in galaxies and clusters of galaxies revealing cooling inflow and cluster evolution.
- First medium and deep X-ray surveys.

ROSAT Röntgensatellit (1990 - 1999), 0.042 to 021 KeV., r=5 *arcsec*$^{-1}$)

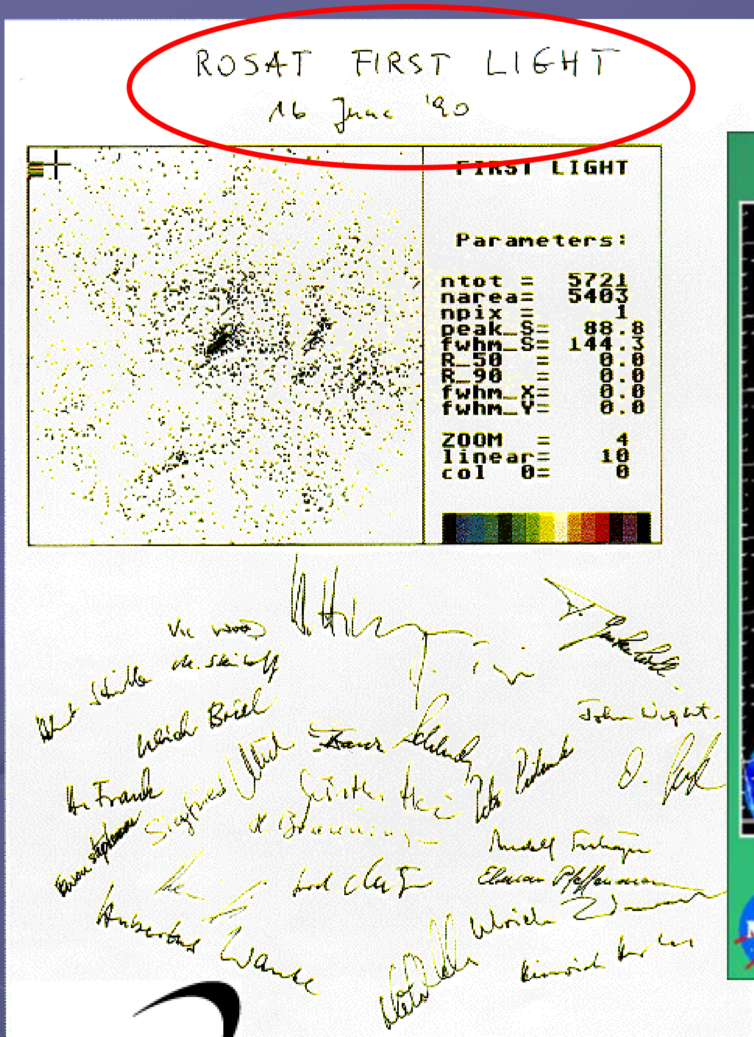

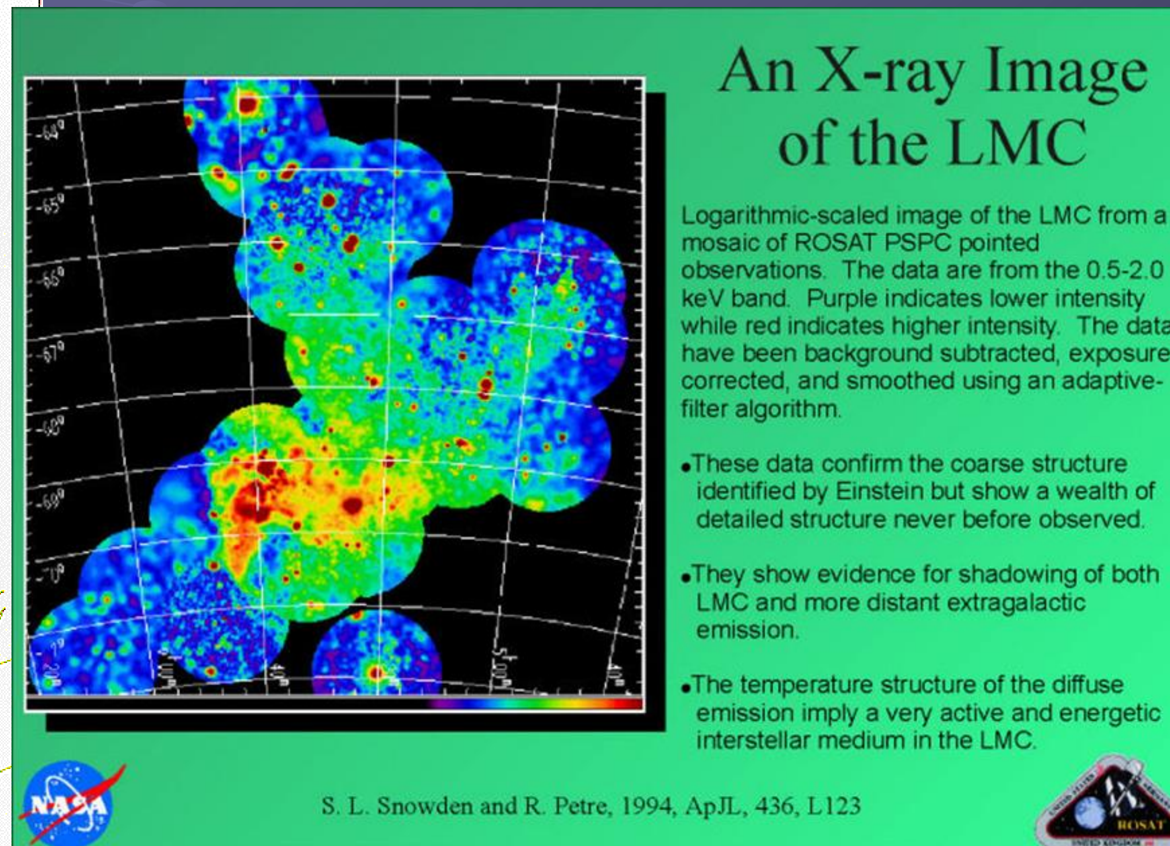

Large Magellanic Cloud.

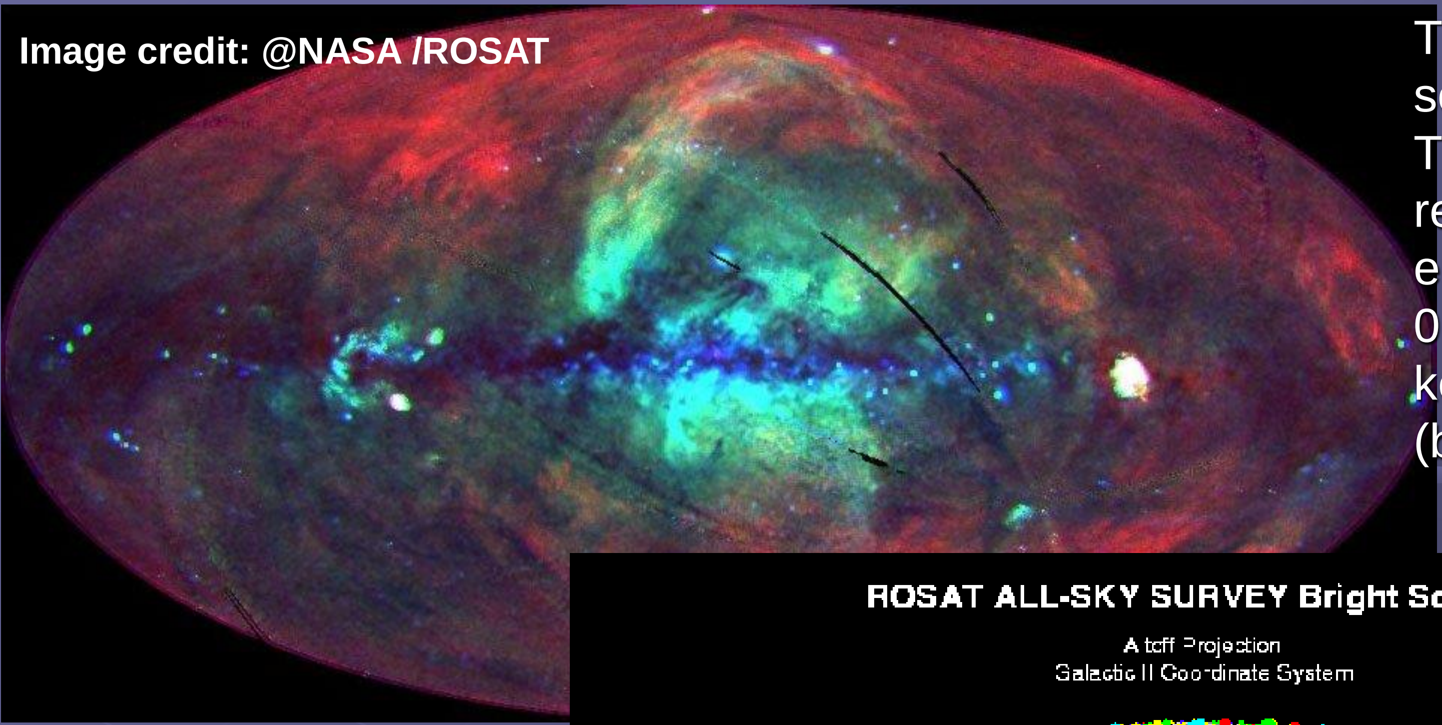

This ROSAT all-sky soft X-ray image. The different colours represent different energy bands: 0.25 keV (red), 0.75 keV (green), 1.5 keV (blue).

150 000 X-ray sourses

and
18 811 Bright Sources
(RASS-BSC)

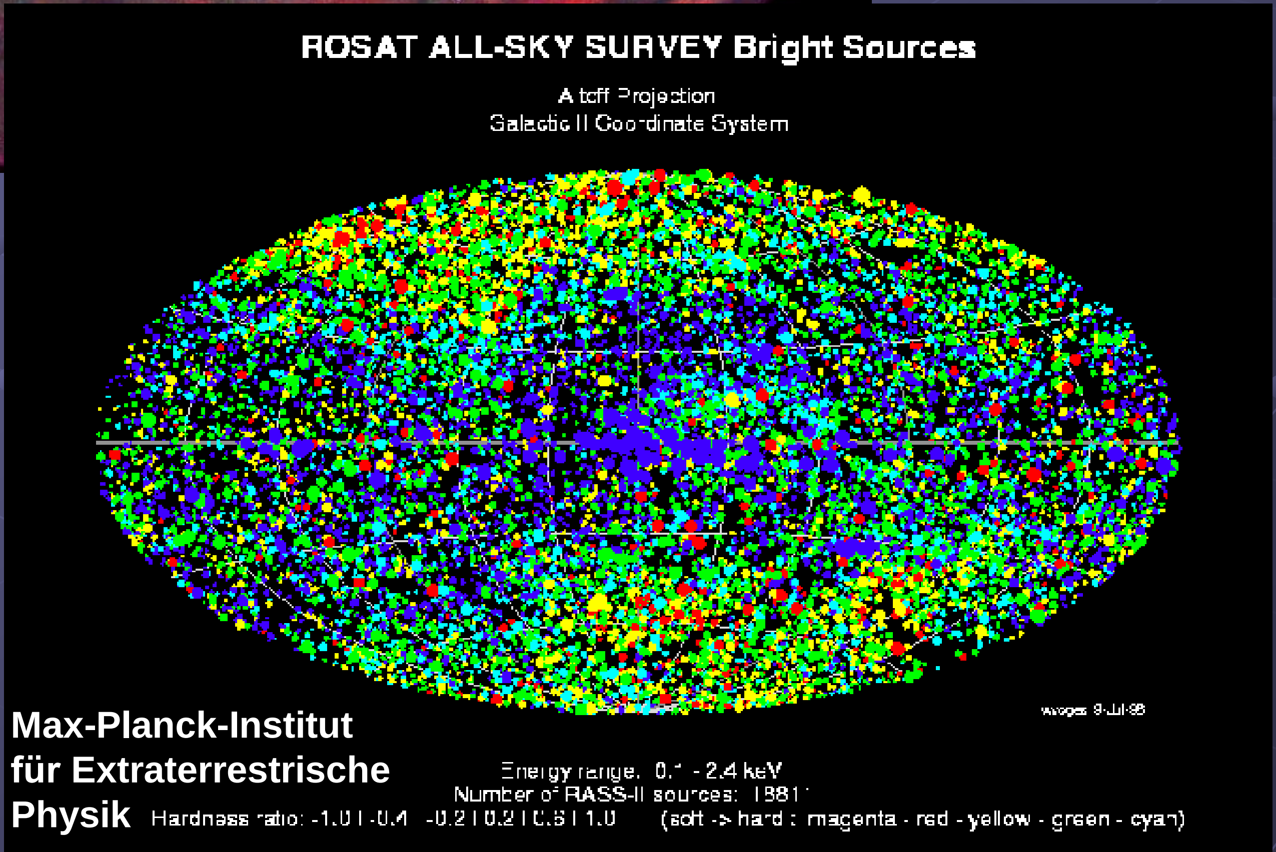

Max-Planck-Institut für Extraterrestrische Physik

Based on 0.1 − 2.4 keV ROSAT DATA:

REFLEX (ROSAT-ESO, Böhringer et al. 2004a) is based on RASS data, covers the southern sky up to a declination $\delta = 2.5$ deg with the galactic plane ($|b| \leq 20$ deg). The total survey area is 13924 deg^2 and the survey is flux-limited (band flux $\geq 3 \times 10^{-12}$ erg s^{-1} cm^{-2}).

NORAS (Northern ROSAT All-Sky galaxy cluster survey B¨ohringer et al. 2000a) is also based on RASS data excluding the same region around the galactic plane, but covers the northern sky.

The **ROSAT BCS** (The ROSAT Brightest Cluster Sample, Ebeling et al. 1998) comprises the brighter sources of the NORAS survey. We use data for the 90 per cent complete BCS, a flux-limited sample (band flux $\geq 4.4 \times 10_{-12}$ erg s^{-1} cm^{-2}) of **$z \leq 0.3$** clusters.

The **eBCS** (The extended ROSAT Brightest Cluster Sample, Ebeling et al. 2000a) is the low flux extension of the BCS (band flux $\geq 2.8 \times 10^{-12}$ erg s^{-1} cm^{-2}).

The **SGP** (A Catalog of Clusters of Galaxies in a Region of 1 Steradian around the South Galactic Pole, Cruddace et al. 2002a) covers a region of 1.013 sr centered on the south Galactic pole and is based on the same X-ray source detection and characterisation procedures as REFLEX. The lowest detected flux is 1.5×10^{-12} erg s^{-1} cm^{-2}, and a complete sub-sample can be obtained by imposing a flux limit of $3 \times 10^{-1}2$ erg s^{-1} cm^{-2} .

The **MACS** (Massive Cluster Survey, Ebeling et al. 2001) is based on the ROSAT Bright Source Catalogue with the aim of increasing the number of known very luminous, **$z \geq 0.3$** clusters.

The **CIZA** (Clusters in the Zone of Avoidance, Ebeling et al. 2002 and Kocevski et al. 2007, respectively CIZAI and CIZAII) catalogues are based on the ROSAT R.

The **MCXC** Catalogue is focused on the region around the galactic plane ($|b| \leq 20$ deg).

Great Observatories Epoch: XMM and Chandra

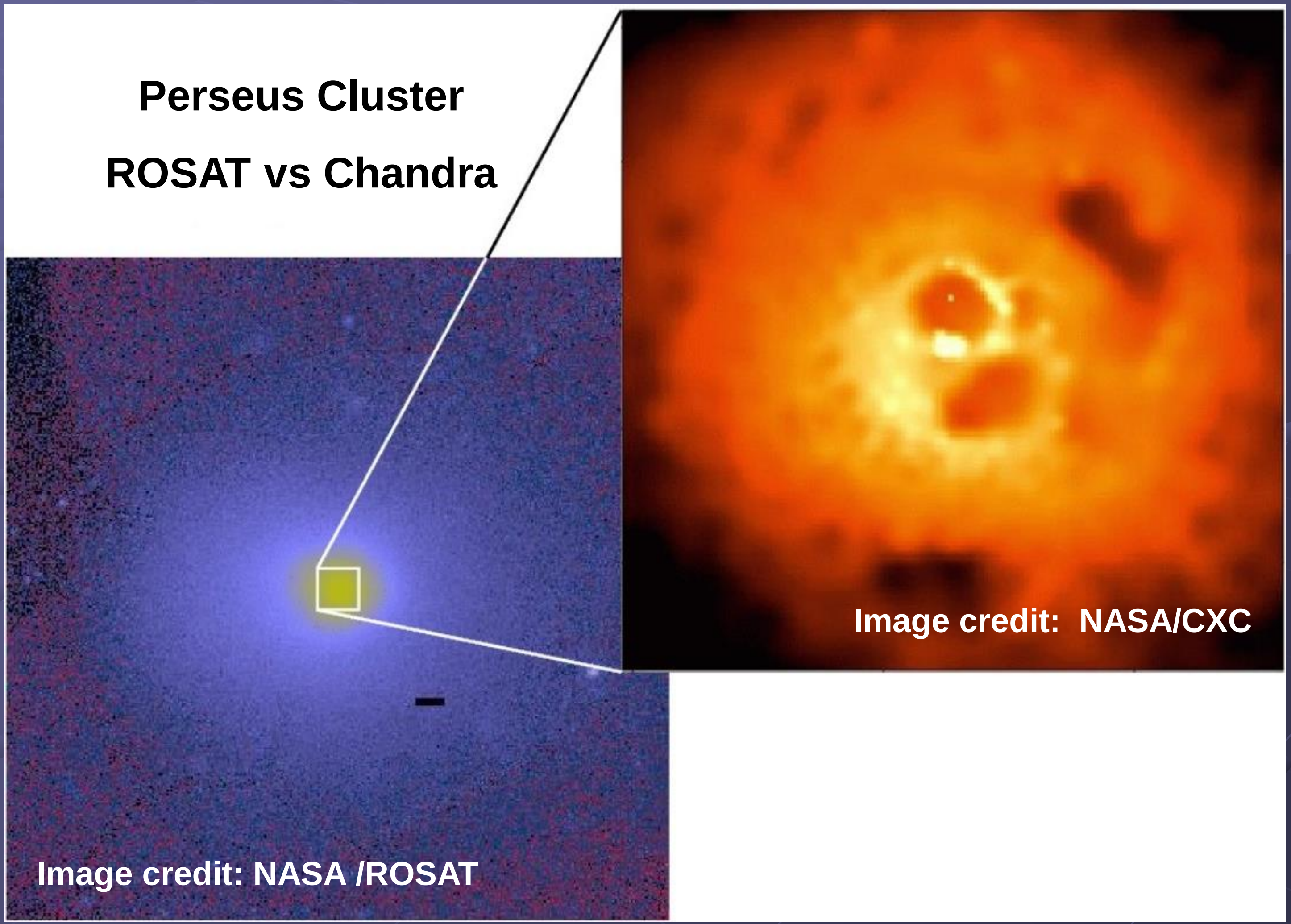

Great Observatories Epoch

XMM Newton

XMM-Newton has 3 mirrors, 2 of which have reflection gratings, providing simultaneous high resolution spectroscopy and imaging.

Band	Energy range	Flux limit
Soft band	0.2-2 keV	5.7×10-13 ergs s^{-1} cm^{-2}
Hard band	2-12 keV	3.7×10-12 ergs s^{-1} cm^{-2}
Full band	0.2-12keV	1.3×10-12 ergs s^{-1} cm^{-2}

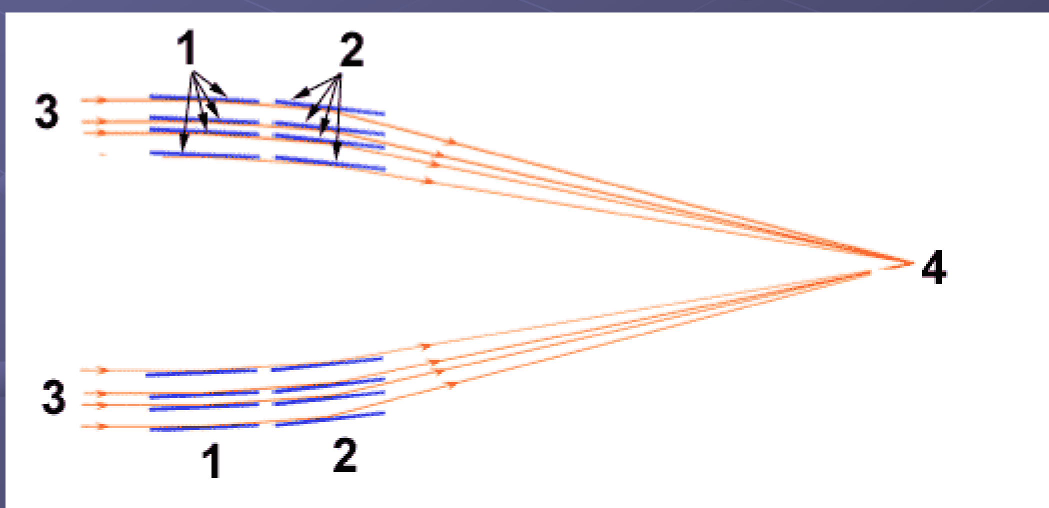

Wolter Type 1 optical system:
1) Parabolic mirrors;
2) Hyperbolic mirrors;
3) X-rays;
4) Focal point.

Great Observatories Epoch

Chandra

Chandra, the best (and most expensive) telescope, giving a sub-arcsecond resolution is a successor to ROSAT.

HRC resolution ~0.2 *arcsec* 0.1–10 keV

And spectrometers:

The High Energy Transmission Grating Spectrometer (HETGS)

0.4–10 keV with a spectral resolution of 60–1000.

The Low Energy Transmission Grating Spectrometer (LETGS)

0.09–3 keV with a spectral resolution of 40–2000.

Advanced CCD Imaging Spectrometer (ACIS),

0.1–10 keV and a time resolution of 16 microseconds.

Chandra vs. XMM-Newton

Chandra is best for:

- Anything requiring better than 5 *arcseconds* spatial resolution.
- High resolution spectroscopy for energies < 0.5 or > 2 keV.

XMM-Newton is best for…

- Imaging or imaging-spectroscopy which does not require a resolution of 5 *arcseconds* or better.
- High resolution spectroscopy for energies 0.5 < E < 2 keV.
- High resolution spectroscopy on extended objects that are larger than 10 *arcseconds* and smaller than 1 *arcminute*.

Characteristic	***Chandra* ACIS-I**	***XMM-Newton* MOS**	***XMM-Newton* pn**
Number of instruments	1	2	1
Energy range in keV	0.3 – 10	0.15 – 12	0.15 – 12
FOV in diameter	16.9′	30′	30′
PSF (FWHM/HEW)	0.2″/0.5″	5″/14″	6″/15″
Pixel size	0.5″	1.1″	4.1″

Chandra + XMM-Newton + … is great!

Solid angles, flux and redshifts of X-ray cluster surveys since 1990

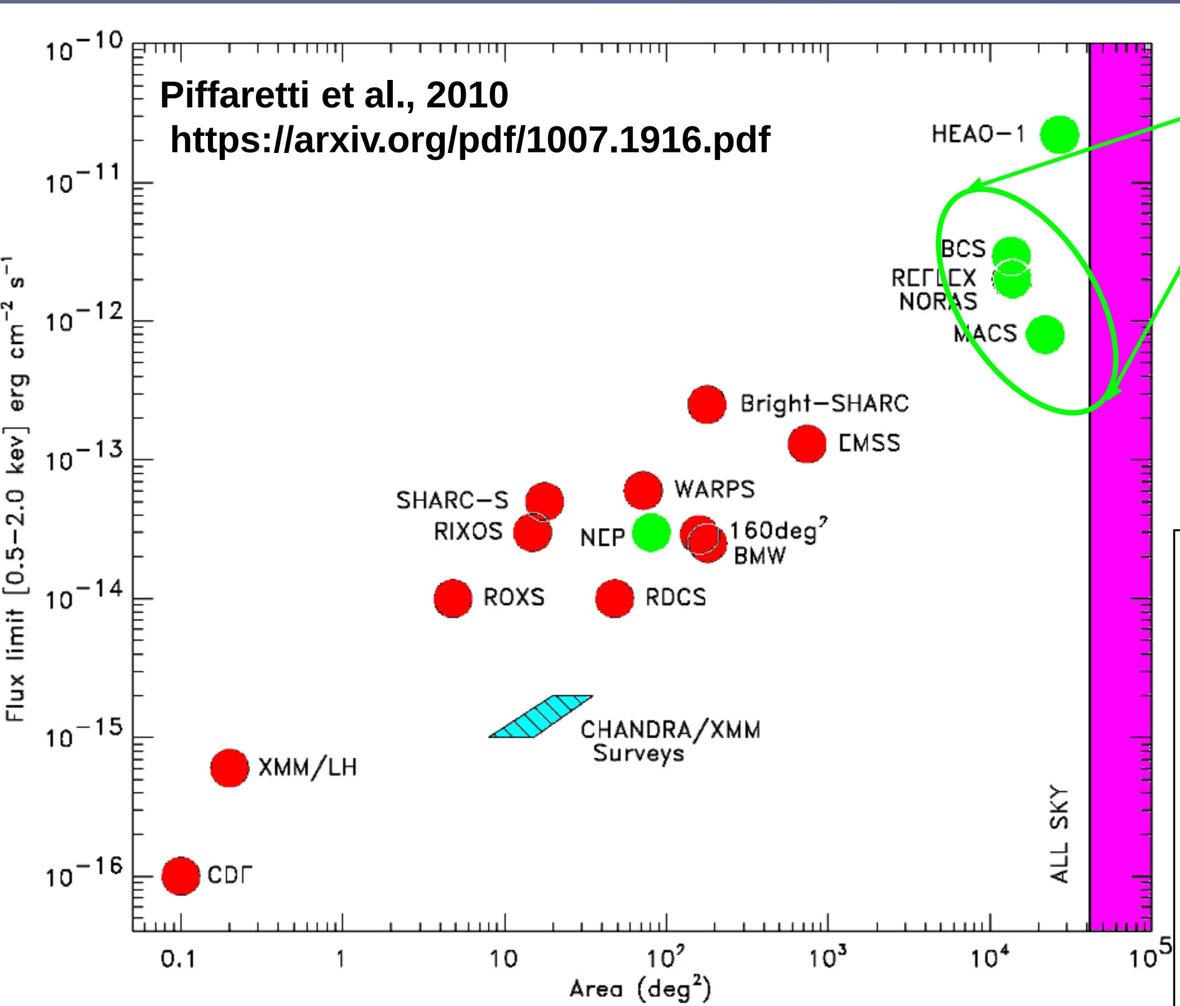

"The MCXC: a Meta-Catalogue of X-ray detected Clusters of galaxies"
Piffaretti et al., 2010
https://arxiv.org/pdf/1007.1916.pdf

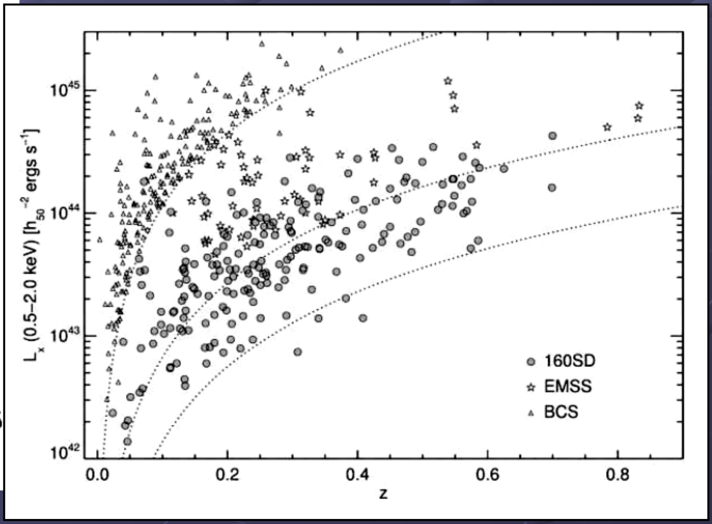

Green circles represent serendipitous surveys constructed from a collection of pointed observations. Red circles represent surveys covering contiguous areas. The pink region is a predicted locus of serendipitous surveys with Chandra and Newton-XMM.

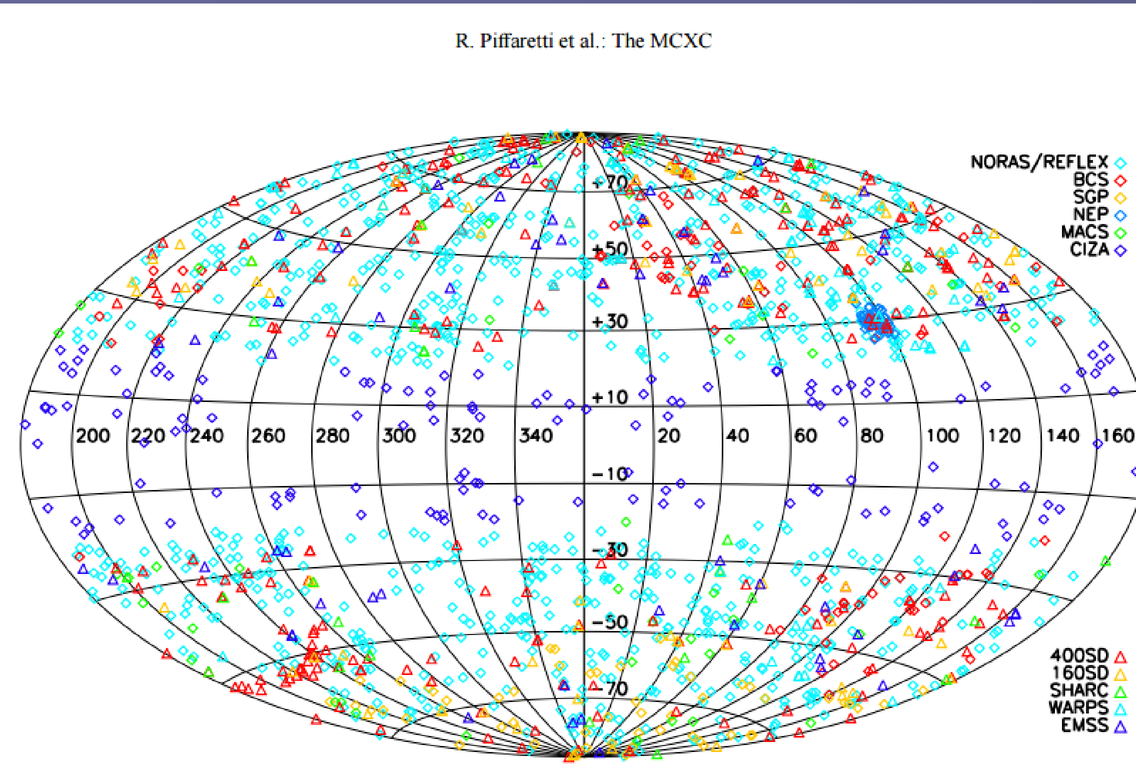

Sky map of the 1743 MCXC clusters in galactic coordinates.

Diamonds and triangles indicate clusters from RASS-based and serendipitous catalogues, respectively

Right: The 0.1 – 2.4 keV band luminosities L_{500} of the 1743 MCXC clusters as a function of redshift.

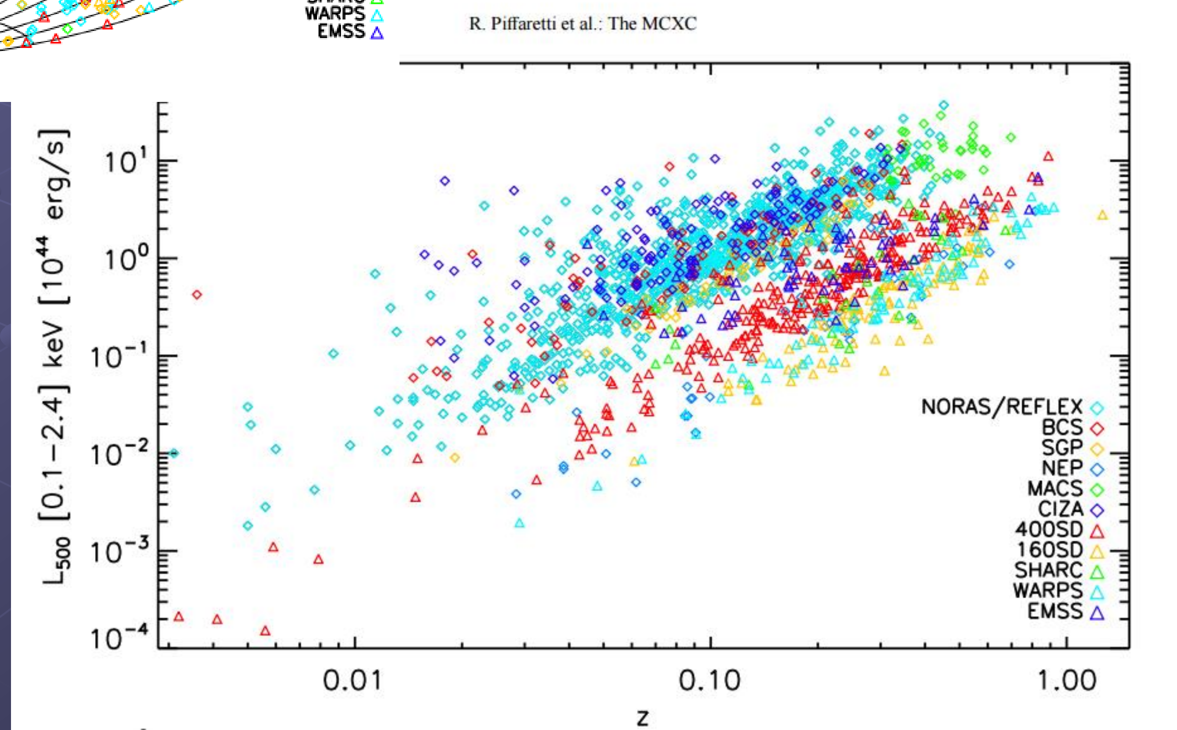

XXL Hunt for Galaxy Clusters

The XXL survey has combined archival data as well as new observations of galaxy clusters covering the wavelength range from 1 × 10^{-4} μm (X-ray, observed with XMM) to more than 1 meter (observed with the Giant Metrewave Radio Telescope GMRT).

Visible light view of a distant galaxy cluster discovered in the XXL survey (PR Image eso1548c)

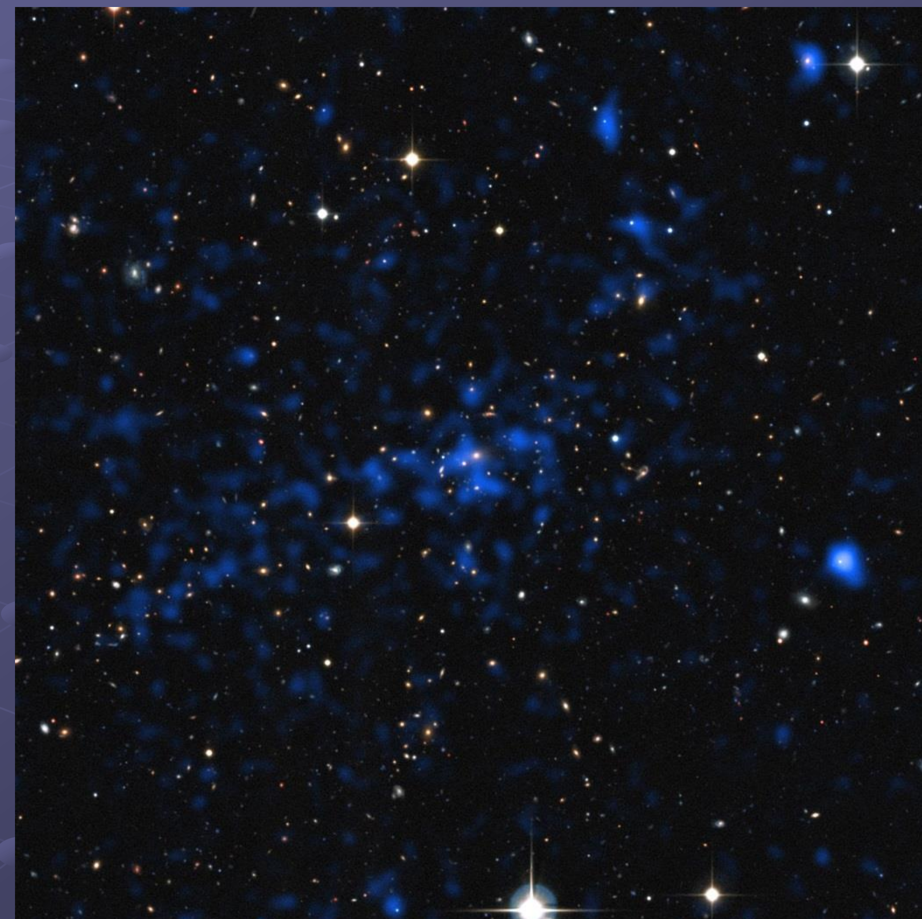

Composite of X-ray and visible light views of a distant cluster of galaxies (PR Image eso1548d)

ESO1548 — Science Release 15 December 2015

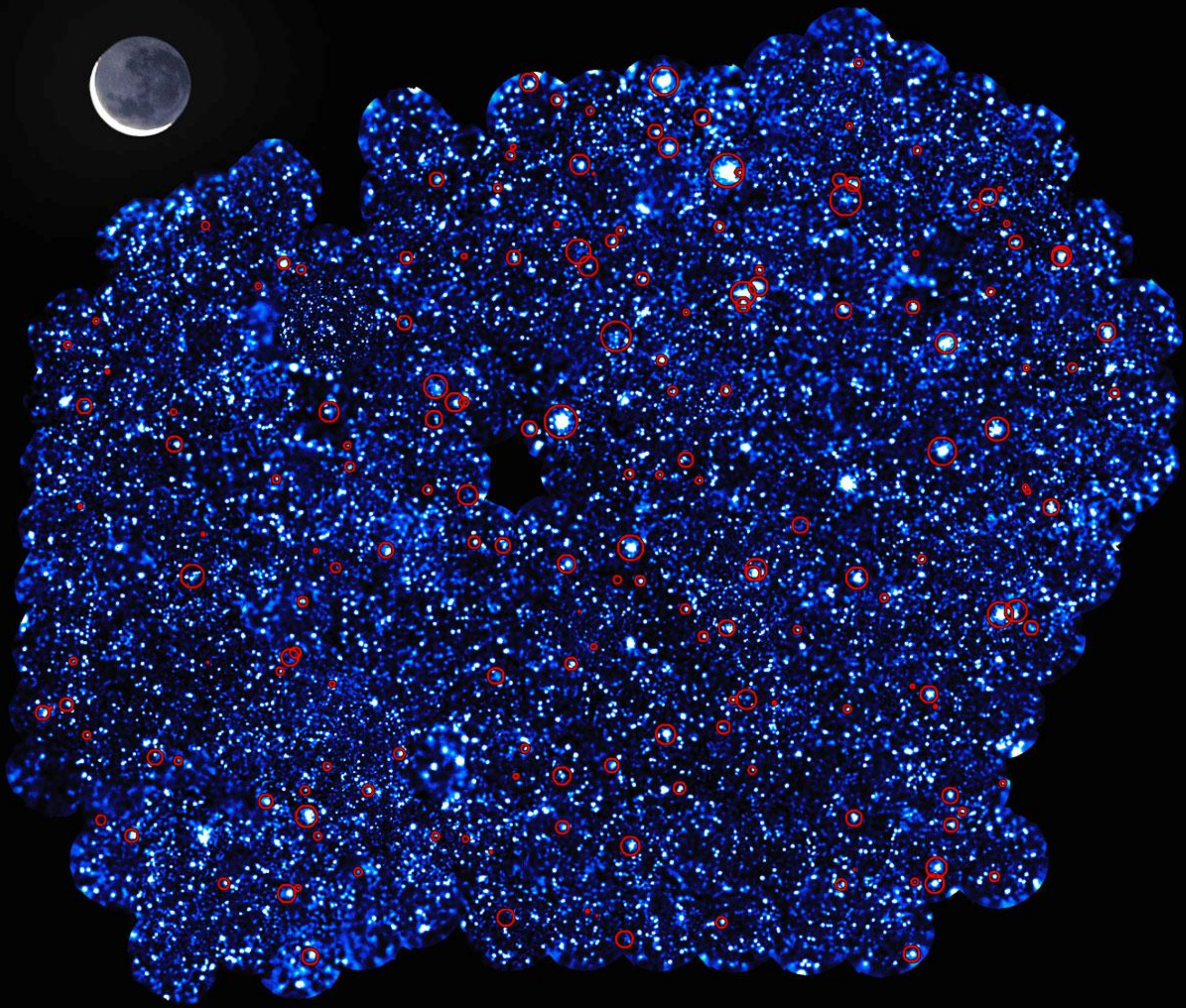

XXL-South Field: region of 25 deg^2 23^{h}30^m -55°00' (J2000)

Image credits: ESA/XMM-Newton/XXL survey consortium (S. Snowden, L. Faccioli, F. Pacaud).

XXL Hunt for Galaxy Clusters

Founded galaxy clusters with z from 0.05 to 1.05.

Observations by the VLT and the NTT complement those from other observatories across the globe and in space.

X-ray image of the XXL-South Field.

Clusters are noted as red circles.

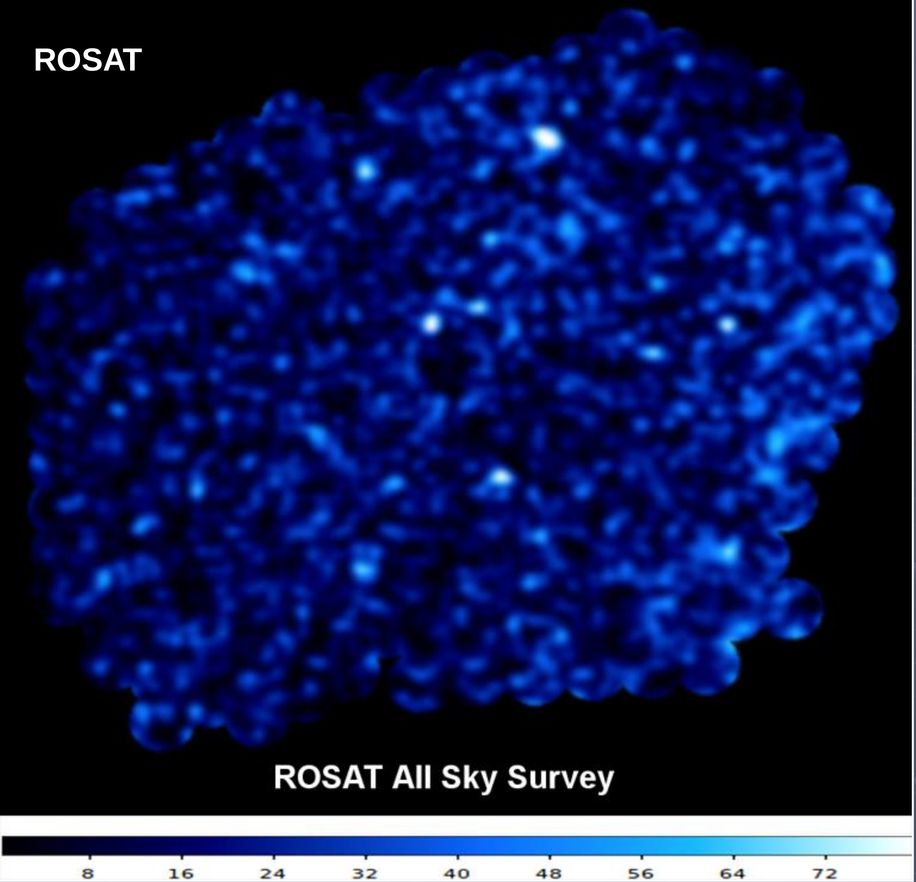

XMM image of field XXL-S. Over **12000 sources** detected in this image. The red circles show the clusters of galaxies.

XXL-N in in the process (*X-Ray Group MPE*).

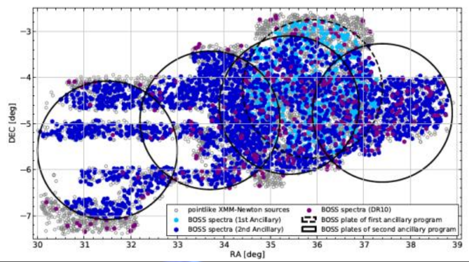

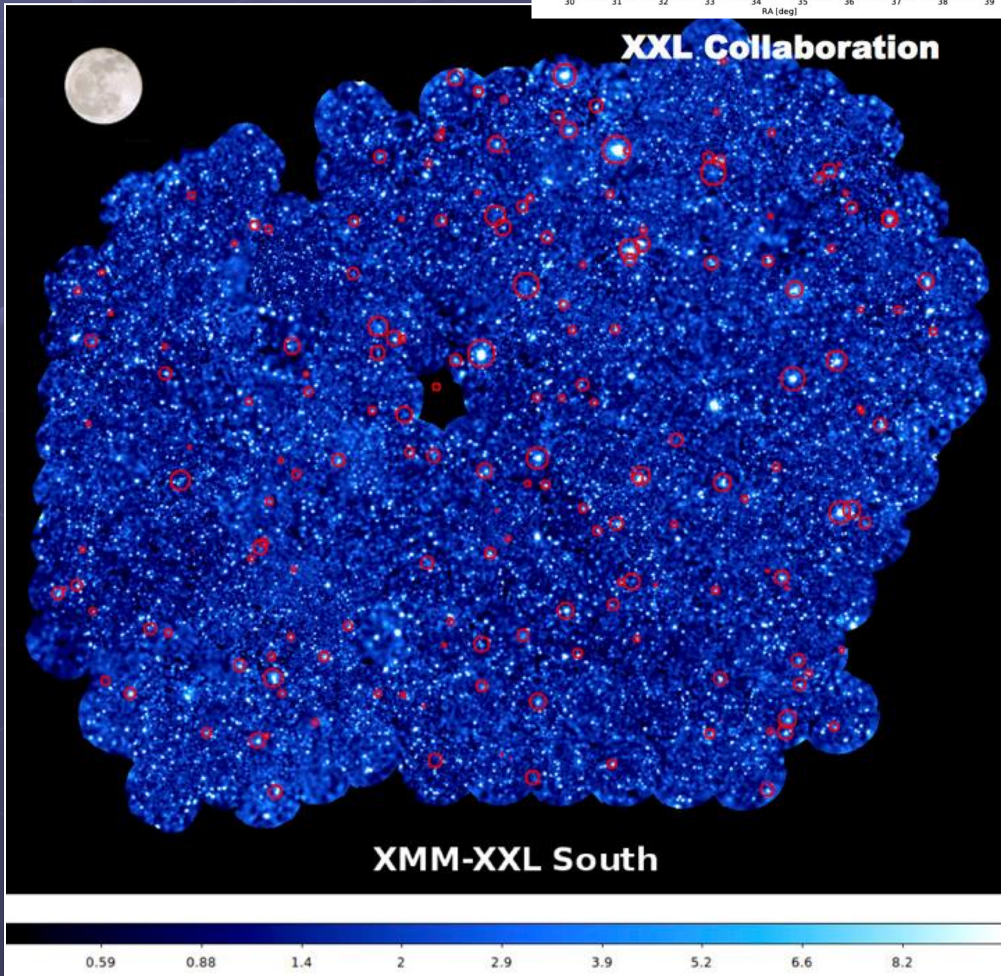

The XXL-S area as observed by ROSAT in 1999, for comparison. Only **45 sources** were detected in this image.

X-ray data and properties of galaxy clusters

Observed relationships between the X-ray–determined bolometric luminosity, L_X, the temperature, T, of the intracluster gas, and the optical measured velocity dispersion, σ, of the cluster' galaxies

If this gas shares the same dynamics as member galaxies, then it is expected to have a typical temperature:

$$k_B T \cong \mu m_p \sigma^2 = 6\left(\frac{\sigma}{10^3\, km/s}\right)^2 KeV$$

Where: m_p is the proton mass; μ is the mean molecular weight (0.6)
for a primordial composition with a 76% fraction contributed by hydrogen).

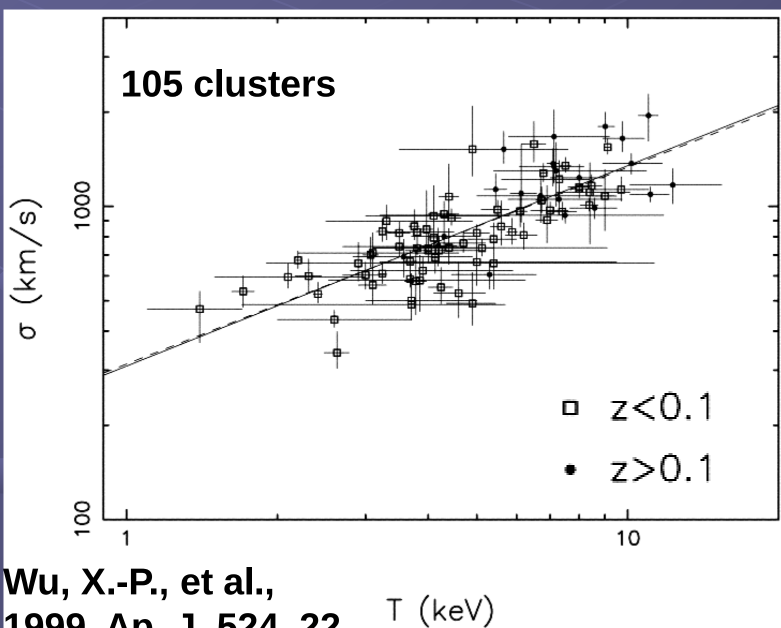

Wu, X.-P., et al., 1999. Ap. J. 524, 22.

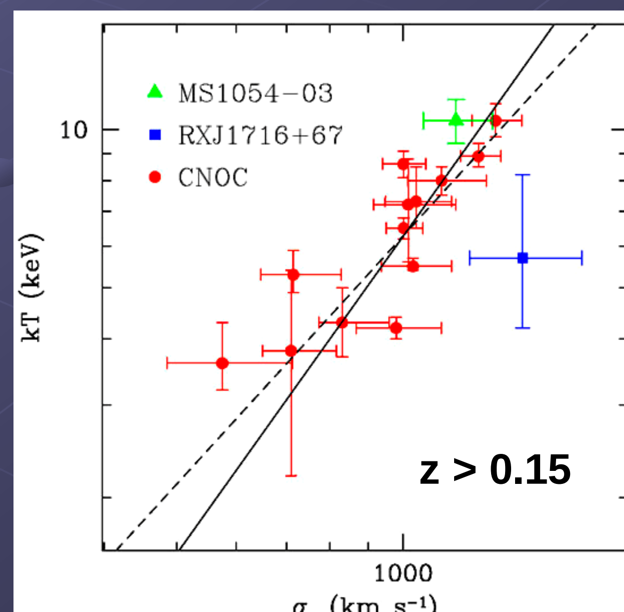

The solid line -- the relation; the dashed line is the best-fit.

https://ned.ipac.caltech.edu/level5/March05/Rosati/Rosati_contents.html

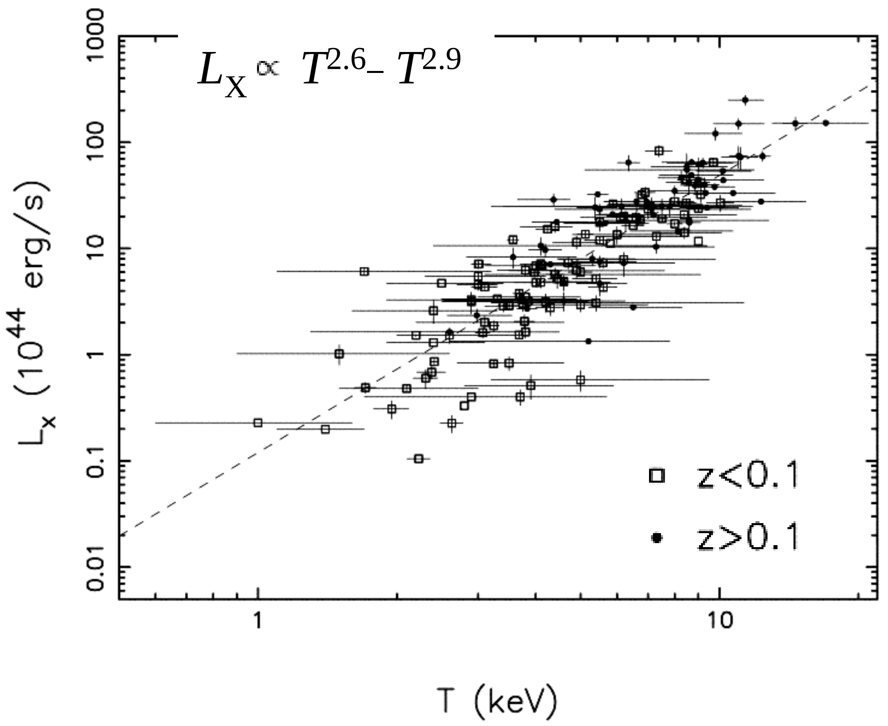

L_X-T relationship for 168 clusters (Wu, X.-P., et al., 1999. Ap. J. 524, 22).

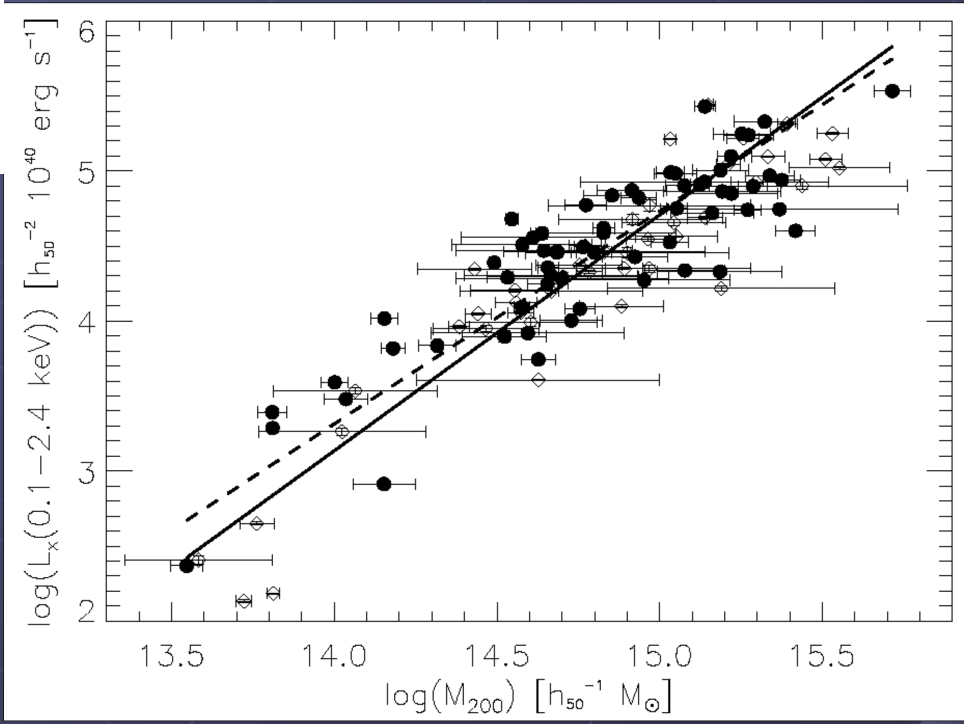

The low-z relation between X-ray luminosity and the mass contained within the radius encompassing an average density 200 ρ_c (from Reiprich & Böhringer, 2002). The two lines are the best log-log linear fit to two different data sets indicated with filled and open circles.

The XXL Survey. Baryon content of the bright cluster sample

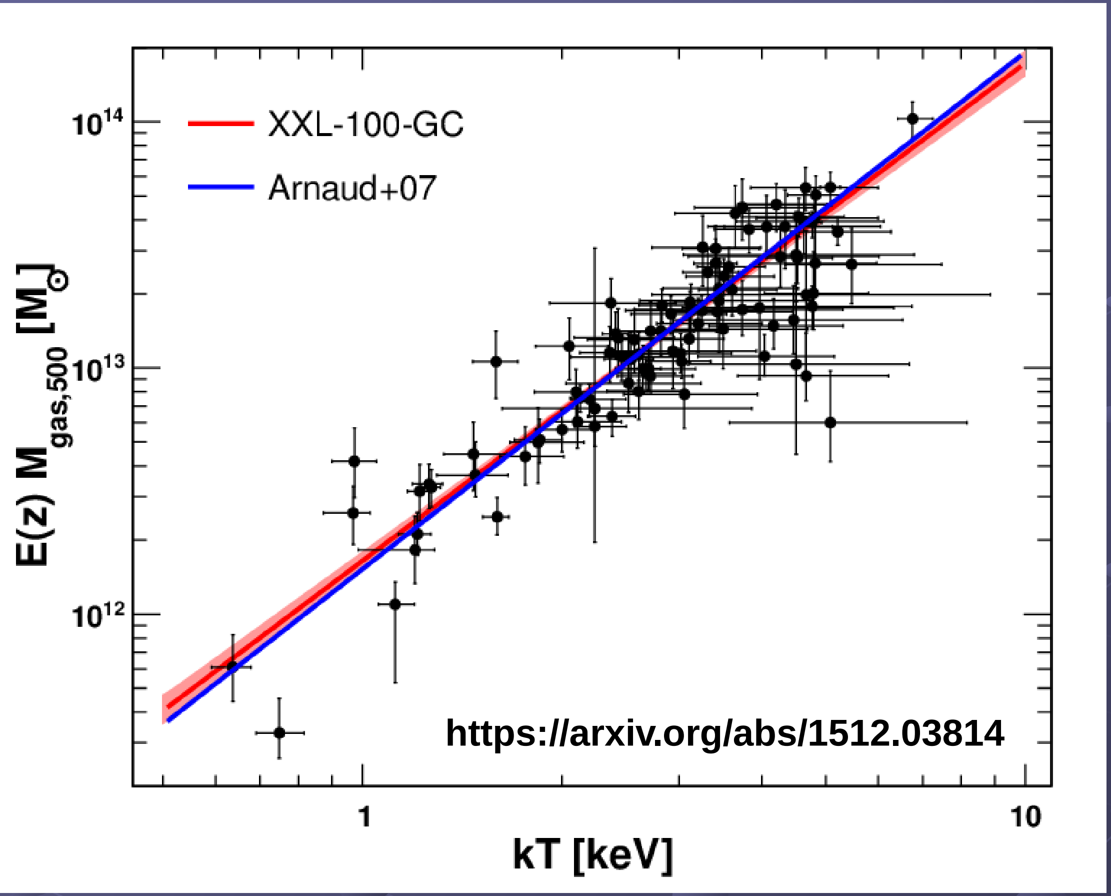

Gas mass within r_{500}, MT for the XXL-100-GC sample as a function of their temperature within a fixed aperture of 300 kpc. The red line and the red shaded area show the best-fit relation and its uncertainty. The blue curve represents the relation of Arnaud et al. (2007).

X-ray images of clusters and the morphology of the intracluster gas

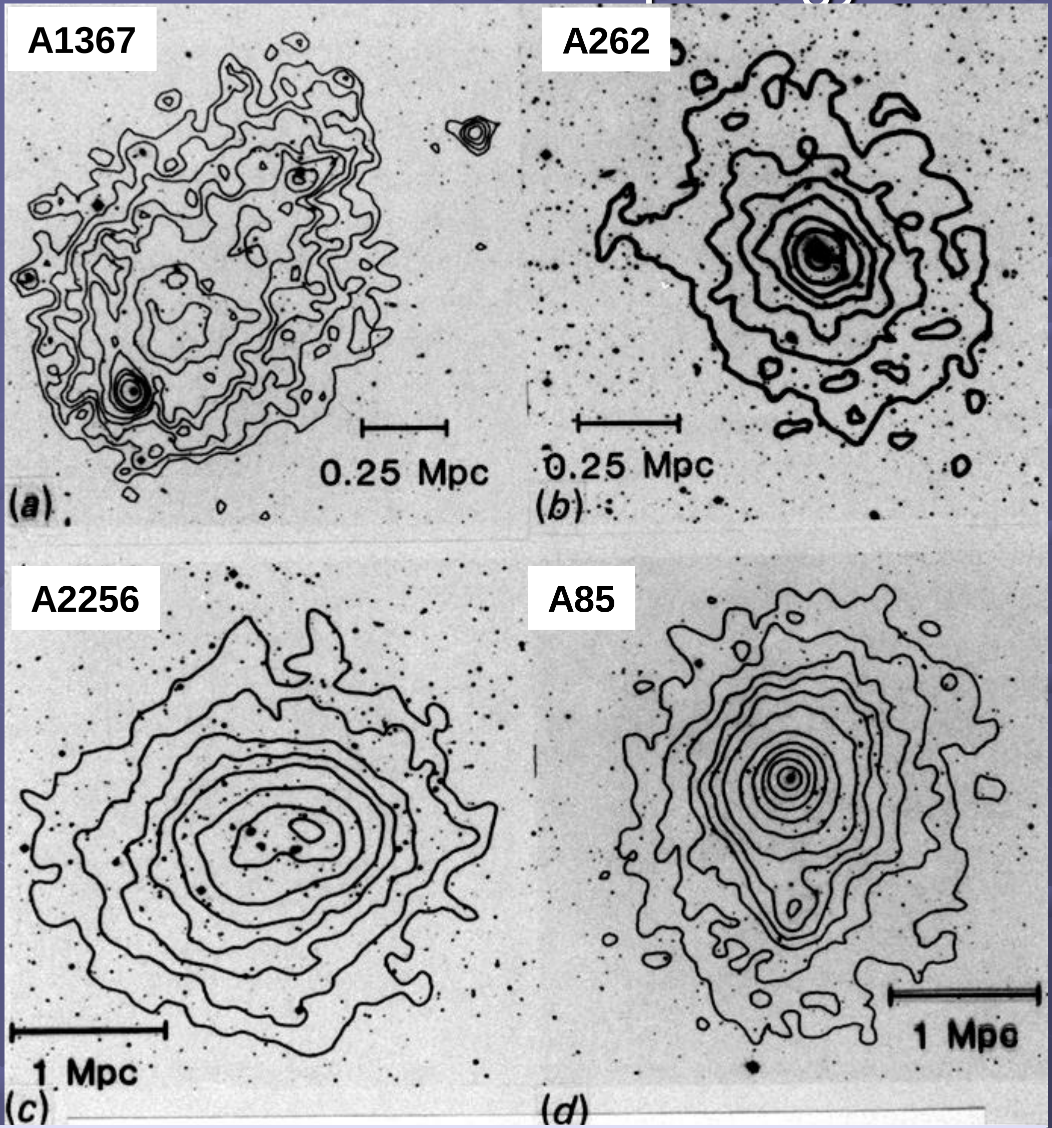

Contours of constant X-ray surface brightness + optical images of the clusters from Jones and Forman (1984).

The first X-ray morphology of clusters of galaxies: Regular, Irregular, Double clusters

The prototypes
A1367: the irregular nXD cluster

A262 the irregular XD cluster.

A2256 the regular nXD cluster

A85: the regular XD cluster, showing the X-ray emission centered on the cD galaxy.

Based on Einstein data

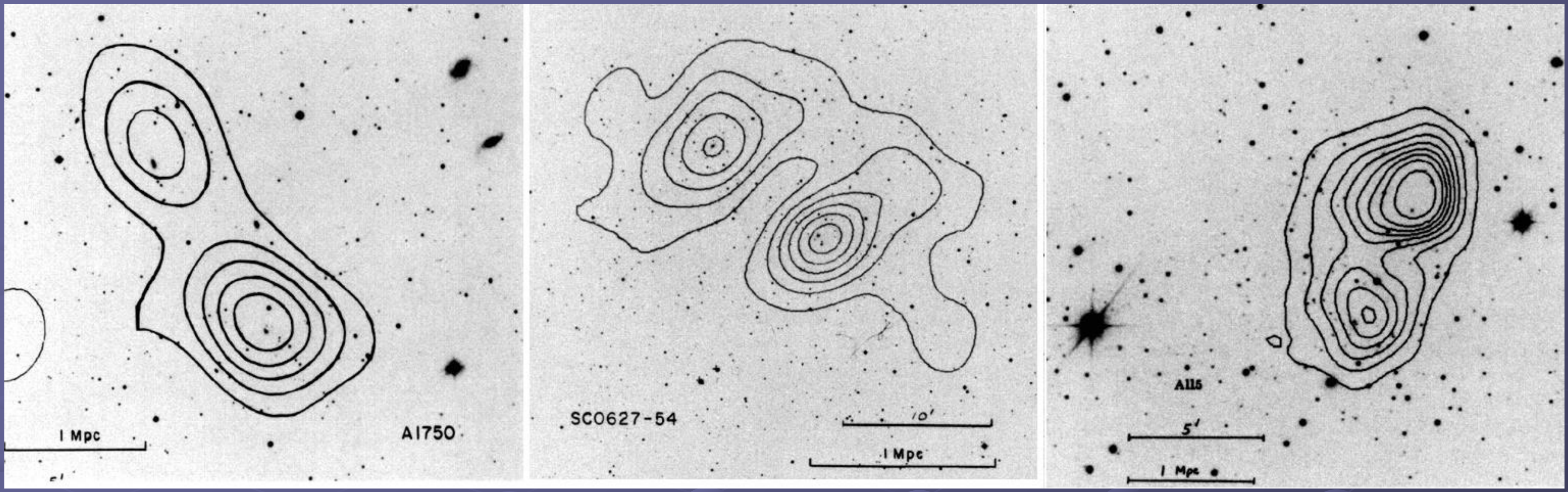

The X-ray surface brightness in double clusters, from Forman et al. (1981). Contours of constant X-ray surface brightness are shown superimposed on optical images of the clusters.

In 1992 Jones and Forman described X-ray types:

single, primary with small secondary, elliptical, off-center and complex. The last 4 classes characterize disturbed clusters.

- single: clusters in which no substructure or departures from symmetry are found
- double: clusters with two subclusters of comparable size and luminosity
- primary with small secondary: clusters in which one of the two subclusters is at least 2 times brighter
- complex: clusters with more than two subclusters
- elliptical: clusters whose X-ray contours are elliptical rather than circular
- offset center: clusters whose peak emission does not lie at the cluster center as determined from lower surface brightness emission

- and one more galaxy-type: in which the emission is dominated by a single galaxy

The morphological classification of clusters is closely related to the study of substructure. The single and galaxy classes contain clusters with appreciable structure. While the double, complex, and primary with small secondary show obvious structure, the elliptical and offset-center clusters generally also are structured systems.

Frequencies of Cluster X-Ray Morphological Classes

(Jones and Forman, ApJ, 511:65 83, 1999)

X-Ray Morphological Class	Example	Number	Percent	Mean L ($\times 10^{43}$ ergs s^{-1})
S (single symmetric peak)...	A401	120	56	29.3
O (offset center)...	A2319	10	5	44.5
E (elliptical)...	A2256	31	14	30.8
C (complex, multiple structures)...	A514	27	13	9.6
D (double)...	A98	13	6	22.1
P (primary with a small secondary)...	A85	7	3	19.9
G (primarily galaxy emission)...	A2666	7	3	0.4

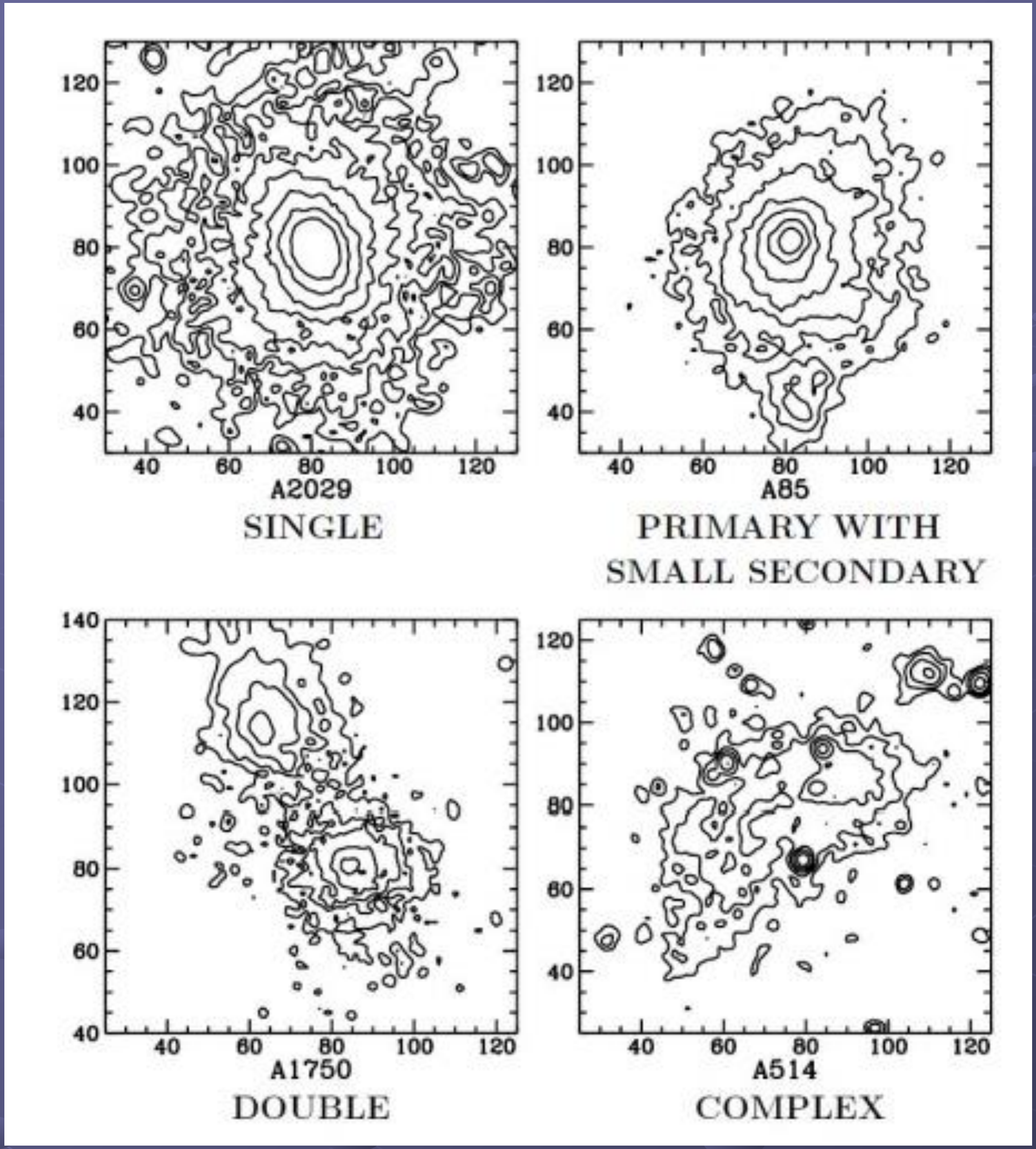

X-ray contours from the ROSAT satellite for four morphological types defined by Jones & Forman (1992).

Figure taken from Buote (2002, in Astrophysics and Space Science Library, Vol. 272, Merging Processes in Galaxy Clusters, ed. L. Feretti, I. M. Gioia, & G. Giovannini, 79–107).

Buote & Tsai (1995, 1996) developed a method to quantify cluster morphology and substructure by "power ratios" that measure the square of the ratio of high order multipole moments of the two-dimensional potential to the monopole moment. This method classifies structures that are apparent to the eye.

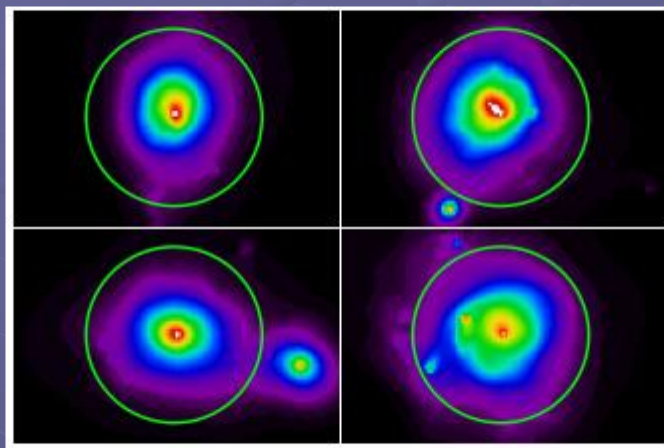

Weißmann, at al. (A&A, 549 (2013), A19) using the Buote & Tsai approach discussed

regular, intermediate, complex, double
as well as
relaxed, mildly disturbed and disturbed clusters.

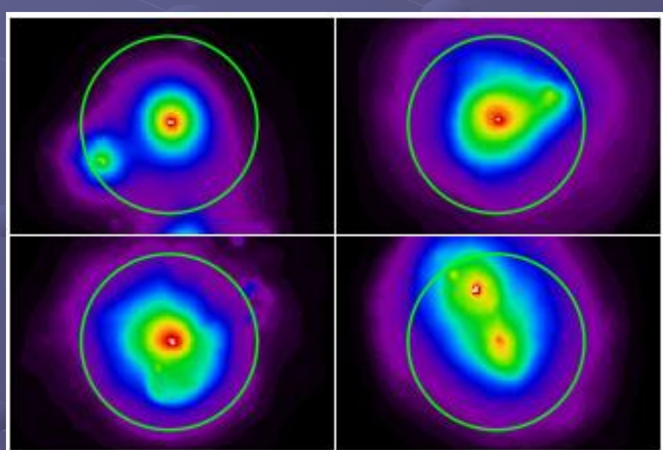

Simulated cluster images for relaxed (up) and disturbed types (r_{500} is shown as green circle).

80 galaxy clusters observed with XMM-Newton were divided as
~ 9% double,
~ 14% complex,
~ 36% intermediate
~ 41% regular objects.

Examples of the another categories.

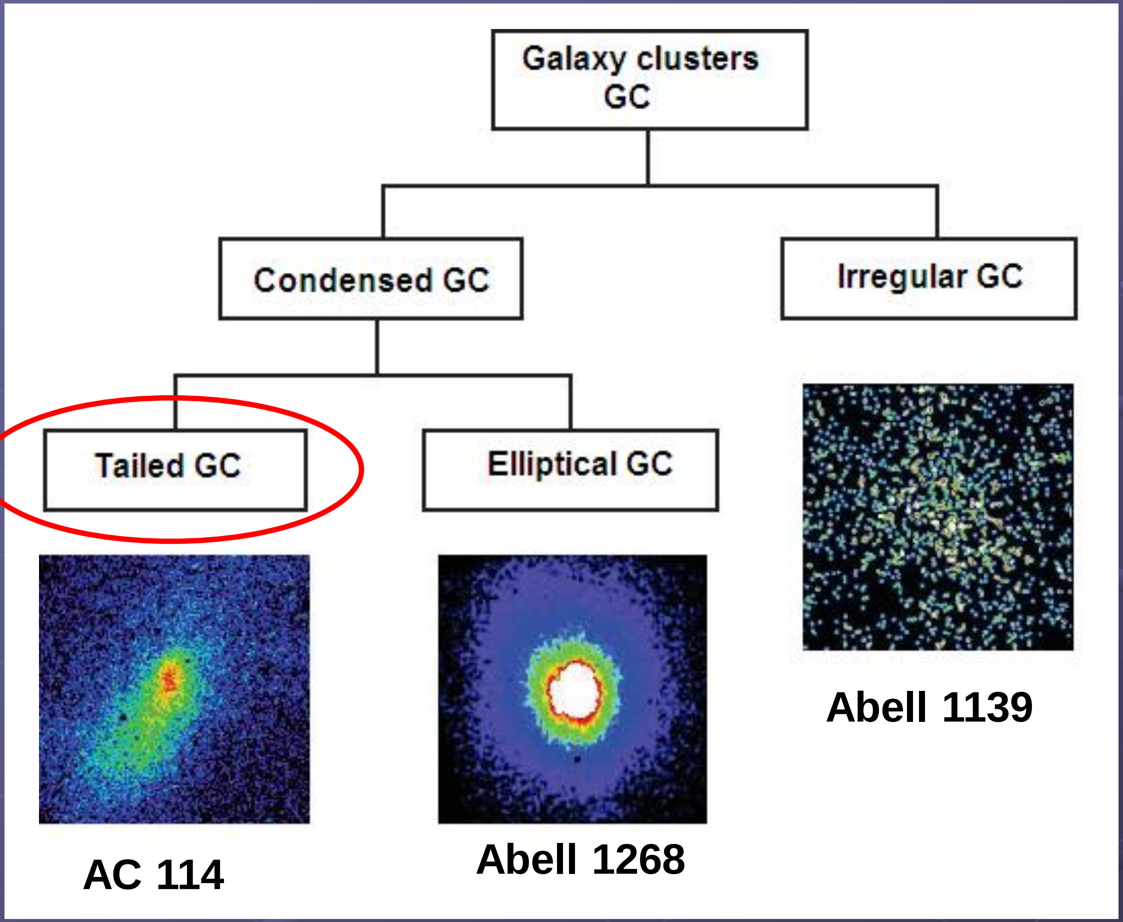

Lei Wang, et al., Classification of X-Ray Galaxy Clusters with Morphological Feature and Tree SVM. **DOI:** 10.1109/ICMLA.2016.0124
A tree structure classifier using support vector machine (SVM)

The XMM-Newton data confirm the substructure in the cluster X-ray morphology

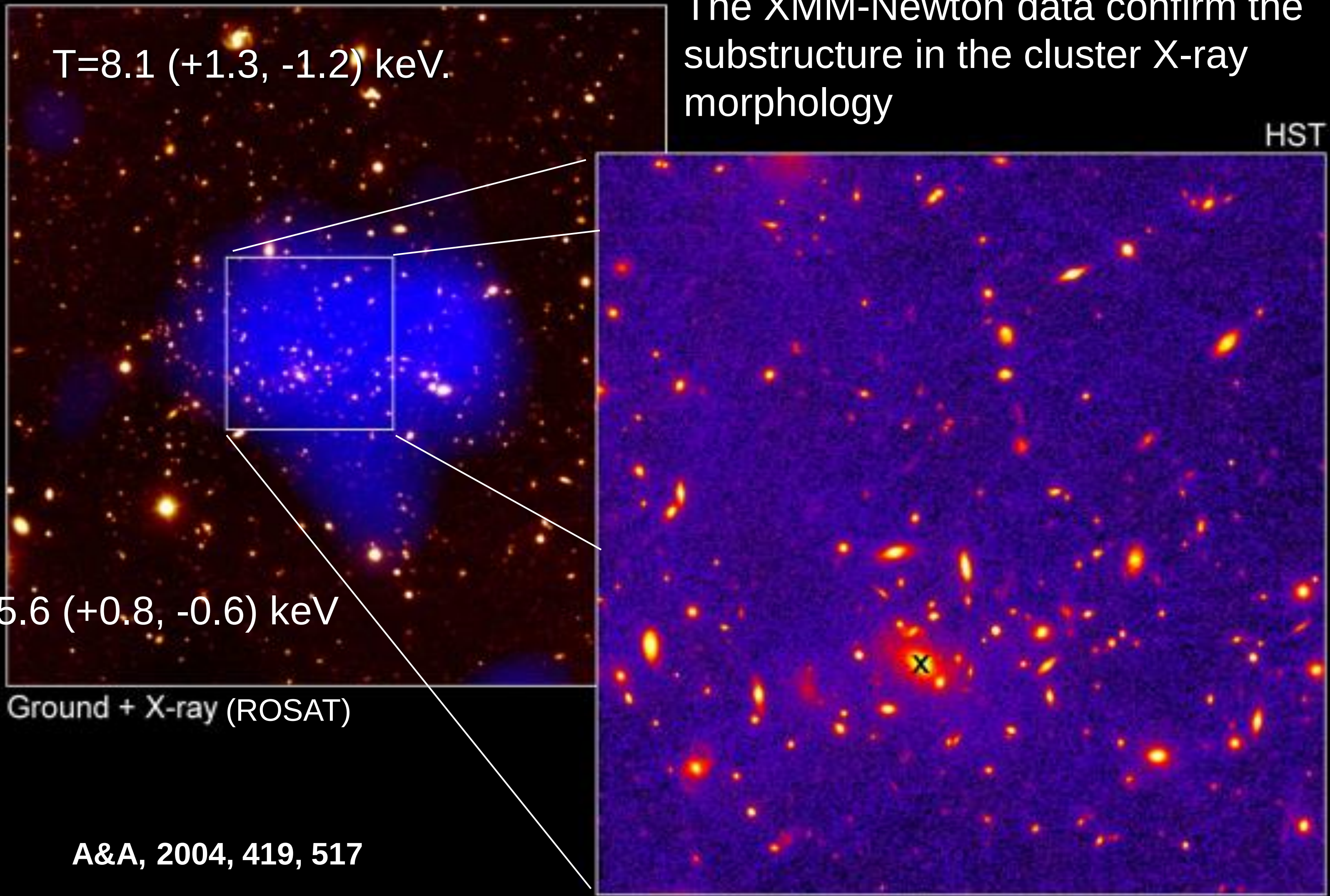

A&A, 2004, 419, 517

Distant Galaxy Cluster MS1054-0321 z=0.83

Hubble Space Telescope • Wide Field Planetary Camera 2

2XMM J083026+524133
z~1

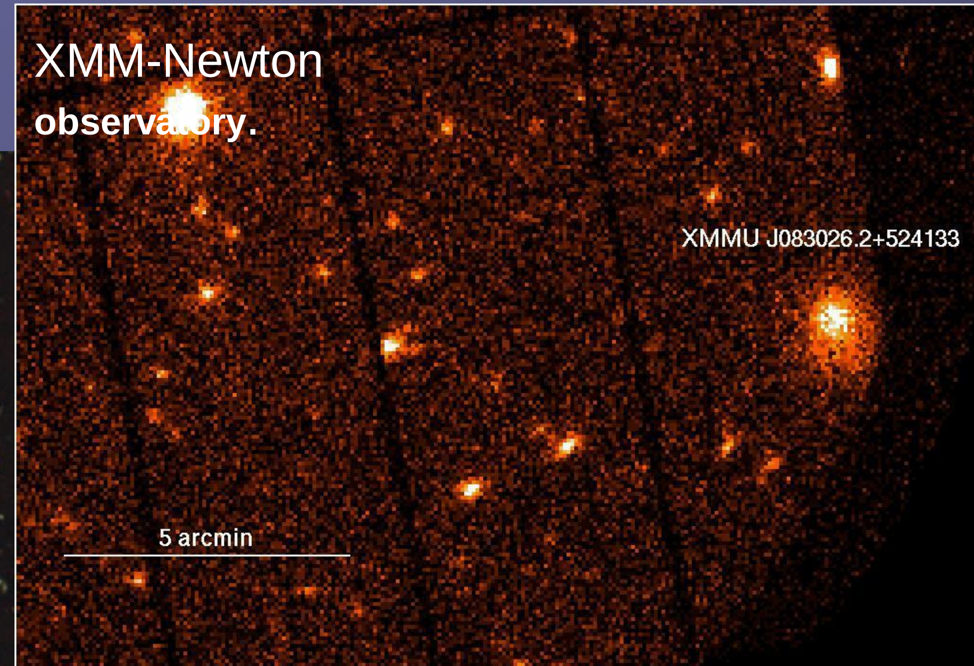

The optical image that confirmed that 2XMM J083026+524133 is a distant cluster of galaxies, taken by the Large Binocular Telescope in Arizona.

The X-ray emission from the cluster of galaxies is shown in blue at the centre of the image. The individual galaxies in the cluster are the small dots inside the blue glow.

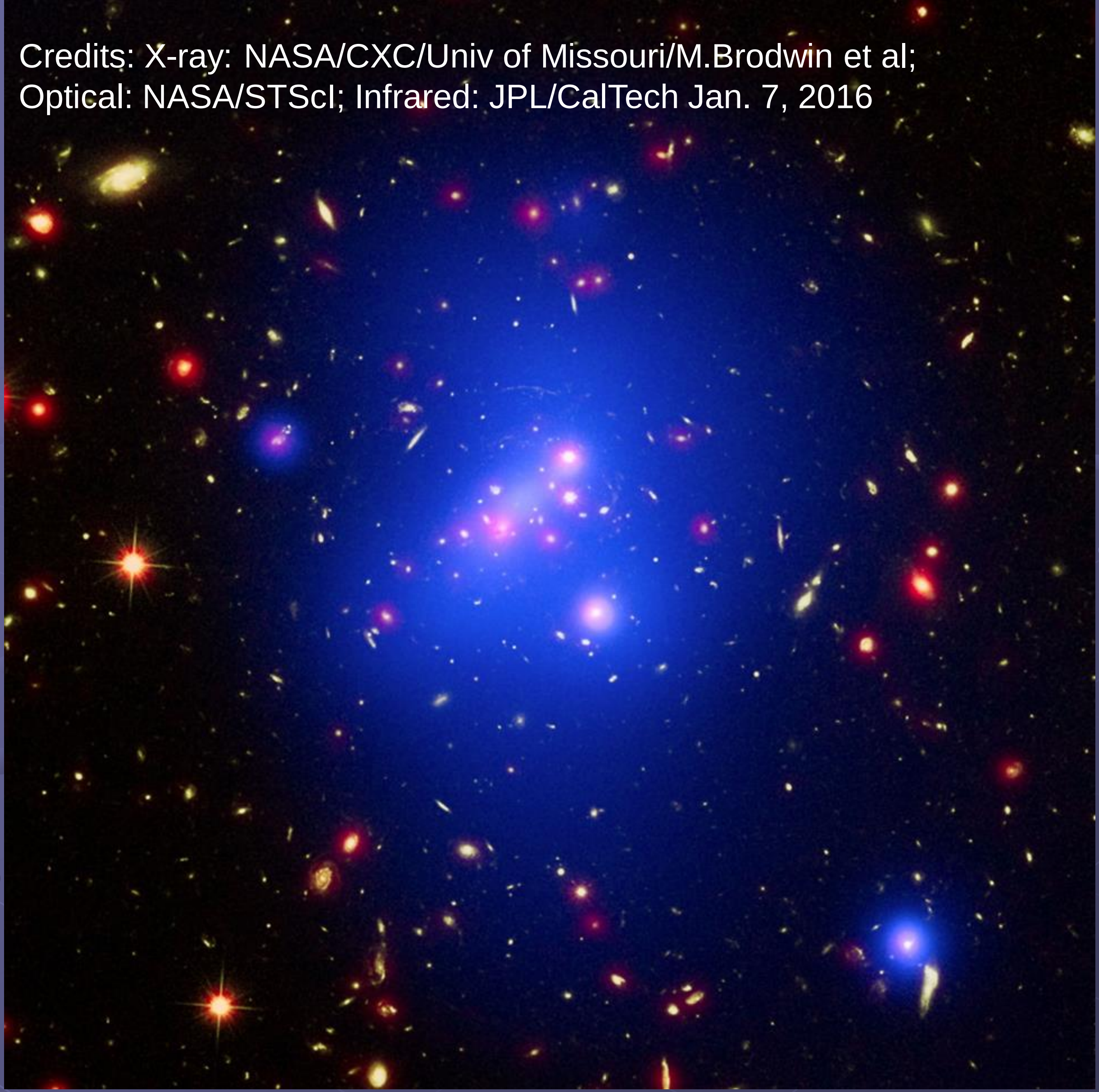

IDCS J1426.5+3508, z=1.75

It is the highest redshift strong lensing cluster known and the most distant cluster for which a weak lensing analysis has been undertaken

$$M = 2.3^{+2.1}_{-1.4}\times 10^{14}\ M_{\odot}$$

Wenli Mo et al., arXiv:1601.07967

This image of IDCS 1426 J1426.5+3508 combines data taken by three major NASA telescopes. The off-center core of X-rays is shown in blue-white near the middle of the cluster, and was captured by Chandra. Visible light from the Hubble Space Telescope, and infrared light from Spitzer is shown in red.

CL J1449+0856, z = 2

Composite image, about 100 arc minutes on a side, shows the X-ray emission (in purple) coming from the diffuse intra-cluster medium of the galaxy cluster CL J1449+0856 as detected by XMM-Newton.

The redshift was found to be 2.00. The cluster luminosity is approximately 7×10^{43} erg/s in the soft X-ray energy range (0.1-2.4 keV). An estimated mass of $5\text{-}8 \times 10^{13}$ solar masses.

R. Gobat et al., A&A 526, A133, 2011
arXiv:1305.3576, 2013

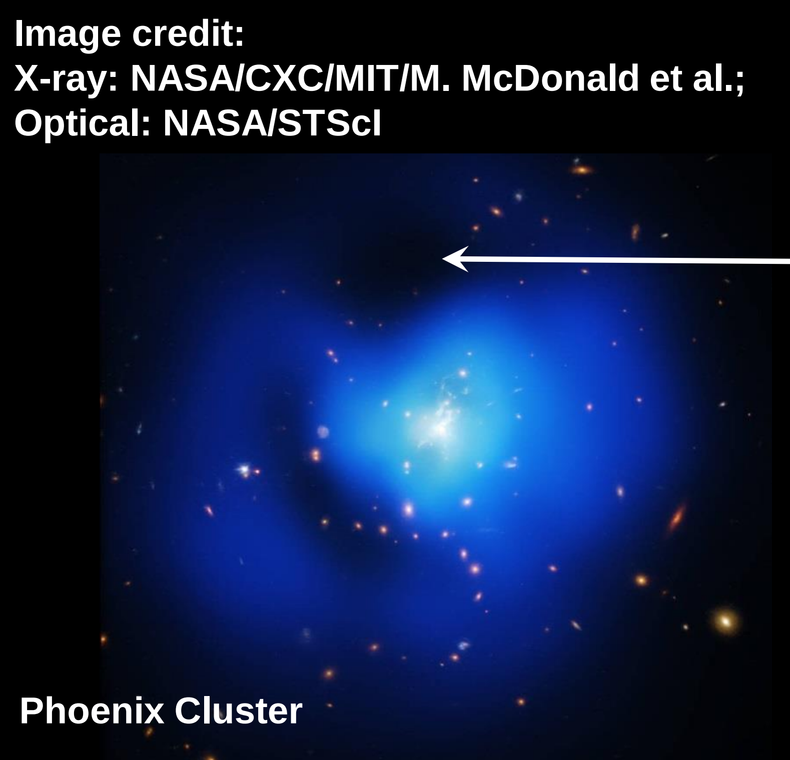

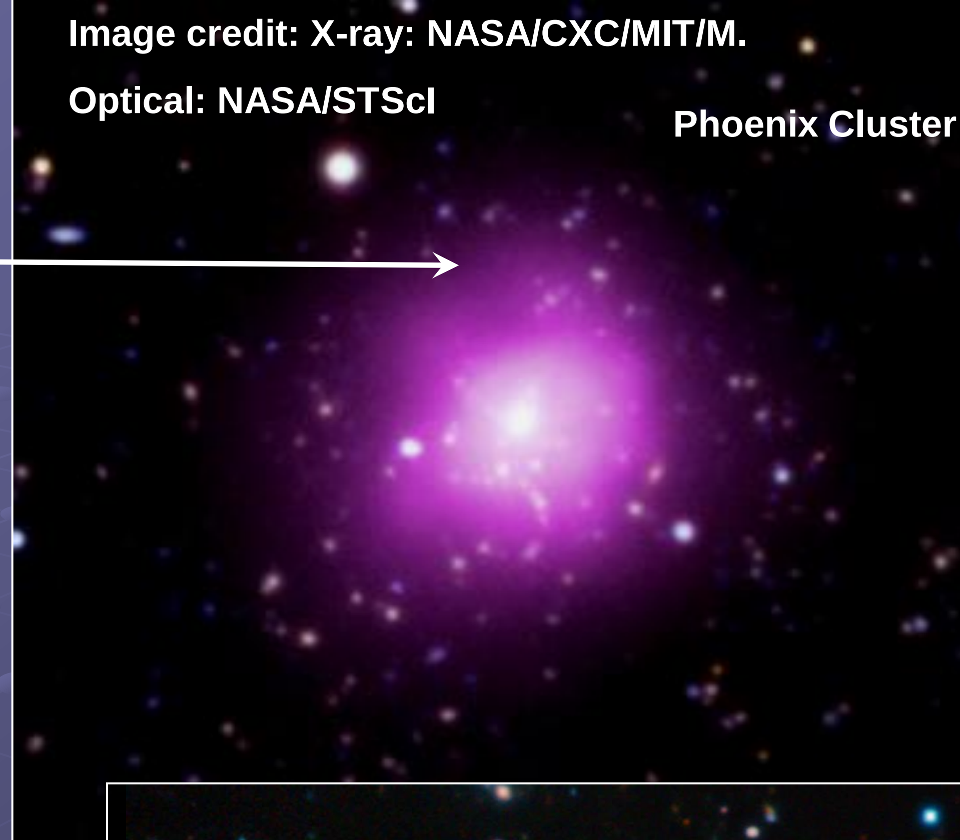

SPT-CLJ2344-4243, the Phoenix Cluster, images with and without cavities, z=**0.596**

CL J1001+0220, regular, 11.1 GLys. *Aug. 7, 2017* "Young, but fully formed galaxy cluster…"

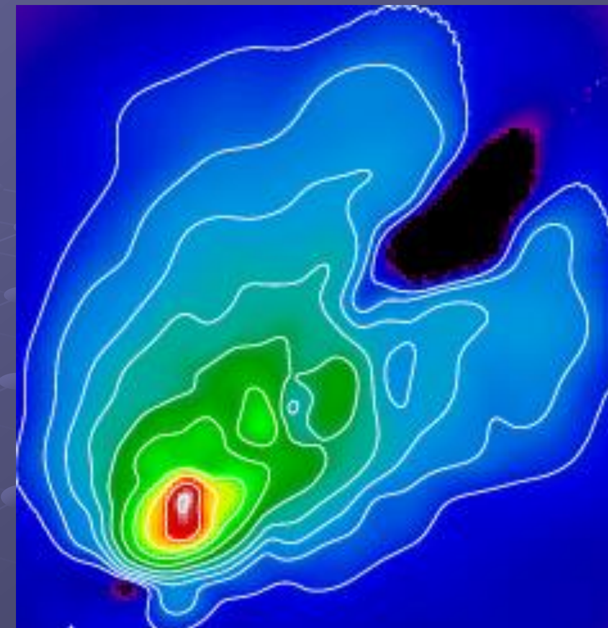

Map of the electron density in the mid-plane, Menanteau et al., ApJ, 2011, 748, 7

'El Gordo' most probably formed in the same manner as the Bullet Cluster

z=0.87

Temperature map of the merging cluster A3921 by Belsole et al. (2005). The temperature map has been produced from XMM-Newton observations obtained with the detectors EMOS1 and EMOS2 with the multi-scale spectro-imaging technique of Bourdin et al. (2004).

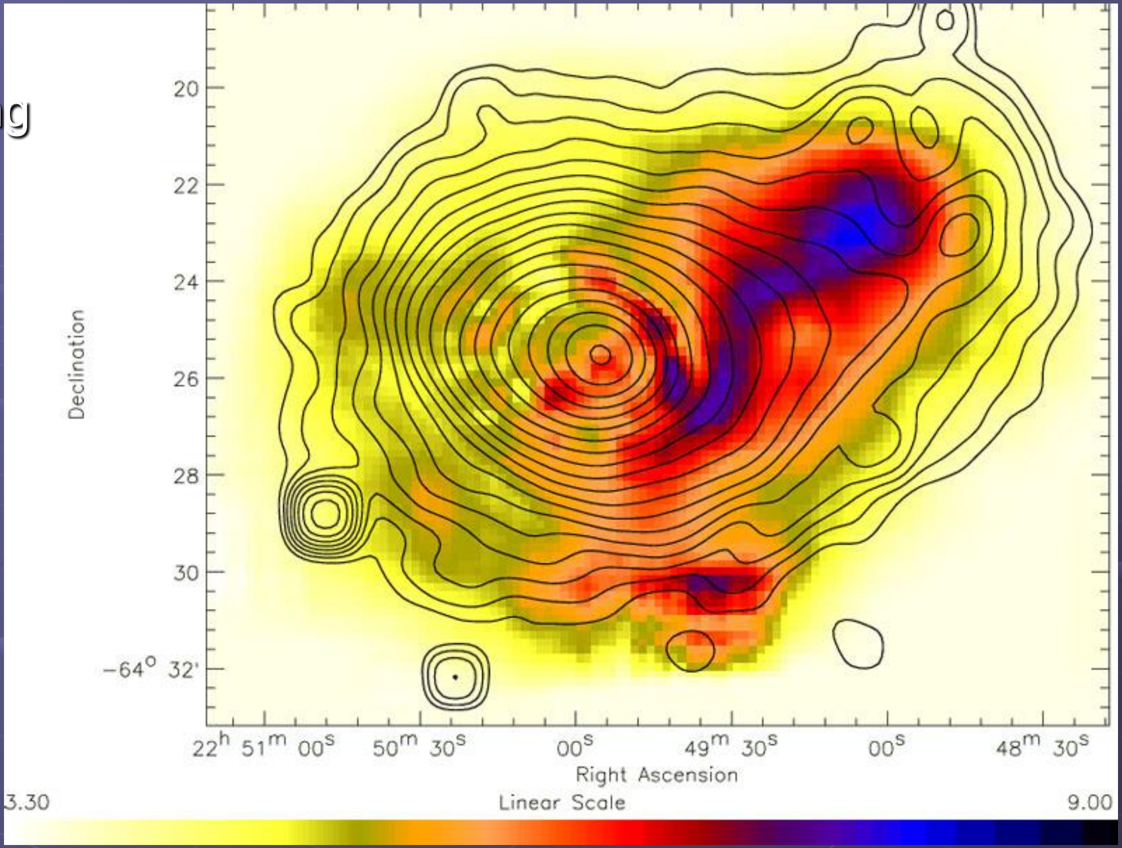

The barlike hot region to the NE is interpretated as the signature of an off-axis merger at a stage short after the first close encounter similar to features observed in simulations (Belsole et al. 2005, Ricker & Sarazin 2001). Superposed to the temperature map are the contour lines of the surface brightness distribution in the 0.3 - 10 keV band which was adaptively smoothed. The contours are spaced logarithmicly (https://ned.ipac.caltech.edu/level5/Sept09/Bohringer/Bohringer3.html)

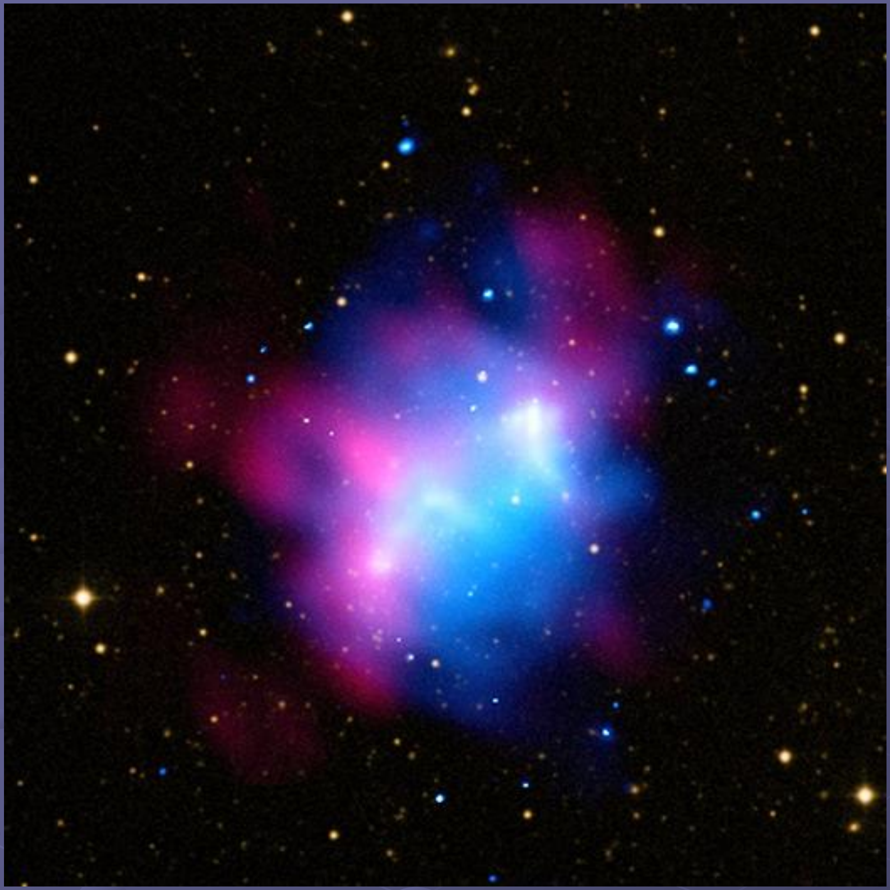

Blue :X-ray (NASA/CXC/SAO/M.Markevitch);
Radio: pink (TIFR/GMRTSAO/INAF/R.Cassano, S.Giacintucci);
Optical (DSS)

Abell 1758 (X-ray+Optical+Radio)
z= **0.28**

Chandra X-ray data reveals hot gas in the cluster and data from the Giant Metrewave Radio Telescope (GMRT) in India shows huge "halos" generated by ultra-relativistic particles and magnetic fields over vast scales.
Radio halos are generated during collisions between galaxy clusters.

Abell 1758 galaxy cluster merger simulation:
X-ray emission vs temperature

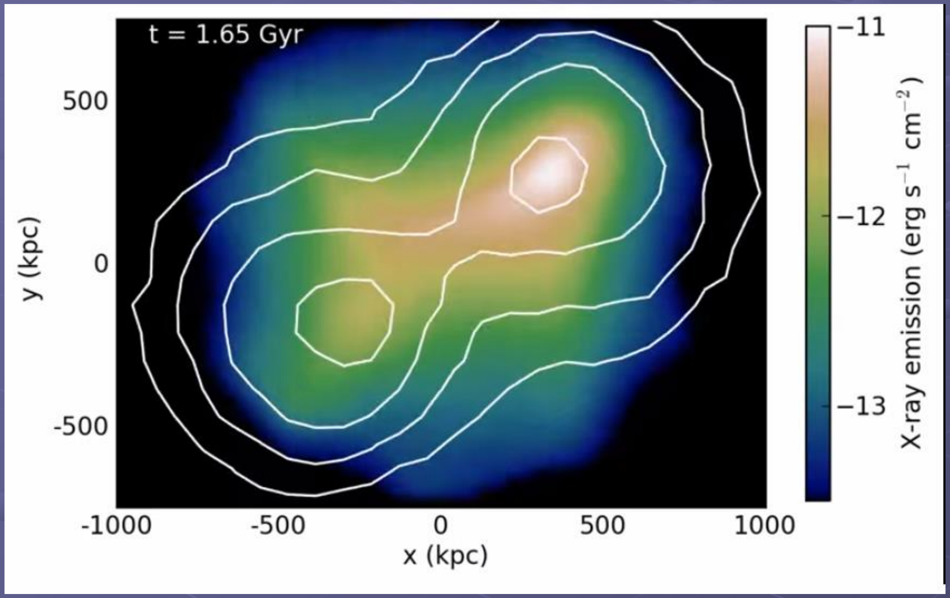

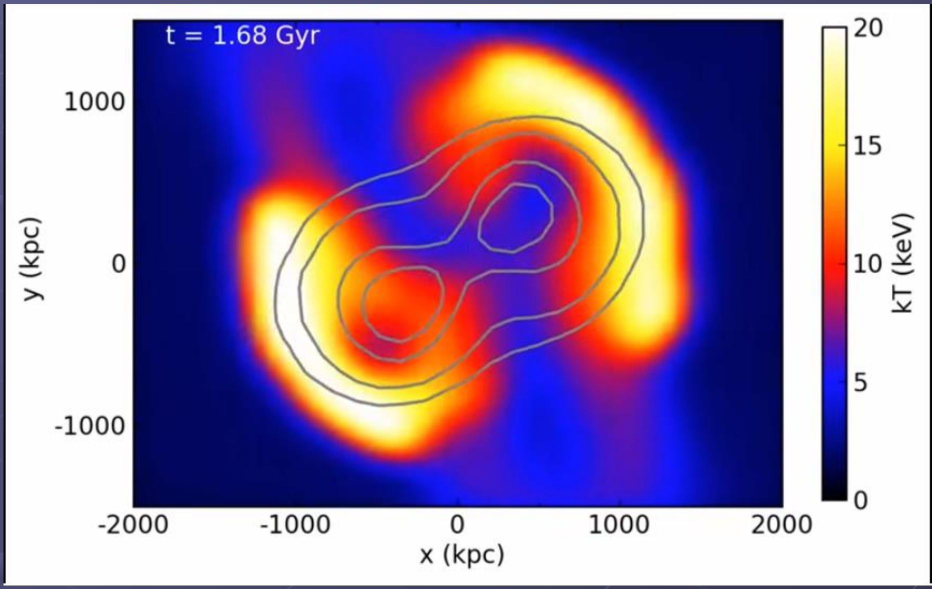

Courtes: R. Machado

https://youtu.be/-YjxxQVc5RE
https://www.youtube.com/watch?v=8loOt892VJQ
http://professor.ufop.br/rgmachado/vídeos-de-simulações

October 27, 2014 RELEASE

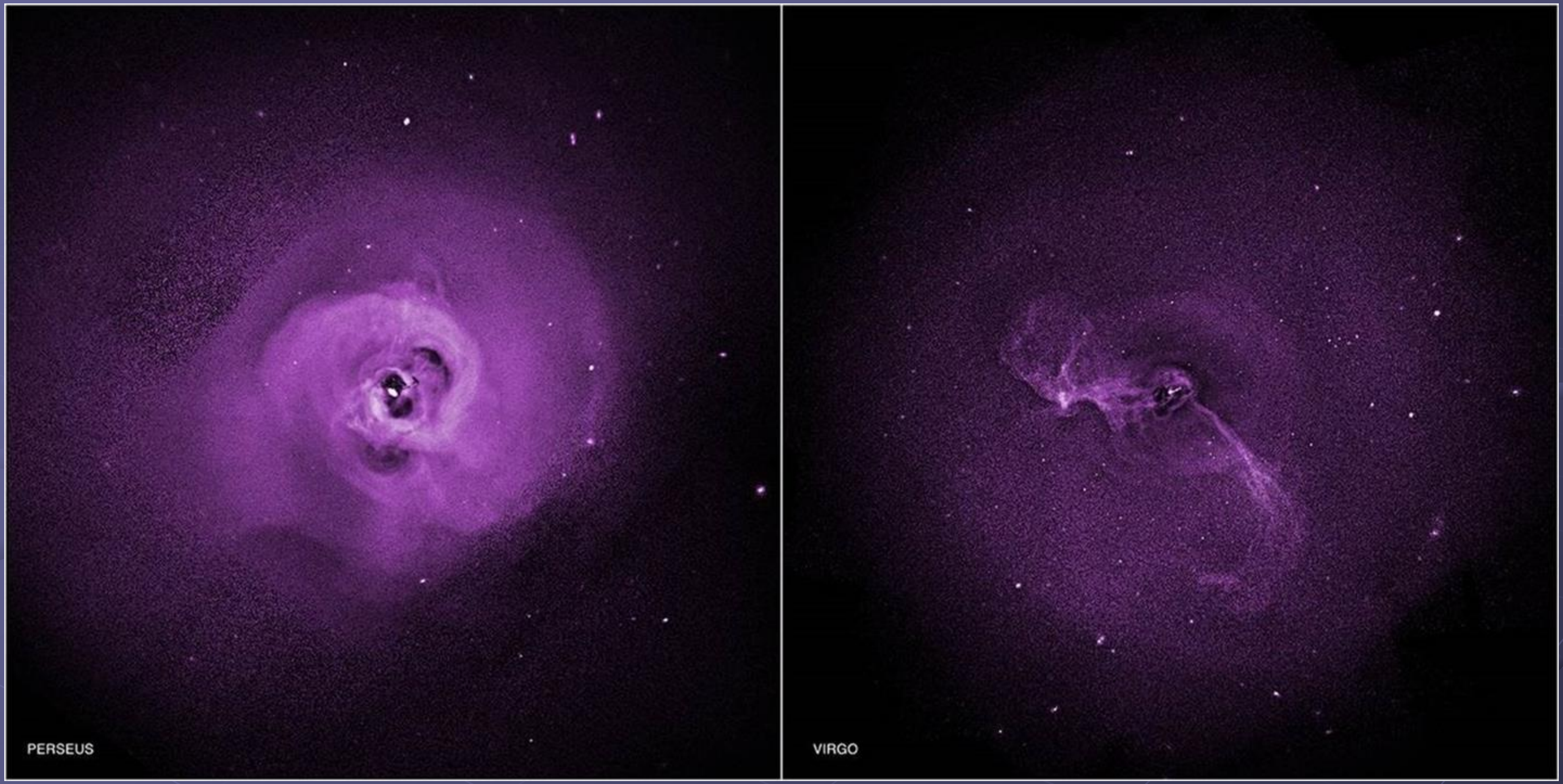

Chandra observations of the Perseus and Virgo galaxy clusters

Also: https://youtu.be/Yu1yF1z7Ins

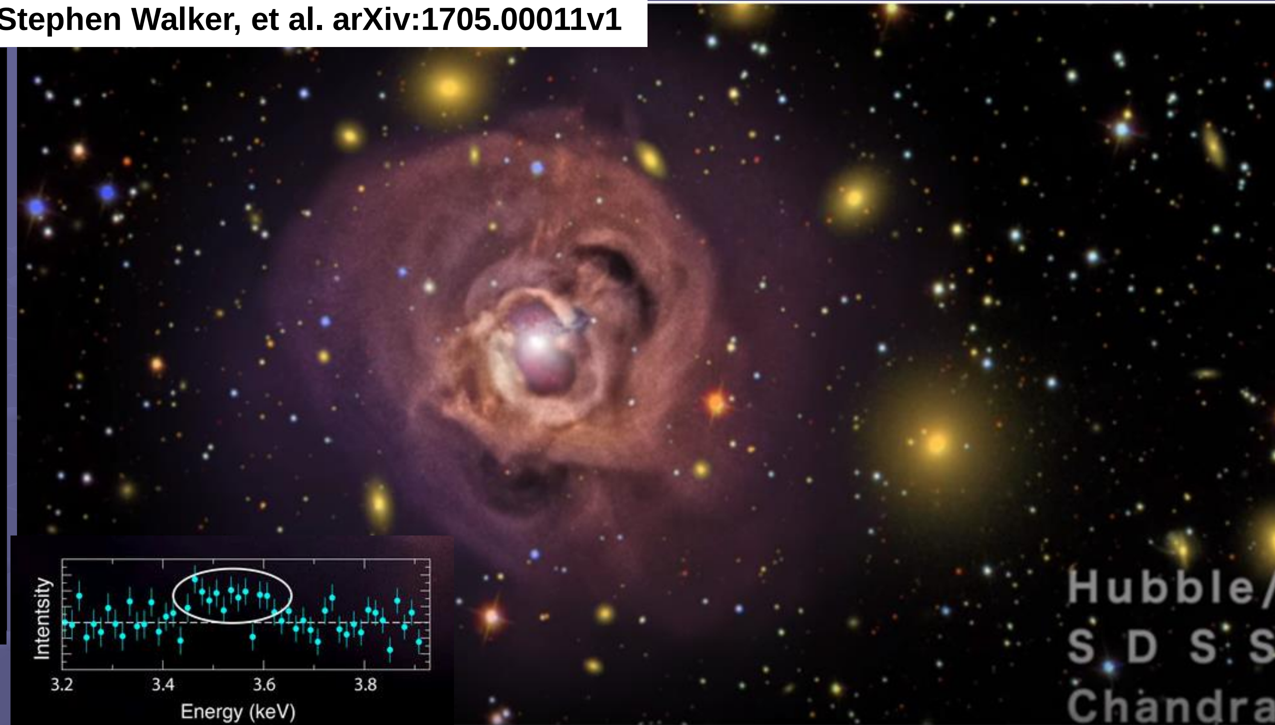

X-ray image of Perseus Galaxy Cluster from the Chandra Observatory. The gravitational disturbance results of the distant flyby of a galaxy cluster about a tenth the mass of the Perseus cluster.
Is it giant Kelvin-Helmholtz instability in hot gas? It is possible: gas in a large cluster similar to Perseus has settled into two components, a "cold" central region (30 10^6 K) and a surrounding zone where the gas is three times hotter.
ESA’s XMM-Newton and NASA’s Chandra observed of the *3.56 keV* line in 73 galaxy clusters (E. Bulbul et al., arXiv:1402.2301)

COLD FRONTS

'Cold Front' in the Perseus Cluster

The Chandra data have been specially processed to brighten the contrast of edges to make subtle details more obvious.

The cold front is about two million light years long and has traveled away from the center of the cluster at about 130 km/s

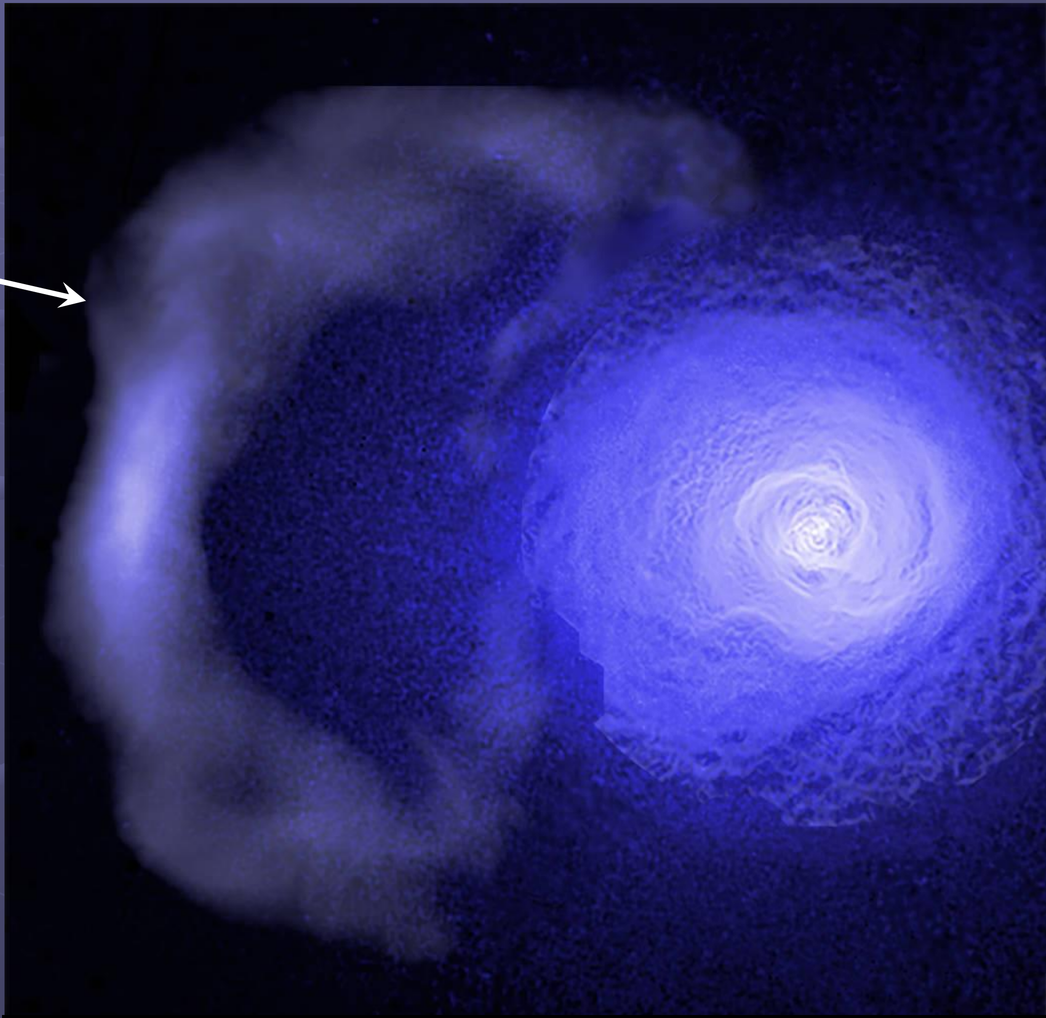

Credit: NASA/CXC/GSFC/S. Walker, ESA/XMM, ROSAT

The motion of gas within or between clusters and the presence of entropy gradients, both of which are conditions that are prevalent in clusters, provide the conditions for the formation of cold fronts.

There are two classes of cold fronts, which were first distinguished in 2005 by Tittley & Henriksen.

They are: “remnant core” cold fronts and “sloshing” cold fronts

The cold fronts potentially tell us very interesting things about the detailed physics of the ICM; puts constraints on transport processes in the plasma; driving turbulence which reaccelerates relativistic particles to produce radio emission

The cores of "relaxed" galaxy clusters are not quite relaxed: many of them exhibit cold fronts produced by gas sloshing.

The cold fronts' relative absence of K-H instabilities may be explained by the cluster magnetic field and Braginskii viscosity.
However, the magnetic field does NOT appear to be sufficient to suppress conduction across the fronts, indicating thermal conduction may be weak in the ICM
Sloshing also drives turbulence, reaccelerating relativistic electrons, producing radio minihalos consistent with observed sources.

In the most general terms, remnant core cold fronts form when a galaxy, or cluster moves through a hotter ambient plasma and the res head wind strips off the outer layer of its atmosphere.

This situation arises when a galaxy or group falls into a larger cluster, and even when two clusters are passing through each other.

This process has also been described as "ram-pressure stripping" in the context of galaxies moving through the ICM of their host clusters

Examples: "Bullet Cluster" or NGC 1404 in the Fornax cluster which moves towards the NW to the Fornax center. NGC 1404 is a classic example of a remnant core cold front, which stretches around the galaxy's atmosphere from NE through NW to SW. Reproduced from Machacek et al. (2005).

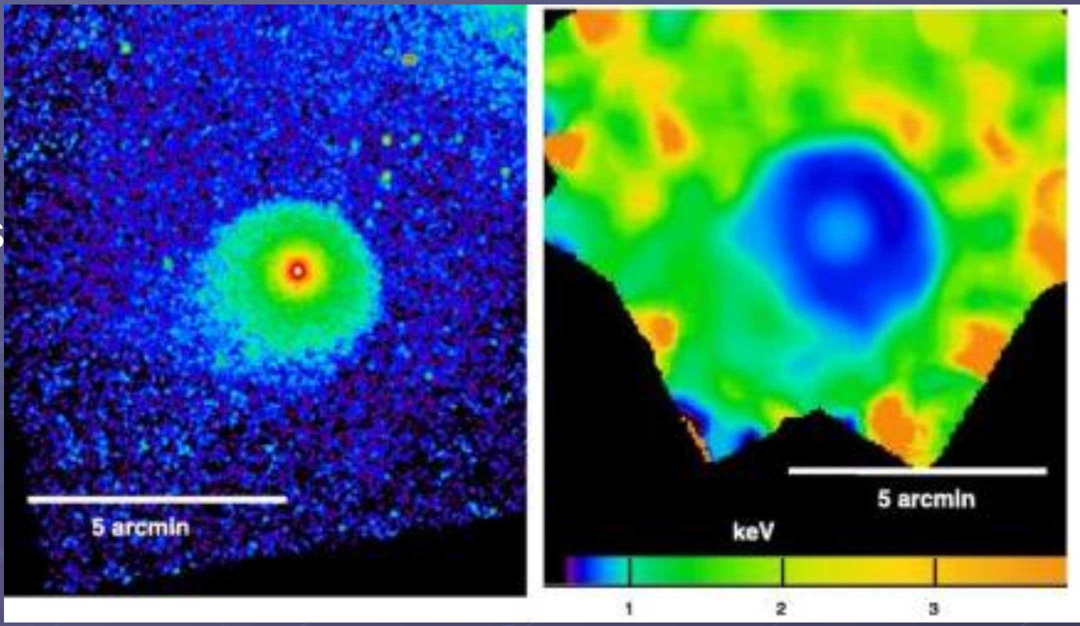

X-ray surface brightness (left) and spectroscopic temperature (right) maps for the elliptical galaxy NGC 1404, which is falling into the Fornax cluster.

The second class of cold front, sloshing cold fronts, arises when some process offsets the bulk of the central ICM in a cluster from its hydrostatic equilibrium in the cluster potential. The ICM then slowly oscillates–or sloshes–around its hydrostatic equilibrium configuration. The variation of sloshing frequency with cluster radius leads to the formation of arc-shaped contact discontinuities staggered on opposite sides of the cluster core. They are particularly visible if the cluster is of the “cool-core” variety, where the cluster has been relatively undisturbed for some time and the temperature in the center has slowly decreased via radiative cooling, causing the central density to go up to maintain hydrostatic equilibrium.

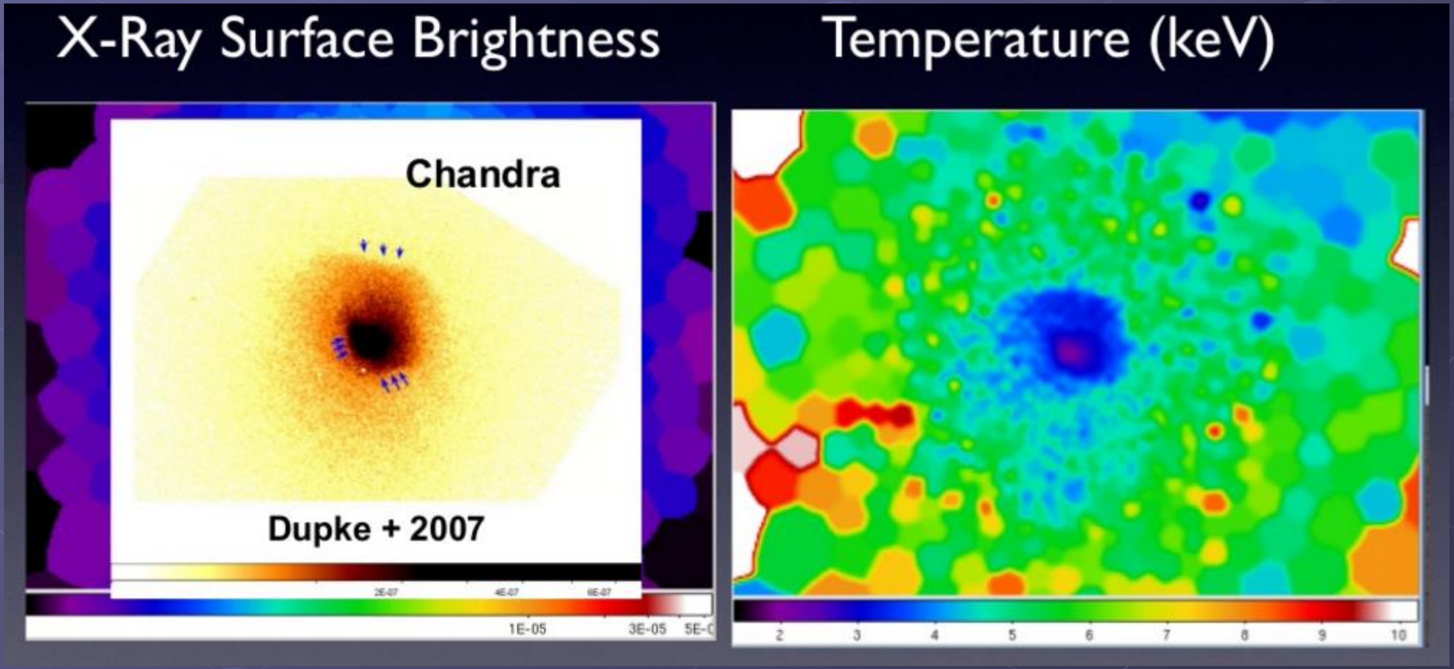

Observations of Gas Sloshing by Chandra and XMM (right). Courtesy S.Chizzardi

What Causes Sloshing?

Interactions with small subclusters (Asascibar & Markevitch 2006)

A passing subcluster accelerates both the gas and dark matter components of the cluster core, but the gas component is decelerated by ram pressure, resulting in a separation between the two

As the ram pressure weakens, the cold core gas falls back into the DM core, but overshoots it and begins to "slosh"

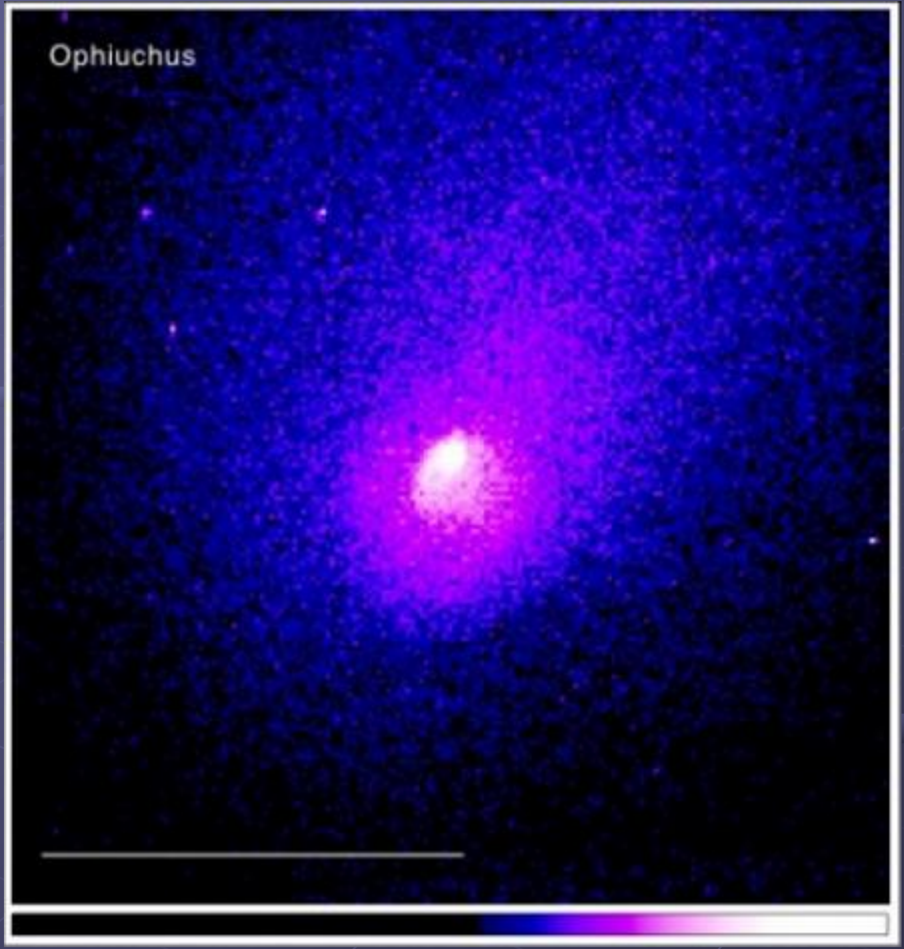

https://www.slideshare.net/jzuhone/the-physics-of-gas-sloshing-in-galaxy-clusters-37471994 (Markevitch et al.)

Gas Sloshing

The signature:

cold fronts in relaxed cool-core clusters

Spiral-shaped discontinuities in surface brightness and projected temperature

Most easily explained by the "sloshing" of the cool core gas in the dark matter potential well

Cold gas has been uplifted from the gravitational potential minimum and formed a contact discontinuity in pressure equilibrium with the hotter, less dense gas

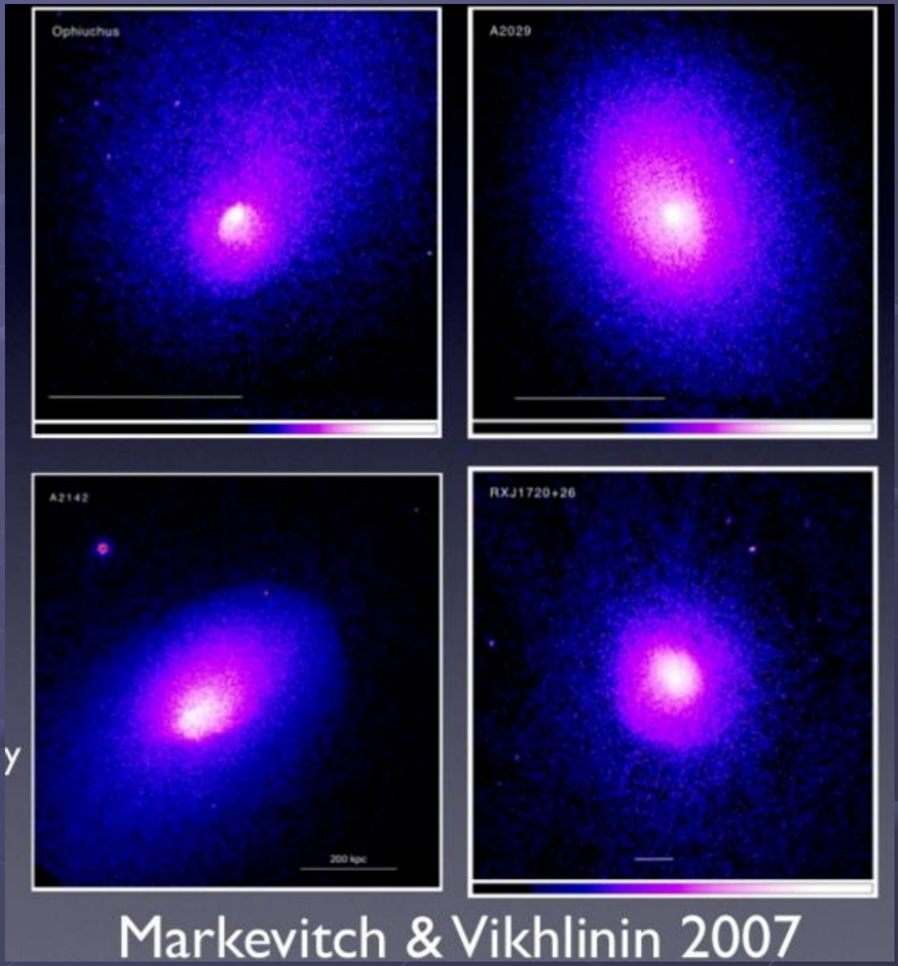

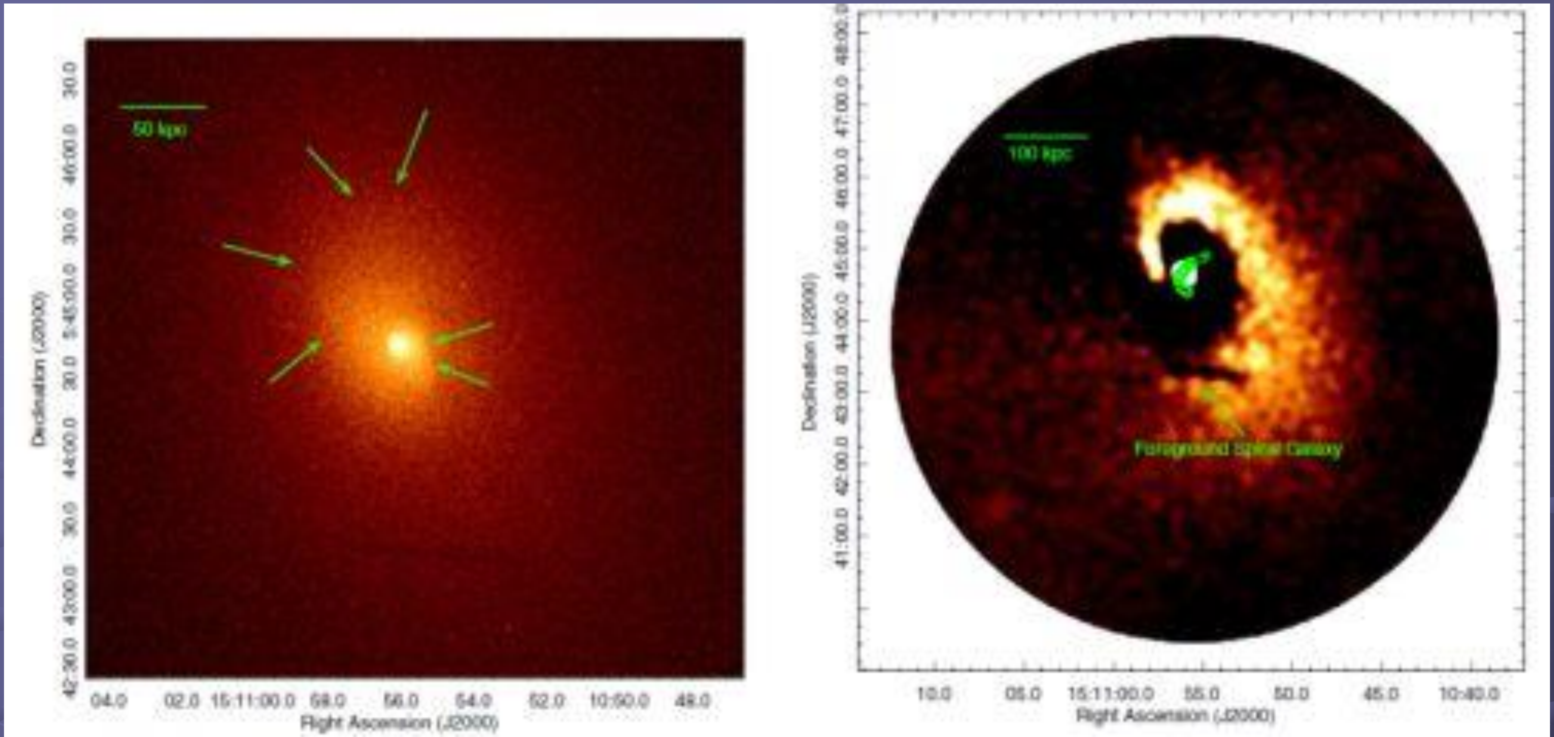

Sloshing in A2029.

Left: X-ray surface brightness image of the central part of the cluster, showing sloshing cold fronts arranged in a spiral pattern.

Right: Surface brightness residual image, highlighting the associated spiral-shaped surface brightness enhancement, and demonstrating the extent of the sloshing motions out to 400 kpc. (From Paterno-Mahler et al., 2013).

A nice key to ICM Plasma Physics

Gaussian Gradient Magnitude (GGM) edge-detecting algorithm
Sanders et al., 2016

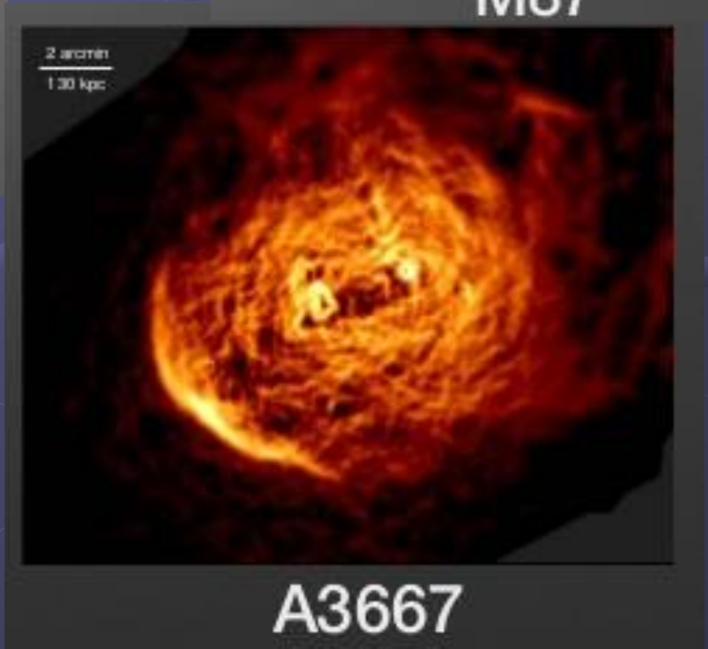

Courtesy: John ZuHone

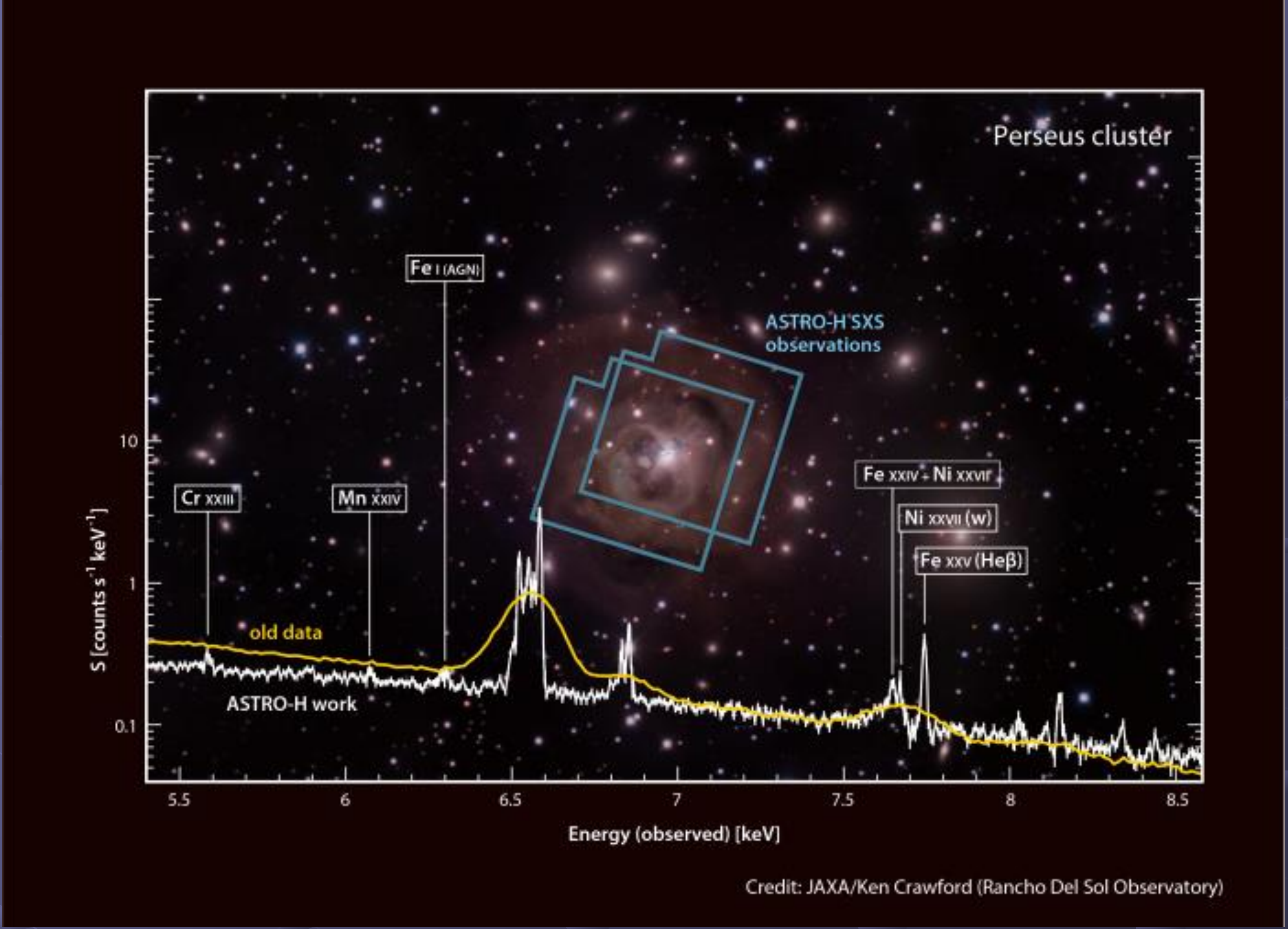

ひとみ　Hitomi (Astro-H, NeXT from New X-ray Telescope)
Lifetime 17.02—26.03.2016

More in: https://ned.ipac.caltech.edu/classic/level5/

LEVEL 5

A Knowledgebase for Extragalactic Astronomy and Cosmology

Star Award
Griffith Observatory

Principal Investigator
Dr. Barry F. Madore

Caltech and Carnegie
Pasadena, California, USA

Originated in 1997 under the sponsorship of NASA's
Applied Information Systems Research Program (AISRP).
Now a component of the NASA/IPAC Extragalactic Database (NED).

- Introduction
- New Additions
- Author Index
- Glossary & Lexicon
- Text Search Engine
- Cosmology
- Annual Reviews Articles
- Cambridge Monographs
- Fundamental Data
- Graphical Relations
- Commentary
- Basic Data: Galaxies
- Atlases & Catalogs
- Tools & Astrostatistics
- Galaxy Reviews
- Spectroscopy
- Particle Physics Reviews
- Database of Galaxy Distances
- Deep Fields
- WEB Links

*****

This site is maintained by Cren Frayer
Database last modified: November 3, 2017

To see the monthly web statistics, click here

https://www.clues-project.org/cms/talks/

Thank you!